Analytical solutions to backreaction on cosmic strings

A dissertation submitted by

Jeremy M. Wachter

in partial fulfillment of the requirements for the degree of

Doctor of Philosophy

in

Physics

Tufts University

May 2017

Advisor: Ken D. Olum

Abstract

We present analytical studies of gravitational and electromagnetic backreaction on cosmic strings. For oscillating loops of cosmic string, we present a general argument for how kinks must change; additionally, we apply this general argument to the geometrically simple case of the Garfinkle-Vachaspati loop. Our results suggest that the formation of cusps on loops is delayed, and so we should expect fewer cuspy signatures to be seen in gravitational wave observations. Electromagnetic backreaction we show to reduce currents on a string at least as rapidly as necessary to avoid a paradox, and currents induced on a superconducting straight string will be asymptotically reduced to zero.

Acknowledgements

First and foremost, I would like to thank Ken for many years of advising. None of the following work would be possible without his aid and guidance; his door was always (metaphorically, and quite often literally) open. In addition, I would like to thank my other committee members: Alex Vilenkin, Larry Ford, Jose Juan Blanco Pillado, and Tim Atherton.

Thanks is due as well to the faculty and staff of the Physics and Astronomy department. Of the faculty, I wish to expressly thank Hugh Gallagher, Roger Tobin, and Tim Atherton for inspiring and encouraging my interest in becoming a better educator.

I have been fortunate to have the friendship and support of many excellent graduate students at Tufts, but the following deserve special recognition: Andrew, Anna, Chris, Dave, Eric, Erin, Josh, Lise.

Finally, I do not have enough space to thank my family for all they have done for me. All that I have done, they have made possible.

While completing this dissertation, I was supported financially by the John F. Burlingame Graduate Fellowship and the Allan Cormack Graduate Fellowship.

CONTENTS

LIST OF FIGURES

Analytical solutions to backreaction on cosmic strings

CHAPTER 1

INTRODUCTION

Cosmic strings are one-dimensional topological defects which may have formed as a consequence of spontaneous symmetry breaking in the early universe [1]. They are generic predictions of field theories and string-theory models of inflation [2, 3]. In this chapter, we give motivations for studying cosmic strings and provide for the non-expert reader an overview of how cosmic strings form, important properties of strings, and some outstanding questions in the field. For a complete review, see Ref. [4].

The first question which ought to be asked of any line of inquiry in physics is, put bluntly, "but how is it useful?". If our ultimate goal is to build a more complete picture of reality, then our research should contribute some novel part of that image, or make clearer an existing one. The broad answer which cosmic strings give to this question is "we inform you about the early conditions and evolution of the universe". Beyond this bare-bones pragmatism, the study of cosmic strings invokes and applies many beautiful and interesting aspects of physics and mathematics, drawing inspiration from (and, in turn, contributing to) fields such as particle physics and astronomy.

We ask the reader to accept, for now, the following claims: that strings are massive; that strings are effectively one-dimensional, possessing a thickness many orders of magnitude smaller than their curvature in most applications; and that strings are generally dynamic. We shall delve into these claims in more detail in Sec. 1.2. For now, we consider the consequences of such objects existing in our universe.

The presence of any massive object immediately suggests that it might be involved in structure formation. Such ideas have been present from the earliest days of cosmic strings [5, 6]. While subsequent investigations and observations have restricted the conditions under which cosmic strings may contribute, such mechanisms remain possible and are the subject of active research [7].

An interesting property of strings is that they may be superconducting [8]. This naturally gives rise to a collection of possibly observable signals, such as ultra-high-energy cosmic rays [9] or fast radio bursts [10] whose sources are still a matter of debate. The presence

of these charged objects and their associated decays at early cosmic times also provides a possible mechanism for the creation of astrophysical magnetic fields [11].

In addition to electromagnetic or particle emission, cosmic strings of all sorts radiate gravitationally. Loops of cosmic string decay by gravitational radiation, as they are massive objects in motion through spacetime. This form of emission should provide a background of gravitational waves, potentially detectable by the current generation of pulsar timing arrays [12] as well as by next generation of gravitational interferometers [13]. In addition, features known as cusps which may arise on strings would be a source of intermittent, but far stronger, gravitational wave signals.

As we have definitively entered the era of gravitational wave astronomy, the importance of understanding and modeling such emissions of cosmic strings is critical to detection. Improving upon the existing understanding of cosmic string loop gravitational waves will be the primary motivator of the bulk of this work, although we will devote some time to investigating another such problem in electromagnetic radiation. Delaying further discussion of the specificities of our motivation for later, we will now consider strings themselves in greater detail.

1.1 Mechanisms for string formation

If we are to study cosmic strings, we should understand the processes by which they might form, and the types of theories which permit such processes. Accepting the basic description of cosmic string as a massive one-dimensional object in three-dimensional space, we might ask: how would one go about finding such an object? A moment's thought convinces us that if we draw a loop which encloses this object (that is, the object pierces the surface whose boundary is given by our loop), we may specify the location of that object by contracting and sliding the loop around. Equivalently, if we work in the plane transverse to our loop, then a cosmic string will be a point in this plane which distinguishes itself from empty space in some fashion.

With this in mind, we will investigate how spontaneous symmetry breaking can give rise to such distinguished points. Symmetry breaking is a familiar topic in a variety of fields of physics. A simple example is found in crystals, which reduce the translational and rotational symmetries to the discrete crystallographic point groups. As seen in the specific case of crystals, spontaneous symmetry breaking is often associated with some form of phase

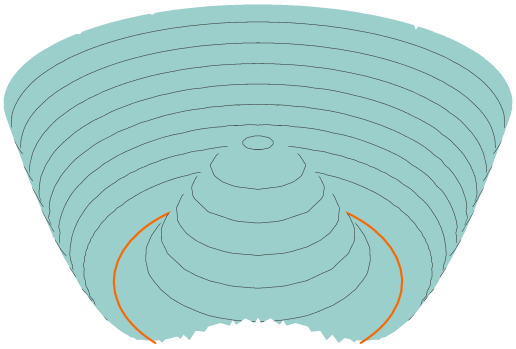

Figure 1.1: The rotationally symmetric cosmic string potential. We have cut away the near part of this potential to show the central peak and (orange) circle of minima more clearly. Black lines indicate $V = const.$

transition. The large number of phase transitions in our universe's life hints at the varied landscape of strings which may be possible.

1.1.1 Strings in the Goldstone model

Perhaps the simplest example of a model with a string-producing spontaneously broken symmetry is the Goldstone model for a complex scalar field ϕ,

$$\mathcal{L} = \left(\partial_\mu \phi^*\right)\left(\partial^\mu \phi\right) - V\left(\phi\right) \ , \tag{1.1}$$

with the potential chosen as

$$V\left(\phi\right) = \frac{1}{4}\lambda\left(\phi^*\phi - \eta^2\right)^2 \ . \tag{1.2}$$

We see that the potential is rotationally symmetric with a non-zero value at $\phi = 0$ and a circle of minima, representing all possible ground states of the theory, for all $\phi = \eta e^{i\theta}$ and θ an arbitrary phase. This sort of potential is termed a *Mexican hat* or *wine bottle bottom* potential for its visual similarity to these objects, as shown in Fig. 1.1. The (real, positive-definite) parameter η is the energy scale at which spontaneous symmetry breaking (and thus string formation) takes place. We shall see in Sec. 1.2 that this energy scale determines the thickness and mass density of a cosmic string.

For spontaneous symmetry breaking to occur in a system, its Lagrangian must respect some symmetry that its ground state does not. In the Goldstone case, this is satisfied: the Lagrangian does not change under global $U(1)$ transformations

$$U_\alpha : \phi \to \phi e^{i\alpha}\,, \tag{1.3}$$

but the ground state does.

$$U_\alpha \left(\eta e^{i\theta}\right) = \eta e^{i(\theta+\alpha)}\,. \tag{1.4}$$

Consider now a two-dimensional space filled by this field. We may represent the value of the complex field at any point by a vector

$$W(x,y) = \Re\left[\phi\right]\hat{x} + \Im\left[\phi\right]\hat{y} \tag{1.5}$$

if the field has undergone spontaneous symmetry breaking and by 0 if it has not (i.e. if it remains on top of the central "peak" of Eq. (1.2)).[1] Now consider some closed path in this space, whose only constraint is that $W \neq 0$ everywhere along its extent (that is, the field has undergone spontaneous symmetry breaking at all points the path visits). As we walk around this path, we keep track of the direction in which W is pointing. When we return to our initial point, W must point in the same direction as when we started, but it is permitted to acquire a nonzero phase shift $\Delta\theta = 2\pi n$.

We now have two general cases: zero phase shift over a path, and nonzero phase shift over a path. Probably there is some interesting physics happening here, so let's see if we can determine what it is. A naïve guess would be that the region the path bounds contains whatever is the source of this difference in phase shift, so our first attempt is to more accurately specify where this effect is. To do this, we shrink our path while preserving the phase shift acquired around the path.

If there is no phase shift as we walk around a closed path, then we may shrink that path to a point without changing the phase shift, as the phase shift for a "path" whose prescription is to remain at a single point is obviously zero. Thus, a closed path with no phase shift contains nothing but vacuum.[2]

The same is not true of a closed path with nonzero phase shift. We can, however, very accurately specify which point must be responsible for the phase shift. If you were to

[1] We are thinking here only of the simple case of a non-fluctuating field.

[2] This presumes we have sufficiently isolated our point of interest before carrying out this procedure. A path with no phase shift may in fact contain a number of points which would produce a phase shift, but the sum of all these shifts is zero.

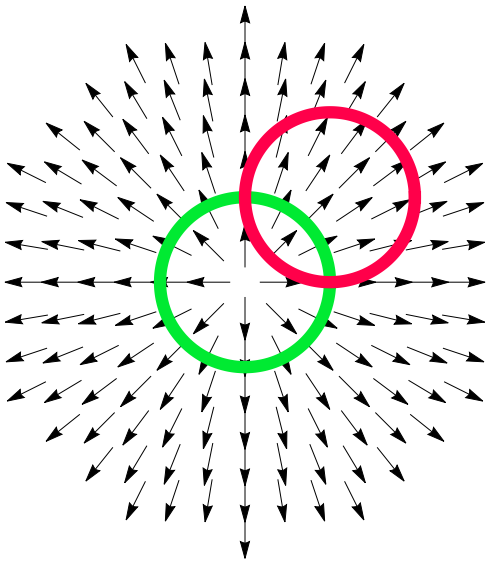

Figure 1.2: A complex field which undergoes spontaneous symmetry breaking in the Goldstone model fills some two-dimensional slice of space. Tracking the field's pointing as you traverse the (centered) green circle yields one full rotation, i.e. a phase shift of 2π. Tracking the field's pointing as you traverse the (off-centered) red circle yields no rotation and thus no phase shift. The crucial difference is that the green circle encloses a point where the field remains in the unbroken phase (and so is represented by a vector of zero length and undefined angle), while the red circle contains only points where the field is in the broken phase.

act out this process on an actual 2D vector field, you would find that the distinguishing characteristic is that a closed path with nonzero phase shift encloses a point where $W = 0$, as shown in Fig. 1.2. (This explains why we specified $W \neq 0$ when first defining our path.) Let's see if we can express this idea in a more mathematical fashion.

Take a point p on a (differentiable) two-dimensional manifold which has some vector field W. Draw a closed path very near p, parameterized by some γ, which avoids $W = 0$. We may then construct a map from this path to the unit circle, given by

$$f(\gamma) = W(\gamma)/\left|W(\gamma)\right| . \tag{1.6}$$

Thus, f will wrap around the unit circle some integer number of times. This corresponds exactly to the number of times we saw W rotate when we walked around our loop! This number is the degree of the map, which for the point p is also its index. We recall that the index of a point in a vector field tells us if that point is a singularity of the field or not. For $W(p) = 0$, the point has an index of $+1$ or -1 (for source/sinks or saddle points, respectively, in two dimensions), while for $W(p) \neq 0$, the index is not defined.

What does this tell us about our vector field? A nonzero phase shift as we traverse a loop means that there must be a point within that loop where $W = 0$. This corresponds to $\phi = 0$, which Eq. (1.2) tells us is a point which has nonzero energy (i.e. a point which is not in the vacuum state). We insist on continuity of this point of energy as we extend the 2D space into our more familiar 3D space—after all, any discontinuity means the line of energy ends, and so we would be able to slide a loop off the line and shrink it to zero. This continuity means that the line must either form in a closed loop, or terminate at the boundaries of our space (provided such a boundary exists).[3] We have thus traced out a one-dimensional object, formed as a consequence of spontaneous symmetry breaking—a cosmic string.

1.1.2 Non-simply connected vacuum manifolds admit strings

While the example given in Sec. 1.1.1 is illuminating, it relies upon a specific model with a specific (and global) symmetry breaking. Furthermore, the presence of spontaneous symmetry breaking alone is not enough to produce strings. Consider as an example a real field ϕ with potential $V \propto \left(\phi^2 - \eta^2\right)^2$. There will clearly be symmetry breaking, with vacuum values of $\phi = \pm\eta$, but it is equally clear that the discreteness of this symmetry breaking means that it produces patches of different vacua separated by "walls", and not strings. We would like a more general way to discover if a theory will permit cosmic strings or not, which we will do by extending our previous ideas about shrinking loops.

The mathematical mechanism we are looking for is homotopy theory. When we consider the homotopy groups of a space $\mathcal{M}$, denoted $\pi_n(\mathcal{M})$, we are asking about our ability to smoothly deform arbitrarily-drawn n-spheres in that space into each other. If two different n-spheres can be smoothly deformed into each other, we say they are *homotopic*, or that they belong to the same element of π_n. Such a deformation is obviously symmetric and transitive, which lets us group n-spheres in a space into homotopy classes.

As an example, consider $\mathbb{R}^3$ with coordinates (x^1, x^2, x^3) with one axis removed: $\mathcal{M} = \mathbb{R}^3 \backslash \{x^1\}$. If we select any point (a 0-sphere) in this space, we may smoothly move it to any other point, as we can always pick a path which avoids the x^1 axis. The zeroth homotopy group is trivial, expressed as

$$\pi_0(\mathcal{M}) = I\,. \tag{1.7}$$

[3] In more complicated situations, strings may exist as finite lengths at whose endpoints reside monopoles, domain walls, or even black holes. For the purposes of this work, we will only be interested in closed loop solutions.

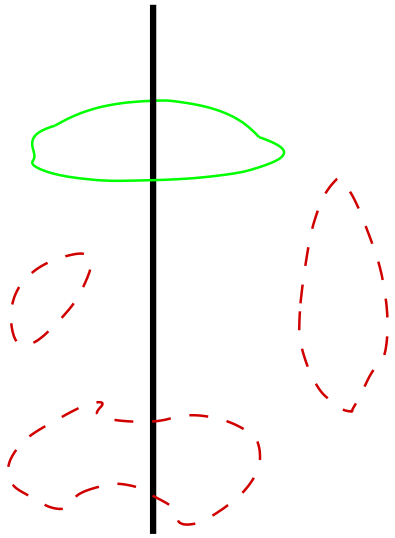

Figure 1.3: The space $\mathbb{R}^3\backslash\{x^1\}$, where the excluded axis is represented by the thick black line (which extends infinitely in both directions). The solid green loop contains this excluded axis, and so it cannot be smoothly deformed into any of the dashed red loops, which do not contain the axis. However, any of the dashed red loops can be smoothly deformed into another, and all may be shrunk to a point.

Put another way, there is only one homotopy class for points in this space. However, when we draw a closed one-dimensional path (that is, we map a 1-sphere into $\mathcal{M}$), it is possible for the path to become "trapped" by the excluded axis, as shown in Fig. 1.3. Consider by way of example all circles which can be drawn in this space whose x^1 coordinate is arbitrary, but whose position is otherwise given by

$$\left(x^2, x^3\right) = (a + \cos\gamma,\, b + \sin\gamma)\ , \tag{1.8}$$

with $0 \leq \gamma \leq 2\pi$. For $a^2 + b^2 > 1$, the excluded axis does not pierce the disk bounded by the circle, and any two such circles can be smoothly deformed into each other. For $a^2 + b^2 < 1$, the circle does contain the excluded axis, and all such circles can be smoothly deformed into each other. Because there is no smooth deformation which can move a circle with $a^2 + b^2 < 1$ to one which has $a^2 + b^2 > 1$, thanks to the excluded axis, we have defined two distinct homotopy classes. The first (or fundamental) homotopy group must be nontrivial,

$$\pi_1\left(\mathcal{M}\right) \neq I\,. \tag{1.9}$$

We will consider an interesting extension of maps of 1-spheres in a moment, but first we consider what happens when we map 2-spheres (or, for a moment dropping mathematical pretense—spheres) into $\mathcal{M}$. Now, there is no way for a sphere drawn in our space to become

trapped by the excluded axis, as just with the points, we can always just move the sphere around it. Because the excluded axis is infinite, we cannot draw a sphere which entirely encloses it and thereby becomes "trapped" as we saw with the closed paths. The second homotopy group is then also trivial,

$$\pi_2(\mathcal{M}) = I\,. \tag{1.10}$$

Here our investigation of homotopy groups obviously ends, for we can only embed an n-sphere in a space with dimension greater than n; that is, for a space with dimension n, $\pi_k(\mathcal{M}) = I$ for $k \geq n$.

Now we return to maps of 1-spheres into $\mathcal{M}$. The expression given in Eq. (1.8) winds once around the point (a, b), but we do not need to limit ourselves by the number (or direction!) of windings in our map. We introduce an integer m and write

$$\left(x^2, x^3\right) = (a + \cos(m\gamma),\, b + \sin(m\gamma))\,. \tag{1.11}$$

Any closed path which is drawn in $\mathcal{M}$ can be smoothly deformed to this form. Paths which are trapped on the excluded axis are now further divided into homotopy classes by m, which we will call a winding number. After all, there is no way to take a path which winds once around the axis to one which winds twice around, nor to take a path which winds clockwise to one which winds counterclockwise.

We are not quite done. The excluded axis makes it impossible for trapped paths with different m to be homotopic, but not so for the paths which were not trapped. Consider a circle which does not contain the excluded axis and winds in one direction. A simple rotation by π around an axis in a parallel plane transforms it into a circle which winds in the opposite direction. Twisting and deforming a circle which is wound once produces a circle which is wound twice. Lastly and most importantly, the paths which are not trapped have an additional freedom: we can shrink them down to a point. This says that any non-trapped circle is homotopic to the case of $m = 0$ (which maps to a point (a, b)), or that they are *null-homotopic*. Our homotopy classes are now the one class of *shrinkable* loops, those with $a^2 + b^2 > 1$, as well as all of the classes of *unshrinkable* loops, those with $a^2 + b^2 < 1$ who are further divided by their winding number.

This distinction between shrinkable and unshrinkable loops lets us find all spaces which could contain cosmic strings. If we claim that unshrinkable loops signal the presence of cosmic strings, then we are interested in spaces which have nontrivial first homotopy groups.

That is, we say a space $\mathcal{M}$ contains strings if $\pi_1(\mathcal{M}) \neq I$; equivalently, if $\mathcal{M}$ is not simply connected. The space which we are so interested in is the *vacuum manifold* of a theory, or (roughly speaking) the space of all possible configurations of the ground state of the theory.

As a simple example, consider the Goldstone model we discussed in Sec. 1.1.1. The group of transformations G under which the Lagrangian is invariant is $U(1)$, whose elements are all complex numbers of absolute value one. If we now spontaneously break this symmetry, permitting the field to take on some vacuum value, we may ask: what elements of G, when acting upon the vacuum value, leave it invariant? Put another way, what are the transformations in G which leave the vacuum value unchanged? By answering this question, we define the invariant subgroup or little group H of G. In our particular example, only multiplication by 1 leaves some $\phi = \eta e^{i\theta}$ unchanged, and so the little group H has only one element, the identity.

Now that we have stated our symmetry group G, and found the little group H of G, we may find the vacuum manifold by $\mathcal{M} = G/H$. It is this operation which allows us to find all possible configurations of the ground state. Of course, since H contains only the identity, it should not be a surprise to learn that $\mathcal{M} = G$ in this case.

The next question we must answer is: does $U(1)$ contain unshrinkable loops? Consider the unit disk. If we remove any part of its interior, then that object obviously contains unshrinkable loops—any closed path we draw on the disk which encloses the void cannot be contracted to a point. Now consider that the unit circle is the boundary of the unit disk—i.e. the disk with its entire interior removed. Thus, it follows that the unit circle contains unshrinkable loops. Since "the unit circle" is another way of saying "all complex numbers of magnitude one", then we have demonstrated that $U(1)$ contains unshrinkable loops. Thus, $U(1)$ is not simply connected, and so the vacuum manifold admits string solutions—as we have already worked out explicitly!

While the approach outlined above allows us to consider which vacua admit string solutions, it does not permit for complete classification of strings. Strings formed by the same symmetry-breaking process are not required to be dynamically identical [14]. We understand this by considering the following: if the non-trivial $\pi_1(\mathcal{M})$ contains multiple distinct elements, we may construct multiple distinct string configurations possessing different inherent properties. Depending on the model used, we can find for example strings with different masses, or different superconducting properties, generated from the same broken symmetry.

At this point, one might be curious about the π_1 homotopy of $U(1)$, which we know to be

non-trivial. Consider again the unit circle. If we wish to draw a closed path in this space, we have only the freedom to choose if we wind around the circle clockwise or counterclockwise, as well as how many times we wind around. Keeping in mind that winding around zero times is a valid choice, and choosing counterclockwise to be a "negative" winding where clockwise is a "positive" winding, we categorize all possible windings by $\ldots -2,\ -1,\ 0,\ 1,\ 2 \ldots$ and so find that by classifying the ways to draw distinct loops in $U(1)$, we have found the integers. Indeed, it is well-established [15] that

$$\pi_1\left(U(1)\right) \cong \mathbb{Z}\,. \tag{1.12}$$

Or, the set of ways to draw a closed loop in $U(1)$ is in one-to-one correspondence with the integers.[4]

1.2 Basic properties of cosmic strings

We now expand upon our description of a cosmic string. Cosmic strings possess a mass per unit length μ, most often given in units of g/cm or GeV^2, and a thickness δ, with common units of cm or GeV^{-1}. The mass per unit length is often found in the company of Newton's constant, G, and so the parameter most often of interest to us in the case of gravitational backreaction will be $G\mu$. This tells us the strength of the string's coupling to gravity. In units where $\hbar = c = 1$, $G\mu$ is dimensionless.

For the Goldstone model previously discussed, we find the string thickness from the general potential of Eq. (1.2). Consider that we may write small perturbations about the minimum of this potential as

$$\phi = \eta + \frac{1}{\sqrt{2}}\left(\phi_1 + i\phi_2\right)\,. \tag{1.13}$$

Thus, ϕ_1 represents radial perturbations, and ϕ_2 angular perturbations. Inserting this into the potential and keeping only terms of second order in the fields, we find that only a term like $\lambda\eta^2\phi_1^2/2$ remains. This gives a mass of $m_1 = \sqrt{\lambda}\eta$ to the ϕ_1 field.[5] This in turn lets us find the thickness of a string as the Compton wavelength of this massive field,

$$\delta \sim \frac{1}{\sqrt{\lambda}\eta}\,. \tag{1.14}$$

[4]Note that the space we studied before, $\mathbb{R}^3\backslash\{x^1\}$, has the same first homotopy group as $U(1)$. The shrinkable loops contribute $m = 0$, while the unshrinkable loops contribute all nonzero integers.

[5]For a globally-broken symmetry, ϕ_2 is massless. If we had considered a complex field with the same potential, but now considered a local symmetry breaking, we would have to use the abelian-Higgs model. The potential remains the same, and so does m_1, but the vector field A_μ associated with the covariant derivative $\mathcal{D}_\mu$ acquires a mass term. We say that the massless ϕ_2 is absorbed into A_μ.

This relationship of $\delta \propto 1/\eta$ is a generic property of cosmic strings, with the exact relationship of course depending upon the model chosen. This typically guarantees that string cores are very thin. If we consider a string formed an energy at just below the GUT scale, $\eta \sim 10^{15}\,\mathrm{GeV}$, we would find $\delta \sim 10^{-15}\,\mathrm{GeV}^{-1} \approx 10^{-29}\,\mathrm{cm}$; or, such a string core is just four orders of magnitude larger than the Planck length.

Next, the mass per unit length is just the energy density of the static string multiplied by the area of the string,

$$\mu \sim V(0)\delta^2 = \left(\lambda\eta^4\right)\left(\frac{1}{\sqrt{\lambda}\eta}\right)^2 = \eta^2\,. \tag{1.15}$$

This relationship $\mu \propto \eta^2$ is likewise a general one. For a choice of $\eta \sim 10^{15}\,\mathrm{GeV}$, this leads to $\mu \sim 10^{30}\,\mathrm{GeV}^2 \approx 10^{20}\,\mathrm{g/cm}$. Cosmic strings have the potential to be quite massive indeed, opening up a number of promising detection schemes and making them potentially significant objects in the evolution of our universe.

In general, we see that as the energy scale of symmetry breaking increases, strings become thinner yet heavier. Equations (1.14) and (1.15) justify our claims made at the start of this chapter that cosmic strings can have a large mass per unit length and a small, though finite, thickness. It is safe to treat them as being one-dimensional in the regime that the radius of curvature of the string is much greater than δ.

Of course, when we say a string is one-dimensional, we refer only to its spatial dimensions. It moves along timelike paths, just as any other massive object. Where a pointlike object traces a worldline in spacetime, a string sweeps out a worldsheet. Where a pointlike object's trajectory may be described by a single parameter, the proper time τ, the string's trajectory requires two parameters. We most often choose τ and σ, a timelike and spacelike parameter respectively, although a common alternate choice are the null parameters $u = \tau + \sigma$ and $v = \tau - \sigma$. We will now show that cosmic strings are generically in motion, making a thorough understanding of their dynamics a topic of considerable interest.

With the general position of a cosmic string given by $x^\mu(\tau, \sigma)$, we can find the equations of motion of a cosmic string by varying the Nambu action, one of whose forms is

$$\mathcal{S} = -\mu \int d\tau d\sigma \sqrt{\left(\frac{\partial x}{\partial \tau}\right)^2 - \left(\frac{\partial x}{\partial \sigma}\right)^2}\,. \tag{1.16}$$

If we work in flat spacetime and pick a gauge wherein the induced metric g_{ab} has elements $g_{\tau\tau} + g_{\sigma\sigma} = 1$, $g_{\tau\sigma} = g_{\sigma\tau} = 0$ (called the conformal gauge), then the string's equations of

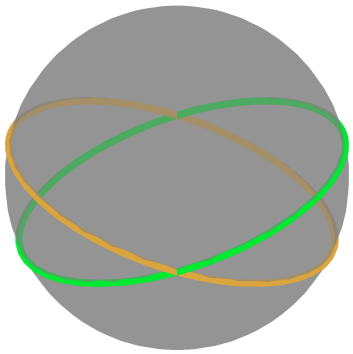

Figure 1.4: The Kibble-Turok sphere for A' and B' both singly-wound circles with angle $\pi/5$ between their normal vectors. Note that in this particular example, the null vectors intersect twice, at antipodal points.

motion are just the two-dimensional wave equation,

$$\frac{\partial^2 x^\mu}{\partial \tau^2} = \frac{\partial^2 x^\mu}{\partial \sigma^2} \,. \tag{1.17}$$

The general solution to this equation is expressed in terms of two independent functions,

$$x^\mu = \frac{A^\mu(\tau - \sigma) + B^\mu(\tau + \sigma)}{2} = \frac{A^\mu(v) + B^\mu(u)}{2} \,. \tag{1.18}$$

There is a final residual gauge freedom, to do with reparameterizations of τ and σ, that we may remove by fixing $\tau = t$. Our gauge conditions now give us $|\vec{A}'| = |\vec{B}'| = 1$. This leads to a convenient visualization of a string's tangent vectors, the Kibble-Turok sphere [16], which is a unit sphere with the spatial tangent vectors inscribed thereon. In a simple example, if $\vec{A}$ and $\vec{B}$ are both singly-wound circles with some arbitrary angle between their normal vectors, then $\vec{A}'$ and $\vec{B}'$ are both singly-wound unit circles, and the Kibble-Turok sphere has two great circles on it (with the same arbitrary angle between their normal vectors), as shown in Fig. 1.4. We shall return to the Kibble-Turok sphere in Chapter 3, where it will be useful to us in analyses of cosmic string behavior.

Fixing $\tau = t$ has also set the equations of motion to be only the spatial parts of the wave equation,

$$\frac{\partial^2 \vec{x}}{\partial t^2} = \frac{\partial^2 \vec{x}}{\partial \sigma^2} \,. \tag{1.19}$$

Because σ points along the string and t points perpendicular to the string, we see that a string's acceleration is proportional to its curvature. We expect curved segments of string to straighten, acquiring some velocity in the process. Straight segments of strings have no

acceleration, and so they are constrained to be either static or to move rigidly in some direction perpendicular to their extent.

Curved strings are generically in motion, and at least to the level of treatment we have so far given them possess no way to slow themselves to a static configuration. If we consider a length of string composed of straight segments—a string whose tangent vectors are piecewise constant—then have we found a static string configuration? We have not, for reasons we will now discuss, but we have discovered an object of string structure which is of considerable interest, particularly to this work.

At the points where distinct straight segments join, which is called a *kink*, one of $\vec{A}'$ or $\vec{B}'$ is discontinuous, and the other continuous (this of course implies that both $\dot{\vec{x}}$ and $\vec{x}'$ are discontinuous, as one would guess). Consider a kink for which $\vec{A}'$ is discontinuous—that is, at some fixed $t-\sigma$, there exists a kink. As t changes, so too must σ, and so the location of the kink on the string changes with time. Note that if we had considered a kink caused by a discontinuity in B', its location is given by fixed $t+\sigma$, and so kinks due to discontinuities in A' and B' move in opposite directions on a string. Thus, any string with kinks cannot remain static.

A property of kinks which will be important later is that they are constrained to move at the speed of light. In the case of a kink due to a discontinuity in A', if we have fixed v, then the kink must evolve in the u direction. The velocity vector of the kink must point in the direction of B', which is null, and so the kink moves along a lightlike path.

We have now proven our third claim made at the start of this chapter: that strings are generally dynamic.[6] More importantly, we have now described a kink, an object of considerable importance to string dynamics and evolution. We will consider the dynamics of loops with kinks in further detail in Chapter 3.

Another important object for cosmic strings arises when $\vec{A}' = \vec{B}'$; that is, where the tangent vectors intersect on the Kibble-Turok sphere. We call this point a *cusp*. Considering our example Kibble-Turok sphere of Fig. 1.4, there must be two points of overlap, and thus two cusps. Unlike kinks, cusps are transient. This is obvious if we consider that the overlap of the tangent vectors requires $t+\sigma = const_1$ and $t-\sigma = const_2$, which has only one solution for t and σ. So each cusp appears once per oscillation at a specific time and at a specific place on the string.

[6]There does exist a static straight string configuration, achieved by taking $\dot{\vec{x}} = 0$ and $|\vec{x}'| = 1$ everywhere and letting it be infinitely long. We will use such a configuration in Chapter 5 when looking at how charges on a string self-interact.

A closer look at Eq. (1.18) suggests that an equivalent way of defining a cusp is that it is where $|\vec{x}'| = 0$. The conformal gauge conditions mean that $\dot{\vec{x}} = 1$, and so we have a point on the string which momentarily doubles back on itself and formally moves at the speed of light.

Our first definition of a cusp leads us to see that kinks inhibit cusps. If neither worldsheet function has discontinuities and the loop is to be periodic, i.e. $A(0) = A(L)$, then we must have that

$$\int_0^L A' dv = 0 \tag{1.20}$$

and likewise for integrating B' with respect to u. Said more loosely, the "center of mass" of the null vectors (in the rest frame of the loop) on the Kibble-Turok sphere must be the origin. Smooth loops are therefore very likely to have crossings, and thus cusps. For kinky strings, the discontinuities in A' and B' allow them to jump from one location to another on the Kibble-Turok sphere, avoiding intersections and therefore avoiding cusps.

Of course, the equations of motion we have been using are not valid in curved spacetimes, and ignore gravitational backreaction entirely. However, they will be a useful starting point for our analysis conducted in Chapter 3. For now, we will move on to address other big-picture aspects of cosmic strings.

1.3 Outstanding questions

Having established why we are interested in cosmic strings, and having given some understanding of how they come to be, we are prepared to consider what questions are most pressing to the cosmic string researcher. Foremost is the question of detection. At this time, cosmic strings have not been detected by any experiment. Pulsar timing arrays [12], CMB analysis [17], lensing surveys [18], and gravitational wave observations [19, 20] have all reported null results, by which we have set an upper bound of $G\mu \lesssim 10^{-8}$ on cosmic string tensions.

This upper bound is set not only by non-observations, but also by the limited sensitivity of detection methods. With the next generation of gravitational wave detectors, we will be able to achieve sensitivities to signals from much lighter strings [13]. However, it is not enough to merely obtain a more powerful trap, so to speak; one should also be more familiar with the nature of one's prey. We are interested then in knowing more about how cosmic

strings form and evolve, as well as the number, frequency, and types of observable signals we expect from them.

The question of how cosmic strings form has been laid out, in its barest bones, in the preceding sections. But as forewarned at the end of Sec. 1.1.2, there are many ways to make a string. Compounded with the large number of generators available in popular particle physics models (e.g. $Spin(10)$, with minimally 45 generators), the string family is large enough that we are still adding species to the cosmic string zoo [21] some four decades after they were first proposed.

Solving for how cosmic string networks evolve is only tractable when done computationally. While recent advances in computing power have greatly improved our capabilities in this endeavor, a straightforward back-of-the-envelope calculation reveals certain limits. If we consider that a cosmic string formed at just below the GUT scale ($\eta \approx 10^{15}\,\mathrm{GeV}$) has a thickness of $\delta \approx 10^{-29}\,\mathrm{cm}$, and that a loop of string has some astrophysically large diameter (take $D \approx 10^{22}\,\mathrm{cm}$, the distance from Earth to the center of the Milky Way), then a simulation of perfect fidelity of a single loop would require a "box" of $\approx 10^{153}$ cells. Never mind simulating an entire expanding universe filled with strings. Of course, perfect fidelity to reality is not a necessary condition for a simulation to test and discover important aspects of the theory. Simulations of cosmic string networks are valuable tools for understanding what those networks look like throughout their lives [22, 23].

Important as well to cosmic string evolution is the question of gravitational backreaction and how it modifies the loop's structure. Particularly interesting to us, and a major subject in Chapter 3, are the questions of how kinks are changed by backreaction and how and when cusps form. The interconnected nature of these questions is evident from the following three facts: that cosmic string loops generically form with kinks, but without cusps [22]; that kinks inhibit cusps [24]; and that cusps are expected to be a source of observable signals with much greater detectability than the stochastic background caused by decaying loops [9, 25, 26]. We will discuss later how gravitational backreaction can modify kinks such that a initially kinky, cuspless loop can develop cusps.

By understanding gravitational backreaction on strings, we understand better both the evolution of loops as well as the nature of signals we should expect from loops in networks. Thence comes our motivation for the investigations to follow.

CHAPTER 2

CONVENTIONS AND EQUATIONS FOR BACKREACTION

In advance of the actual work, there are a few general results which we should establish now, that we need not repeat ourselves later. Throughout this work, we will adhere to the following conventions.

- We use the East Coast/general relativist/spacelike/"mostly plusses" metric sign convention, $(-+++)$. A four-vector with negative length is timelike, while one with positive length is spacelike.
- We use natural units, setting $c = \hbar = \epsilon_0 = 1$. In this unit system, Newton's gravitational constant takes the value $G = 1/M_p^2 \approx 10^{-38}\,\mathrm{GeV}^{-2}$ (where M_p is the Planck mass).
- Our MTW sign [27] is $(+++)$.

Sections of this chapter are based upon Ref. [30].

2.1 The method of Green's functions

The essence of any problem of backreaction is to find the answer to the question "given a point in spacetime, how is that point's motion affected by sources in its past?". For our particular cases, we will be concerned with interactions propagating at the speed of light, and so we may specify further to ask about sources which lie on a point's past lightcone.

To find how a function f is influenced by a source g, we must solve the equation

$$\Box f = g\,, \tag{2.1}$$

with $\Box = -\partial^2/\partial t^2 + \nabla^2$. The general solution in four dimensions is given by

$$f(x) = \int d^4x' D_r(x - x') g(x')\,. \tag{2.2}$$

Here, x is the spacetime location of the observation point and x' the spacetime location of the source. The function

$$D_r(x, x') = -\frac{\theta(t - t')\delta\left([x - x']^2\right)}{2\pi}\,, \tag{2.3}$$

known as the *retarded Green's function*, is the solution to

$$\Box D_r(y, y') = \delta(y - y') \tag{2.4}$$

with the additional constraint that we are only interested in things from the past[1]. Thus, the right-hand side of Eq. (2.3) is telling us to include all sources whose x' lies on the past lightcone of the point x. The $\delta\left([x - x']^2\right)$ in the retarded Green's function is enforcing the null connected condition, while the θ function is ensuring that we only select sources in the past.

2.2 The metric perturbation of a piecewise linear string

Our first task is to determine the metric perturbation caused by a piecewise linear cosmic string.

We consider a string with $G\mu \ll 1$. Thus, we can work in linearized gravity, where $g_{\alpha\beta} = \eta_{\alpha\beta} + h_{\alpha\beta}$, $g^{\alpha\beta} = \eta^{\alpha\beta} - h^{\alpha\beta}$, and $|h_{\alpha\beta}| \ll 1$. We consider this string to have always been in existence in flat space. We will turn on gravitational effects at some time and analyze the resulting evolution.

We parameterize the string worldsheet by a temporal parameter τ and a spatial parameter σ. We will always work in the conformal gauge, with the gauge conditions

$$\dot{x} \cdot x' = 0\,, \tag{2.5a}$$

$$\dot{x}^2 + x'^2 = 0\,, \tag{2.5b}$$

where a dot means the derivative with respect to τ and a prime the derivative with respect to σ.

When gravitational effects are turned off, the string is moving in flat space. In that case, we may additionally choose $t = x^0 = \tau$. Then the equations of motion are just the homogeneous wave equation,

$$\ddot{x} = x''\,. \tag{2.6}$$

These have the general solution given by Eq. (1.18), where we will now take B to be a function of $\tau_+ = \tau + \sigma$ and A to be a function of $\tau_- = \tau - \sigma$. We recall that A and B are four-vector functions whose tangent vectors A' and B' are null vectors with unit time component.

[1]The full solution includes as well the advanced Green's function, which has instead $\theta(t' - t)$. As this represents signals coming from the future, we disregard it as being unphysical.

We now consider the case where the functions A and B are made of linear pieces, so A' and B' each take on a succession of constant values. The places where each linear piece joins its successor is a kink. The angles of these kinks could be small, and we could use many pieces to approximate a smooth curve. In the case of a string loop, these angles could be large and represent actual kinks in the shape of the loop, which could result from previous intersections.

By Eq. (1.18), the shape of the string at any fixed time will also be piecewise linear. The region of the world sheet where a particular linear segment of A combines with a particular segment of B in Eq. (1.18) is part of a plane in spacetime, traced out by a piece of straight string moving at a constant velocity. The vectors A' and B', constant over this region, are tangent to that plane.

As we are working in linearized gravity, we may find the metric perturbation in the harmonic gauge due to a given source with stress-energy tensor $T_{\alpha\beta}$ by solving

$$\Box h_{\alpha\beta} = -16G\pi S_{\alpha\beta}\,, \tag{2.7}$$

where $S_{\alpha\beta} = T_{\alpha\beta} - (1/2)g_{\alpha\beta}T^{\gamma}_{\gamma}$ is the trace-reversed stress energy tensor of the source, given by [4, 28]

$$S^{\alpha\beta}(x) = \mu \int d\tau d\sigma\, \sigma^{\alpha\beta}\delta^{(4)}\left(x - x(\tau,\sigma)\right) = \frac{\mu}{2}\int d\tau_- d\tau_+\, \sigma^{\alpha\beta}\delta^{(4)}\left(x - x(\tau_-,\tau_+)\right)\,, \tag{2.8}$$

with

$$\sigma^{\alpha\beta} = \dot{x}^{\alpha}\dot{x}^{\beta} - x'^{\alpha}x'^{\beta} - \frac{1}{2}\eta^{\alpha\beta}\left[x'^2 - \dot{x}^2\right] = \frac{1}{2}\left[A'^{\alpha}B'^{\beta} + A'^{\beta}B'^{\alpha} - \eta^{\alpha\beta}(A'\cdot B')\right]\,. \tag{2.9}$$

Considering that the edges of regions of constant null vectors are, in the absence of external forces, traced out by null lines, it may be more convenient to reparameterize the worldsheet in terms of local null parameters. We choose parameters u and v, which are defined separately for each region by

$$u = \tau_+ - \tau_+^{(0)}\,, \tag{2.10a}$$

$$v = \tau_- - \tau_-^{(0)}\,, \tag{2.10b}$$

where $\tau_\pm^{(0)}$ set the zero of each pair of local null parameters. Each region of the worldsheet is now given by

$$x(u,v) = \frac{1}{2}\left[vA' + uB'\right]\,, \tag{2.11}$$

where A' and B' are the unit null tangent vectors to that region.

We solve Eq. (2.7) using Green's functions,

$$h_{\alpha\beta}(x) = -16G\pi \sum \int d^4x' S_{\alpha\beta}(x') D_r(x, x') \,. \tag{2.12}$$

The sum is over all contributing source regions. In this particular case of the piecewise linear string, we know that the retarded Green's function's null-connected constraint is that

$$x - x' = \Omega - [vA' + uB']/2 \tag{2.13}$$

has zero length, where Ω is the vector which connects the local origin $(u, v) = (0, 0)$ to the observation point. Using Eq. (2.8), the metric perturbation for a single region is thus

$$h_{\alpha\beta}(x) = 4G\mu \int d^4x' \, \delta\left([x - x']^2\right) \int du dv \, \sigma_{\alpha\beta} \delta^{(4)}\left(x' - x(u, v)\right) \,. \tag{2.14}$$

Because the segments move at a constant rate, $\sigma_{\alpha\beta}$ is constant for each region and can be taken outside the integral. We integrate over x', consuming the four-dimensional Dirac delta term, and find

$$h_{\alpha\beta}(x) = 4G\mu\sigma_{\alpha\beta} \int du dv \, \delta\left([x - x'(u, v)]^2\right) \,. \tag{2.15}$$

The squared distance from the source to the observation point is

$$[x - x']^2 = \frac{A' \cdot B'}{2} uv + \Omega^2 - (A' \cdot \Omega)v - (B' \cdot \Omega)u \,. \tag{2.16}$$

Setting $[x - x']^2 = 0$ gives a hyperbola in u and v. This hyperbola has two branches, and we are interested in the one corresponding to the past lightcone. As this corresponds to the intersection of the past lightcone with the string worldsheet, we will refer to it as the *intersection hyperbola*. Solving $[x - x']^2 = 0$ for u as a function of v gives

$$u(v) = \frac{(A' \cdot \Omega)v - \Omega^2}{(A' \cdot B')v/2 - (B' \cdot \Omega)} \,, \tag{2.17}$$

and for v as a function of u,

$$v(u) = \frac{(B' \cdot \Omega)u - \Omega^2}{(A' \cdot B')u/2 - (A' \cdot \Omega)} \,. \tag{2.18}$$

These expressions will be used later in finding the limits of integration. For now, we will rewrite the δ function via

$$\delta([x - x]^2) = \frac{\delta(v - v(u))}{|\partial([x - x'])^2/\partial v|} \,, \tag{2.19}$$

with

$$\frac{\partial([x - x'])^2}{\partial v} = \frac{A' \cdot B'}{2} u - (A' \cdot \Omega) \tag{2.20}$$

from Eq. (2.16). Integrating Eq. (2.15) over v then yields

$$h_{\alpha\beta} = -\frac{8G\mu\sigma_{\alpha\beta}}{A'\cdot B'}\int_{u_-}^{u_+}\frac{du}{2A'\cdot\Omega/(A'\cdot B')-u} = -\frac{8G\mu\sigma_{\alpha\beta}}{A'\cdot B'}\ln\left[\frac{2A'\cdot\Omega}{A'\cdot B'}-u\right]\Bigg|_{u_+}^{u_-}. \quad (2.21)$$

Equation (2.21) holds also under the exchanges $A' \leftrightarrow B'$, $v \leftrightarrow u$.

We are now equipped to find the first-order effect of gravitational backreaction on the motion of some string segment. If the unperturbed trajectory of the segment is given by Eq. (1.18), the perturbation can be found from the equations of motion [28],

$$x^\lambda_{,uv} = -\Gamma^\lambda_{\alpha\beta}x^\alpha_{,u}x^\beta_{,v} = -\frac{1}{4}\Gamma^\lambda_{\alpha\beta}B'^\alpha A'^\beta\,, \quad (2.22)$$

where the Christoffel symbol, to first order in the metric perturbation, is given by

$$\Gamma^\lambda_{\alpha\beta} = \frac{1}{2}\eta^{\lambda\rho}\left[h_{\beta\rho,\alpha}+h_{\rho\alpha,\beta}-h_{\alpha\beta,\rho}\right]. \quad (2.23)$$

Once we have allowed the string to perturb spacetime, we can no longer set $t=\tau$ (although the definitions made in Eq. (2.10) will hold always).

Note that the metric perturbation gets its tensor structure from the $\sigma_{\alpha\beta}$ of the source region. But from Eq. (2.9) we can see that any contraction of $\sigma_{\alpha\beta}$ with A' or B' will vanish. Thus if we consider the effect of the source region on itself (or any other region with identical null vectors), all terms in Eq. (2.23) vanish in Eq. (2.22) and there is no effect.

2.3 Specializing to finite regions

We have so far kept our equations agnostic as to the nature of the string beyond its piecewise linearity and $G\mu \ll 1$. In particular, we have placed no constraints on the size of the regions, and so the above may apply to finite or infinite strings. (Even more generally, while we assumed the boundaries between regions to be due to kinks—i.e. unperturbed piecewise linear strings—there is nowhere anything enforcing this; in Chapter 4, we will apply this formalism to a perturbed infinite string.) However, string loops, all of whose regions are parallelograms of finite size, are of particular interest to us. It behooves us to further specialize our equations to this case.

The first observation we make is that every unique region of the worldsheet is due to some unique combination of a segment of A and a segment of B. The line where this segment of A joins its successor is given by fixed τ_- and thus fixed A, while τ_+ varies, so that the line points in the null direction B'. There is a parallel line where this segment of A joins its predecessor. The two lines where B joins its adjacent segments point in the direction of

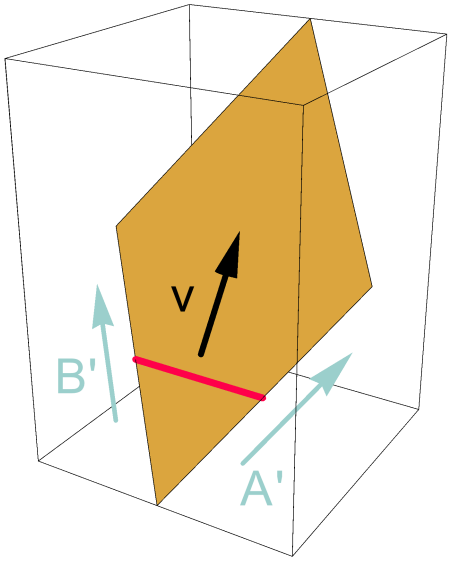

Figure 2.1: An element of a piecewise linear string, which we call a diamond. The red line on the diamond is a segment of the string at a fixed time. This segment moves in the direction indicated by v, and in so doing sweeps out the diamond. The blue arrows indicate A' and B', which are null, unit length, tangent to the worldsheet, and each parallel to two of the diamond's edges. The diamond shown is a special case where all four edges have the same spatial length. This is true of all diamonds in the Garfinkle-Vachaspati loop we will discuss in Sec. 3.2.

A'. These four lines bound a region of the worldsheet as shown in Fig. 2.1. In general the region has the shape of a parallelogram, but we shall refer it as being a *diamond*, which is the case for the rectangular loop we will discuss in Sec. 3.2.

Next, we consider the definitions of the local null parameters on a piecewise linear loop. We wish to set the point $u = v = 0$ to be the center of the diamond, and so take $\tau_{\pm}^{(0)}$ as the values of $\tau_{\pm}$ at that center. By this definition, the range of u is $[-L_B, L_B]$, with L_B the length of the edge of the diamond spanned by B. The range of v is defined similarly for L_A. The edges of the worldsheet may be traced out by holding either $u = \pm L_B$ or $v = \pm L_A$ fixed and allowing the other null parameter to vary over its full range.

Finally, we note that Ω is defined as being the four-vector which points from the diamond center to the point of observation.

We now turn to Eq. (2.21). The limits of integration, $u_{\pm}$, are chosen depending on how the intersection hyperbola crosses the diamond. Because the hyperbola must lie on the null past lightcone, it may never be a timelike path, and is only null in the special case where the tip of the lightcone is on the diamond. As such, it may never connect worldsheet edges

which are timelike separated, meaning that there are only four kinds of hyperbola which we will need to consider: those connecting two edges where $u = \pm L_B$, those connecting two edges where $v = \pm L_A$, those connecting the two future edges ($u = L_B$ and $v = L_A$) and those connecting two past edges ($u = -L_B$ and $v = -L_A$).

For the case of the intersection hyperbola connecting opposite edges of constant u, we choose $u_- = -L_B$ and $u_+ = L_B$ to get

$$h_{\alpha\beta} = -\frac{8G\mu\sigma_{\alpha\beta}}{A'\cdot B'} \ln\left[\frac{-L_B A'\cdot B'/2 - A'\cdot\Omega}{L_B A'\cdot B'/2 - A'\cdot\Omega}\right] . \tag{2.24}$$

The hyperbola which connects opposite edges of constant v has the same solution, but with $A' \leftrightarrow B'$ and $L_B \to L_A$. For the case of the intersection hyperbola connecting the past edges, we choose $u_- = -L_B$ and find u_+ from Eq. (2.17) with $v = -L_A$. We find

$$h_{\alpha\beta} = -\frac{8G\mu\sigma_{\alpha\beta}}{A'\cdot B'} \ln\left[\frac{(L_B A'\cdot B'/2 + A'\cdot\Omega)(L_A A'\cdot B'/2 + B'\cdot\Omega)}{(A'\cdot\Omega)(B'\cdot\Omega) - \Omega^2(A'\cdot B')/2}\right] . \tag{2.25}$$

For the case of the intersection hyperbola connecting the future edges, we choose $u_+ = L_B$ and find u_- from Eq. (2.17) with $v = L_A$ to get

$$h_{\alpha\beta} = -\frac{8G\mu\sigma_{\alpha\beta}}{A'\cdot B'} \ln\left[\frac{(A'\cdot\Omega)(B'\cdot\Omega) - \Omega^2(A'\cdot B')/2}{(L_B A'\cdot B'/2 - A'\cdot\Omega)\,(L_A A'\cdot B'/2 - B'\cdot\Omega)}\right] . \tag{2.26}$$

Thus, by knowing the location of the source diamonds and the manner in which the intersection hyperbola crosses each diamond, we may find the metric perturbation at an arbitrary point.

To find the acceleration felt by a point on a piecewise linear loop, we must find the derivatives of the metric perturbation. These follow easily from Eqs. (2.24-2.26).

We find that for Eq. (2.24) connecting constant-u edges,

$$h_{\alpha\beta,\gamma} = \frac{8G\mu L_B (A'\cdot\Omega)\sigma_{\alpha\beta}A'_\gamma}{(A'\cdot\Omega)^2 - L_B^2(A'\cdot B')^2/4} \tag{2.27}$$

For Eq. (2.25) connecting past edges,

$$\begin{aligned} h_{\alpha\beta,\gamma} = -\frac{8G\mu\sigma_{\alpha\beta}}{A'\cdot B'}\Bigg[&\frac{A'_\gamma}{L_B A'\cdot B'/2 + A'\cdot\Omega} + \frac{B'_\gamma}{L_A A'\cdot B'/2 + B'\cdot\Omega} \\ &- \frac{(A'\cdot\Omega)B'_\gamma + (B'\cdot\Omega)A'_\gamma - (A'\cdot B')\Omega_\gamma}{(A'\cdot\Omega)(B'\cdot\Omega) - \Omega^2(A'\cdot B')/2}\Bigg] . \end{aligned} \tag{2.28}$$

Finally, for Eq. (2.26) connecting future edges,

$$\begin{aligned} h_{\alpha\beta,\gamma} = -\frac{8G\mu\sigma_{\alpha\beta}}{A'\cdot B'}\Bigg[&\frac{A'_\gamma}{L_B A'\cdot B'/2 - A'\cdot\Omega} + \frac{B'_\gamma}{L_A A'\cdot B'/2 - B'\cdot\Omega} \\ &+ \frac{(A'\cdot\Omega)B'_\gamma + (B'\cdot\Omega)A'_\gamma - (A'\cdot B')\Omega_\gamma}{(A'\cdot\Omega)(B'\cdot\Omega) - \Omega^2(A'\cdot B')/2}\Bigg] . \end{aligned} \tag{2.29}$$

We now have a number of very general and very useful formulae. Let's apply them to solve some interesting problems in backreaction on cosmic strings.

CHAPTER 3

GRAVITATIONAL BACKREACTION ON LOOPS

Because cosmic strings are massive objects in motion, they will produce gravitational waves. Similar to the process by which a pair of co-orbiting massive objects lose energy to gravitational wave production and thus spiral in, cosmic string loops will shrink as they oscillate and emit gravitational waves, eventually emitting all of their energy into waves, which is termed evaporation. We know how to calculate the power radiated into gravitational waves by an arbitrary loop [24]. While we thereby know the timescale on which loops evaporate, what is not so well understood is how backreaction changes the structure of the loop. There are two questions, not independent of each other, that we will address in this chapter.

We first ask, How are kinks on loops changed due to backreaction? We know that loops form without cusps, but with kinks [22]. It was previously thought that kinks were "smoothed" by backreaction in the sense that the kink was rounded off. We will demonstrate that this is not the case, and show that kinks instead have their angles modified, while the straight segments which connect them acquire bends. We will continue to call this phenomenon "kink smoothing", but that the kinks remain is an important consequence of our investigation.

We additionally know that kinks inhibit cusps. Our second question, now knowing that kinks persist on loops, is: How likely is it that cusps will form on a loop? Here we do not offer a definitive answer for all loops, instead focusing on the results of an analytical study of a specific class of string loops, the Garfinkle-Vachaspati loops. By comparing rates of kink smoothing and loop dissipation, we show that those loops closest to the maximally symmetric case may never acquire cusps before dissipating. The maximally symmetric loop, which we call (in a slight abuse of geometric terminology) the "square" loop, experiences no kink smoothing and instead shrinks rigidly to nothing. This invites comparison to another known rigidly shrinking loop, commonly called the Allen-Casper-Ottewill (ACO) loop [29], which we will touch on in Sec. 3.5.1.

The work in this chapter is based upon Refs. [30] and [31].

3.1 General arguments about the effect of backreaction

Consider a string loop which is small compared to the Hubble distance, and so can be considered to evolve in flat space. This allows us to employ Eq. (1.18) and note that the usual gauge conditions set $|\vec{A}'| = |\vec{B}'| = 1$. Thus, $\vec{A}'$ and $\vec{B}'$ are paths on the Kibble-Turok sphere of unit vectors [16, 32, 24]. If the string is smooth, these paths will generically (though not always [24]) intersect, producing cusps. The string doubles back on itself at a cusp and moves (formally) at the speed of light. Cusps lead to emission of bursts of gravitational waves, which may be detectable [33, 26, 34, 35].

Simulations show that loops just formed from the long string network essentially never have cusps [22]. Instead they have several large-angle kinks. But most loops which exist at any given time have lost a very significant fraction of their length to gravitational radiation and thus may have very different shapes from those they had at formation. If gravitational backreaction rounds off the kinks, then the paths of $\vec{A}'$ and $\vec{B}'$ will cross, producing cusps. Generally there will be two cusps per oscillation [22].

In certain systems, the effect of gravitational backreaction is easy to understand. Consider, for example, a straight, static string with small wiggles of various wavelengths. In this case one can straightforwardly compute the gravitational power from wiggles of some frequency ω and energy density E interacting with other wiggles going the opposite direction [36, 37]. This power should come from a decrease in the energy of the wiggles in question, and so one arrives at the damping rate of these wiggles, $dE/dt \propto -Ec\omega$, where c is a constant depending on the opposite-direction wiggles (as long as the wiggles going in the two directions have similar wavelengths [37]). After some interval t, E will decrease by $e^{-tc\omega}$.

If this process were linear, one could argue that when there is a superposition of waves of different frequencies, the short waves are damped more rapidly in proportion to their wavelength. Then the fate of any pattern of excitations on the string could be found by Fourier analysis, and we would conclude that effect of backreaction on the position of a string would be to convolve it with a Lorentzian, because the Lorentzian is the function whose Fourier transform declines exponentially with frequency.

Indeed, this was the procedure used in Ref. [22] to produce a toy model of the effects of backreaction. Convolution rounds off kinks, so the result was that cusps were generated, as described above. However, radiation is not a linear process, and this model is qualitatively incorrect, as we will describe below.

Gravitational backreaction on string loops was studied numerically by Quashnock and Spergel [28]. However their simulations were limited by the computer power available at the time, and so the detailed fate of the kinks is not clear. Ref. [28] says that "the kink angles are opened", but the same results have been interpreted by other authors (e.g., Ref. [4]) to show that the kinks are rounded off.

To determine whether rounding off, straightening out, or some other model is correct, we will analyze the general properties of backreaction. We know how to find the metric perturbation given some source distribution (Eq. (2.12)), as well as how to find the change in the motion of the string resulting from that perturbation (Eq. (2.22)). Thus after some time, the function $\vec{A}'(v) = 2\vec{x}_{,v}$ will change by the quantity [28]

$$\Delta A'^{\lambda} = -2 \int du \, \Gamma^{\lambda}_{\alpha\beta} x^{\alpha}_{,u} x^{\beta}_{,v} \,, \tag{3.1}$$

and similarly for $\vec{B}'(u)$.

How does $h_{\alpha\beta}(x)$ depend on the observation point x? Equation (2.12) is an integral over the intersection of the past light cone of x with the world sheet of the string. If the world sheet is smooth, moving x changes this intersection in a smooth fashion, so $h_{\alpha\beta}(x)$ changes smoothly. Kinks in the world sheet are lightlike lines where the world sheet has a slope discontinuity. Generically, the backward light cone from x intersects such lines in isolated points. Moving x moves the intersection points without changing their nature, and thus $h_{\alpha\beta}(x)$ is still smooth.

When the backward light cone crosses the point where two kinks pass through each other, this no longer applies. The two kinks divide the world sheet into four regions. The backward light cone of x intersects three of these, and moving x causes the intersection with one region to gradually decrease to zero and then the intersection with the fourth region to increase from zero. Thus there is a jump in the first derivative of $h_{\alpha\beta}(x)$ at such points. The Christoffel symbol there has a discontinuity but remains bounded.

Now consider the effect of Eq. (2.22) on the string very near a kink. As we approach the kink, $x_{,u}$ and $x_{,v}$ have constant limits and $\Gamma^{\lambda}_{\alpha\beta}$ is bounded. Thus the force which changes the direction of the string approaches a constant as we approach the kink tip, so the original direction is perturbed in a uniform way. The perturbed string near the kink may point in a different direction, but the kink itself remains. Thus kinks are not rounded off. Rounding off would require that after even a small number of oscillations, the string very near the kink would be substantially modified, which would be possible only if the force diverged as

one approached the kink, which is not the case.

As we cross over to the other side of the kink, $\Gamma^{\lambda}_{\alpha\beta}$ has no sudden change, but $x_{,u}$ or $x_{,v}$ changes discontinuously to produce a sharp kink. Thus the force on the other side of the kink may be different. This means that the two sides may be turned in different directions and so the angle of the kink may change.

If the kinks were rounded off, the paths of $\vec{A}'$ and $\vec{B}'$ would become continuous, which would almost always lead to cusps. Opening the kink angle makes cusps more likely, as the curvature introduced by backreaction spreads out the unit vectors on the Kibble-Turok sphere away from their discontinuous jumps, and so their paths may overlap. But it is still possible for $\vec{A}'$ to jump over $\vec{B}'$, or vice versa, so cusps are by no means certain.

One might argue that cusps become inevitable once backreaction completely straightens kinks, but this is not guaranteed to happen. Consider a kink due to a discontinuity in A' with a very shallow angle $\zeta \ll 1$. This kink will change its angle in a way that depends on the difference in force across the kink. There will be a factor $G\mu$ from $h_{\alpha\beta}(x)$, a term like $1/L$ due to the derivatives of $h_{\alpha\beta}(x)$ found in the Christoffel symbol, and a dimensionless prefactor which depends on the contraction of null vectors with the Christoffel symbol. Under the small-angle approximation, the difference in null vectors will be linear in ζ, and so altogether we have

$$\frac{d\zeta}{dt} = -\frac{\Gamma_\zeta G\mu}{L}\zeta\,, \tag{3.2}$$

where Γ_ζ is a constant. The total radiation power of a loop is usually written $\Gamma G\mu^2$, with $\Gamma \sim 50$ depending on the loop shape. As a result, the length of the loop decreases as $L(t) = L_0 - \Gamma G\mu t$. If we put this into Eq. (3.2) and solve the resulting differential equation for initial kink angle ζ_0, we find

$$\zeta(t) = \zeta_0 \left(1 - \frac{\Gamma G\mu t}{L_0}\right)^{\Gamma_\zeta/\Gamma}\,, \tag{3.3}$$

so the kink angle depends on the fraction of the loop remaining raised to some power. When $\Gamma_\zeta \sim \Gamma$, small kink angles are opened at about the same rate as the loop dissipates. If a kink was preventing a cusp, such Γ_ζ will lead to the cusp appearing on average when the loop has half evaporated. Larger Γ_ζ causes cusps to appear sooner, and $\Gamma_\zeta \ll \Gamma$ means that small kinks persist very late in the lifetime of the loop. Because many kinks comprise a generic loop at formation, this persistence has the potential to greatly reduce the frequency of cusps. Unfortunately, we do not know at this point the typical magnitude of Γ_ζ.

We have therefore shown from general arguments two important features of how backreaction affects loops. First, kinks are opened up rather than being smoothed out, and so the appearance of cusps on a loop will be delayed. Second, very small kinks may persist all the way to the end of a loop's life. Both of these results serve to change the distribution of loops with cusps, and therefore the signals we expect from loops.

3.2 Rectangular loops

Having given the general argument for how backreaction affects kinks on a loop, we ought to supply an example. We shall do this by specializing to the rectangular loop of Garfinkle and Vachaspati [24], which is simple enough that the entire problem can be solved analytically. In doing so, we will rely heavily upon Chapter 2, and in particular the equations found in Sec. 2.3.

3.2.1 Geometry

In the rectangular loop, $A'(\tau_-)$ has some constant value $A'(0)$ for $\tau_- \in \{0, L/2\}$ and the constant value $-A'(0)$ for $\tau_- \in \{L/2, L\}$, and $B'(\tau_+)$ behaves similarly, with some angle 2ϕ between $A'(0)$ and $B'(0)$. By the symmetries of the loop, $\tau_\pm$ should be taken to be modulo L.

We will choose coordinates so that $\vec{A}'(0) + \vec{B}'(0)$ points in the x direction and $B'^0(0) - A'^0(0)$ points in the y direction. The loop then oscillates through all configurations of a rectangle which may be inscribed within a rhombus of angle 2ϕ, as shown in Fig. 3.1. Without loss of generality we can choose $0 < \phi \leq \pi/4$. The x axis will always be the longer of the rhombus's two diagonals, while the y axis will always be the shorter.

We let $w = \cos\phi$ and $h = \sin\phi$. We then have

$$A'^\gamma = (1, \pm w, \mp h, 0)\,, \tag{3.4a}$$

$$B'^\gamma = (1, \pm w, \pm h, 0)\,. \tag{3.4b}$$

One oscillation of the loop is the time it takes for the loop to go through all configurations shown in Fig. 3.1, for example from the double line on the x axis to the double line on the y axis and back again. As this loop lies entirely in a plane, it is guaranteed to self-intersect, and therefore annihilate, in this case when it reaches the double-line configurations. But we will take the loop to be infinitesimally thin and not to interact with itself, except in one

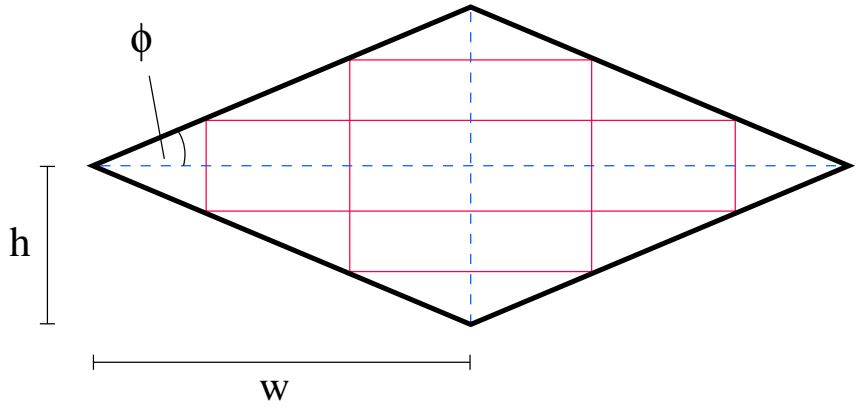

Figure 3.1: The rectangular loop oscillates through all spatial rectangles which may be inscribed within a rhombus whose diagonals (dashed blue) measure $2w$ and $2h$ on the long and short directions respectively. The acute angle of this rhombus is 2ϕ, and so $\tan\phi = h/w$. The solid red rectangles are examples of configurations the loop takes on during its oscillation. The dashed blue lines are additionally degenerate rectangles, also called the double lines, which form when two kinks lie on top of one another.

case below where to avoid a divergence we will need to say that the two parts of the loop pass by each other by some infinitesimal distance.

We will choose $L = 4$. Some particulars of the loop's geometry are that

- $L_A = L_B = 1$, so each diamond is a rhombus.
- The double line on the x axis extends $\pm w$.
- The double line on the y axis extends $\pm h$.
- The speed of a segment moving in the x direction is w, and moving in the y direction is h.
- The period of oscillation is $T = 2$.

Consider a diamond swept out by a string segment moving in the positive x direction in a rectangular loop. We refer to such a diamond as a $+x$ *diamond*. Let the loop be centered on the origin and let the segment pass through the origin at some time t_0, so that the diamond center is $(t_0, 0, 0)$, its futuremost point is at $(t_0 + 1, w, 0)$ and its pastmost point at $(t_0 - 1, -w, 0)$. We will solve for the effect of backreaction on the $+x$ diamond, and we can then recover the effect on other diamonds as follows.

- For the $-x$ diamond, exchange $x \leftrightarrow -x$.

- For the $+y$ diamond, exchange $x \leftrightarrow y$ and $h \leftrightarrow w$.
- For the $-y$ diamond, exchange $x \leftrightarrow -y$ and $h \leftrightarrow w$.

Any of the above may be combined with a redefinition of t_0 to change the diamond's position in time.

For the $+x$ diamond, the null vectors are

$$A'^{\gamma} = (1, w, -h, 0)\,, \tag{3.5a}$$

$$B'^{\gamma} = (1, w, h, 0)\,, \tag{3.5b}$$

and we have

$$\sigma_{\alpha\beta} = \begin{pmatrix} w^2 & -w & 0 & 0 \\ -w & 1 & 0 & 0 \\ 0 & 0 & 0 & 0 \\ 0 & 0 & 0 & h^2 \end{pmatrix}. \tag{3.6}$$

Another object which we will frequently discuss in the context of the rectangular loop is the combination of a diamond and its spatial mirror image, which we call a *butterfly*. A $+x$ and $-x$ diamond with the same t_0 taken together are an x *butterfly*, while $\pm y$ diamonds with common t_0 together make a y *butterfly*. The futuremost edges of an x butterfly meet the pastmost edges of the y butterfly whose t_0 is greater by 1. Similarly, the pastmost edges of an x butterfly meet the futuremost edges of the y butterfly whose t_0 is less by 1. Figure 3.2 illustrates the general appearance of a rectangular loop's worldsheet, and shows how we extract a butterfly from that worldsheet.

3.2.2 Metric perturbations

How does the backward lightcone of some observation point intersect the worldsheet of a rectangular loop? Because the loop and the lightcone are both continuous objects, the total intersection of the lightcone with the worldsheet must be a closed path. Which diamonds does it cross and how does it cross them?

First suppose that the intersection path connects a past and a future edge of some diamond. Suppose, for example, that the path crosses a $+y$ diamond from the edge it shares with the past $+x$ diamond to the edge it shares with the future $+x$ diamond, as shown in Fig. 3.3. This $+y$ diamond intersects a $-y$ diamond along their common centerline. To get from a past edge to a future edge, the intersection path must cross this centerline. (It may

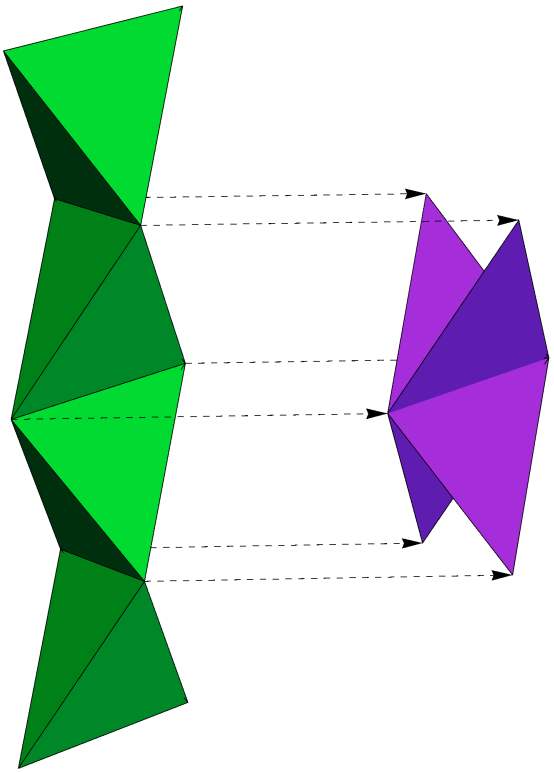

Figure 3.2: On the left is the worldsheet of a loop with $\phi = \pi/6$ over two oscillations, starting from the double-line configuration. Up is forward in time, with the transverse plane being the plane in which the loop is oscillating. By slicing the worldsheet in this transverse plane, we recover all possible configurations of the loop, such as the ones shown (in red and blue) in Fig. 3.1. On the right is an example of a butterfly whose t_0 is at the midpoint of the temporal range of the worldsheet.

only cross once, as it has to get from one side to the other, and no hyperbola can cross a line three times or more.) At the place it crosses, it must also cross part of the intersection path lying on the $-y$ diamond, which thus must also run from the past $+x$ diamond to the future $+x$ diamond. (It cannot enter the past $-x$ diamond, because all interior points on that diamond are in the chronological past of all points on the future $+x$ diamond, and no two points on the intersection path can be timelike separated. The same applies to the future $-x$ diamond.)

Now the two crossings into the future $+x$ diamond must be connected to each other via a hyperbola, and so must the two crossings into the past $+x$ diamond. Thus we have a closed loop made up of four diamonds, two y diamonds of the same butterfly and the $+x$ diamonds in its past and future. We call this a *figure-eight* intersection.

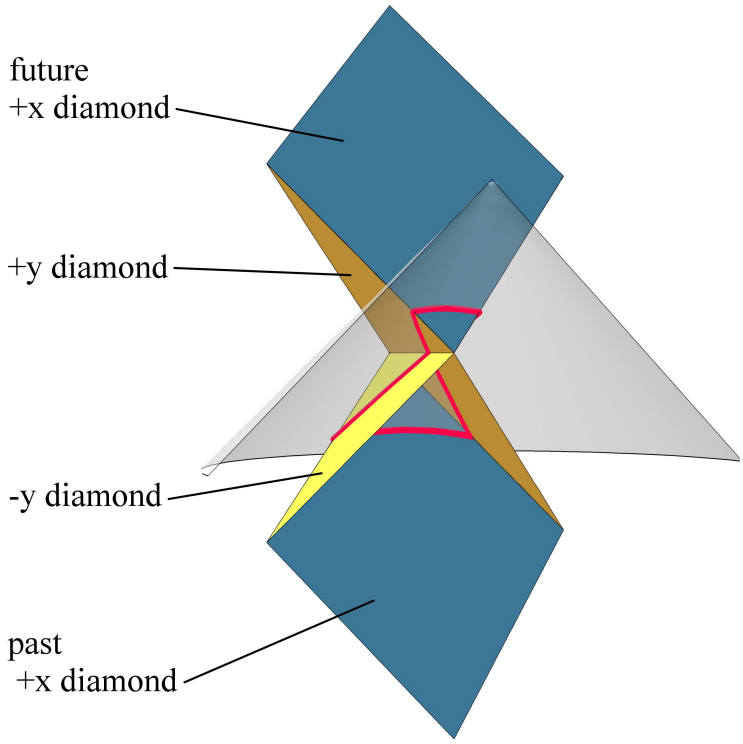

Figure 3.3: The thick red line shows the intersection of the lightcone with the loop worldsheet for a figure-eight intersection. The intersection line passes through two parallel diamonds plus the butterfly in between them for a total of four unique diamonds. We have indicated the diamonds crossed as described in the text.

The only other possibility is that the intersection path never connects a past and a future edge of the same diamond, but only crosses from past to past and from future to future. Suppose the path connects two past edges of a $+x$ diamond. At these two places it comes in across the future edges of the $-y$ and $+y$ diamonds. It must leave these diamonds across their other future edges, which connect to the same $-x$ diamond. We thus have a closed loop crossing both diamonds of an x butterfly and both diamonds of the prior y butterfly, as shown in Fig. 3.4. We call this a *ring* intersection, although it's possible that the parts of the ring lying on the x butterfly may cross each other at the double line and then cross back again.

We will now calculate the metric perturbation at an observation point (t, x, y, z) whose backward light cone yields either the specific kind of figure-eight intersection or the specific kind of ring intersection described above. Once we find those effects, we may recover the perturbation for any intersection through the appropriate transpositions and substitutions.

We will eventually take the observation point to the worldsheet of a $+x$ diamond to

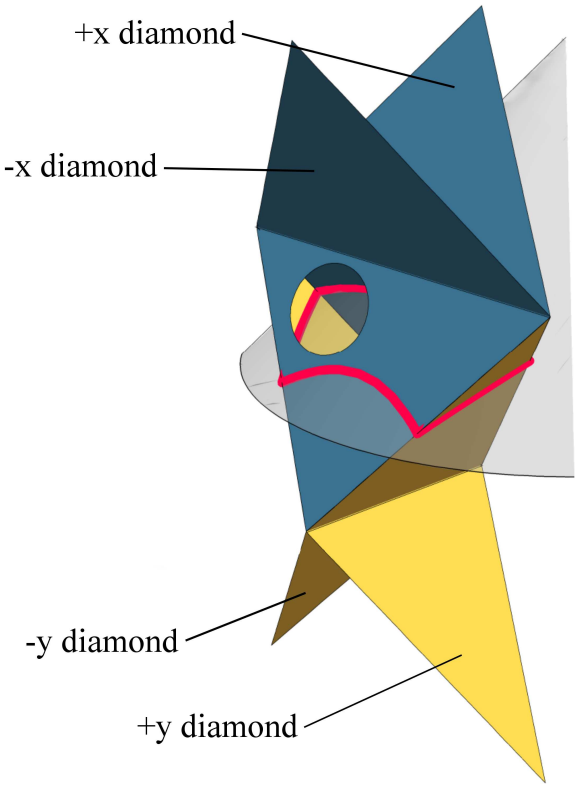

Figure 3.4: The thick red line shows the intersection of the lightcone with the loop worldsheet for a ring intersection. The intersection line passes through two subsequent butterflies for a total of four unique diamonds. We have indicated the diamonds crossed as described in the text.

study how backreaction affects that diamond. When constrained to that worldsheet, the observation point will only ever see figure-eight and ring intersections of the specific sort we have described above, where the same y butterfly is involved in both. There are only five diamonds total that we need to consider when finding the effect of backreaction on such a point: an x butterfly containing the observation point, the y butterfly below the x butterfly, and the $+x$ diamond below the y butterfly. We will call the components of the x butterfly simply the $+x$ diamond (though it is the same one we called the "future $+x$ diamond" earlier) and the $-x$ diamond, while the $+x$ diamond below the y butterfly we will call the past $+x$ diamond. Putting Figs. 3.3 and 3.4 together and color-coding them for later convenience produces Fig. 3.5.

We first consider the perturbations associated with the figure-eight intersection. We assume the center of the x butterfly is at $t = 0$. Using Eqs. (2.25,3.5), we find

$$h_{\alpha\beta}^{(+x)} = \frac{4G\mu}{h^2}\sigma_{\alpha\beta}^{(+x)} \ln\left[\frac{(h^2 + t - xw)^2 - y^2h^2}{(x - tw)^2 + h^2z^2}\right] . \tag{3.7}$$

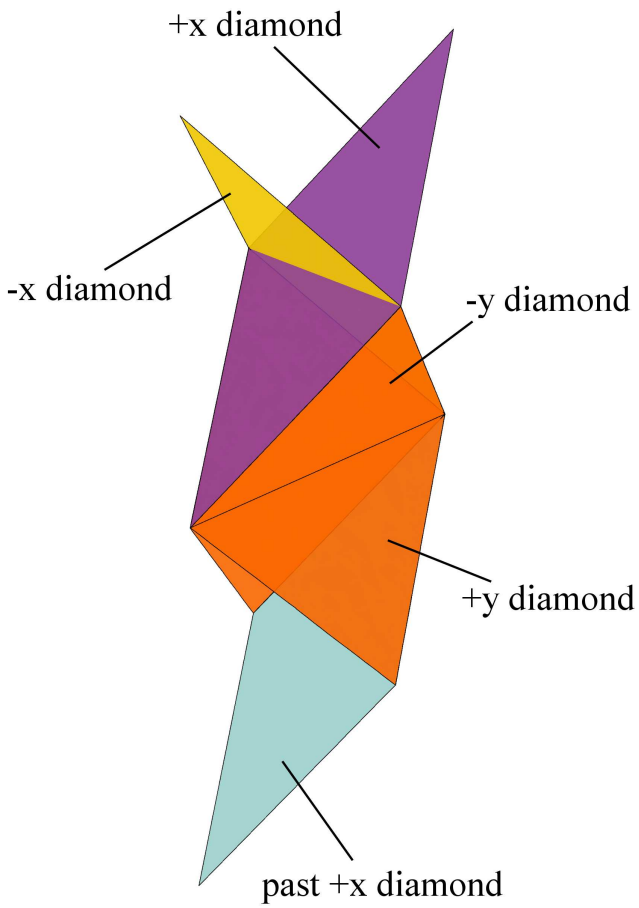

Figure 3.5: The worldsheet of a rectangular loop obtained by combining Figs. 3.3 and 3.4.

The y diamonds, whose centers are at $t = -1$, have perturbations given by Eq. (2.24) and its $A' \leftrightarrow B'$ version.

$$h_{\alpha\beta}^{(+y)} = \frac{4G\mu}{w^2}\sigma_{\alpha\beta}^{(+y)} \ln\left[\frac{1+t-xw-yh+w^2}{1+t-xw-yh-w^2}\right], \tag{3.8a}$$

$$h_{\alpha\beta}^{(-y)} = \frac{4G\mu}{w^2}\sigma_{\alpha\beta}^{(-y)} \ln\left[\frac{1+t-xw+yh+w^2}{1+t-xw+yh-w^2}\right]. \tag{3.8b}$$

For the past $+x$ diamond, which has its center at $t = -2$, equations (2.26,3.5) give

$$h_{\alpha\beta}^{(past\ +x)} = \frac{4G\mu}{h^2}\sigma_{\alpha\beta}^{(+x)} \ln\left[\frac{(x-tw-2w)^2+h^2z^2}{(h^2-t-2+xw)^2-y^2h^2}\right], \tag{3.9}$$

For the ring intersection, we see that the y butterfly is the same as the one involved in the figure-eight intersection. However, the nature of the crossings has changed; we must

now use Eq. (2.26), and find

$$h^{(+y)}_{\alpha\beta} = \frac{4G\mu}{w^2}\sigma^{(+y)}_{\alpha\beta} \ln\left[\frac{(y-th-h)^2+w^2z^2}{(w^2-t-1+yh)^2-x^2w^2}\right], \tag{3.10a}$$

$$h^{(-y)}_{\alpha\beta} = \frac{4G\mu}{w^2}\sigma^{(-y)}_{\alpha\beta} \ln\left[\frac{(y+th+h)^2+w^2z^2}{(w^2-t-1-yh)^2-x^2w^2}\right]. \tag{3.10b}$$

The futuremost $+x$ diamond from the figure-eight intersection is also involved in this ring intersection, and has the same form. The pastmost $+x$ diamond is not involved in the ring intersection, and we must instead consider the perturbation due to a $-x$ diamond whose center is at $t = 0$. Using Eq. (2.25),

$$h^{(-x)}_{\alpha\beta} = \frac{4G\mu}{h^2}\sigma^{(-x)}_{\alpha\beta} \ln\left[\frac{(h^2+t+xw)^2-y^2h^2}{(x+tw)^2+h^2z^2}\right]. \tag{3.11}$$

3.3 The modified worldsheet

3.3.1 Acceleration

We are now equipped to find the four-acceleration felt at an arbitrary point due to the loop worldsheet. All accelerations we find from Eq. (2.22). As we will eventually take the observation point to lie on the worldsheet of a $+x$ diamond, we take it now to be on a string moving transversely at speed w in the $+x$ direction. As such, its null vectors are identical to that of the $+x$ diamond.

The acceleration of the string is found by contracting the metric derivatives of Eq. (2.27-2.29) with A' and B', according to Eq. (2.22). This means that at least one of A' and B' must be contracted with $\sigma_{\alpha\beta}$. For the $+x$ and past $+x$ diamonds, this contraction vanishes, as discussed earlier.

The $-y$ diamond has the same A' as the observation string. Thus its $\sigma_{\alpha\beta}$ can only be contracted with B', which leaves A' to contract with the direction of differentiation. For a figure-eight intersection, the metric derivative is given by Eq. (2.27), which vanishes on contraction with A'^{γ}. The $+y$ diamond is symmetrical and its contribution likewise vanishes, leaving no backreaction effect at all for a figure-eight intersection.

When we consider a ring intersection, the effect of the $-y$ diamond is instead given by Eq. (2.29). Contracting with A'^{γ} leaves only the middle term,

$$h_{\alpha\beta,\gamma}A'^{\gamma} = -\frac{8G\mu\sigma_{\alpha\beta}}{L_A A'\cdot B'/2 - B'\cdot\Omega} = -\frac{8G\mu\sigma_{\alpha\beta}}{h^2+t+wx+hy}. \tag{3.12}$$

For the $+y$ diamond, the only non-vanishing contraction is

$$h_{\alpha\beta,\gamma}B'^{\gamma} = -\frac{8G\mu\sigma_{\alpha\beta}}{L_B A'\cdot B'/2 - A'\cdot\Omega} = -\frac{8G\mu\sigma_{\alpha\beta}}{h^2+t+wx-hy}. \tag{3.13}$$

For the $-x$ diamond, there is no such simplification. Equation (2.28) becomes

$$h_{\alpha\beta,\gamma} = \frac{4G\mu\sigma_{\alpha\beta}}{h^2}\left[\frac{(1,w,-h,0)}{h^2+t+wx-hy}+\frac{(1,w,h,0)}{h^2+t+wx+hy} -2\frac{\big(w^2t+wx,wt+x,0,h^2z\big)}{(wt+x)^2+h^2z^2}\right]. \tag{3.14}$$

Combining Eqs. (3.12-3.14) with Eqs. (2.22,2.23), using $\sigma^{(-x)}_{\alpha\beta}A'^{(+x)\beta} = \sigma^{(-x)}_{\alpha\beta}B'^{(+x)\beta} = (2w^2, 2w, 0, 0)$ and $\sigma^{(-x)}_{\alpha\beta}A'^{(+x)\alpha}B'^{(+x)\beta} = 4w^2$, and taking $z = 0$, we find the components of the acceleration for a point which sees the ring intersection,

$$x^0_{,uv} = \frac{2G\mu w^2}{h^2}\left[-\frac{2w}{x+tw}+\frac{1-h^2/w^2}{h^2+t+xw+yh}+\frac{1-h^2/w^2}{h^2+t+xw-yh}\right], \tag{3.15a}$$

$$x^1_{,uv} = \frac{2G\mu w}{h^2}\left[\frac{2w}{x+tw}-\frac{1}{h^2+t+xw+yh}-\frac{1}{h^2+t+xw-yh}\right], \tag{3.15b}$$

$$x^2_{,uv} = \frac{2G\mu}{h}\left[\frac{1}{h^2+t+xw+yh}-\frac{1}{h^2+t+xw-yh}\right], \tag{3.15c}$$

$$x^3_{,uv} = 0\,. \tag{3.15d}$$

We now transport our observation point to the worldsheet of the $+x$ diamond, and so take $\Delta t = x/w$. It would be good to know where on this worldsheet feels an acceleration and where does not. The line which divides the $+x$ diamond into such regions is given by

$$t = -1 + \sqrt{(x-w)^2+y^2}\,, \tag{3.16}$$

which we call the *critical line*. It is a hyperbola formed by the intersection of the $+x$ diamond's worldsheet with the future lightcone of the point on the futuremost tip of the past $+x$ diamond, which lies at $(t,x,y) = (-1,w,0)$. The critical line intersects the spacelike separated tips of the $+x$ diamond. A point in the future of the critical line sees a ring intersection, while a point in the past of the critical line sees the figure-eight intersection.

An example of the ring intersection for a point above the critical line is shown in Fig. 3.6, while an example of the figure-eight intersection for a point below the critical line is shown in Fig. 3.7.

It is most convenient to analyze the effect of backreaction in null coordinates, so we use

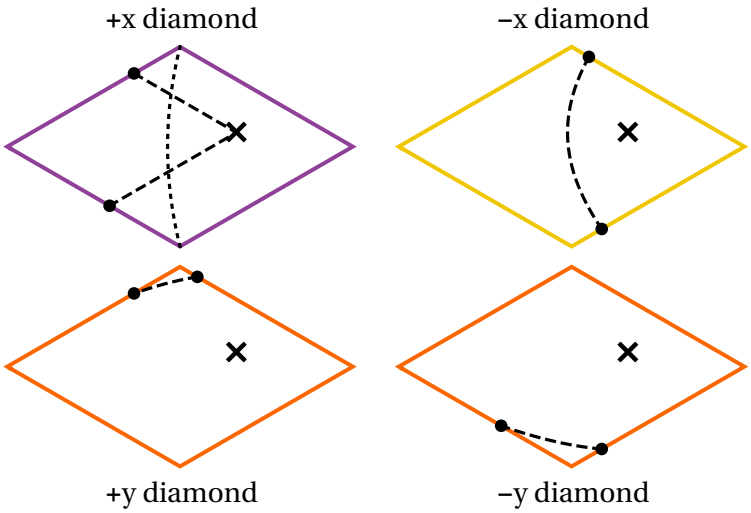

Figure 3.6: The intersections of the past lightcone with various diamonds for a point × on a $+x$ diamond above the critical line (shown dotted). Solid lines indicate the worldsheet boundaries, while dashed lines indicate the intersection. Color choices are consistent with Fig. 3.5

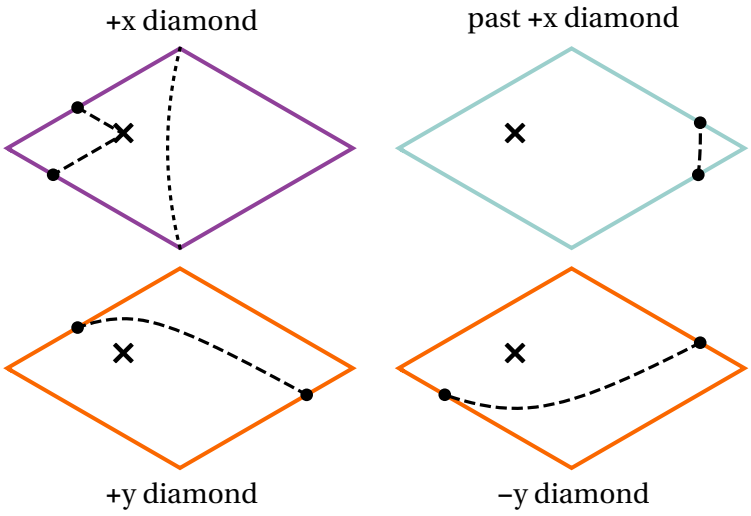

Figure 3.7: As in Fig. 3.6 for an observation point × which is below the critical line. Note that the intersection line now connects opposite edges of the y diamonds, instead of connecting adjacent edges.

$x = w(u+v)/2$ and $y = h(u-v)/2$, in agreement with Eq. (3.5), to write

$$x^0_{,uv} = \frac{2G\mu w^2}{h^2}\left[-\frac{2}{u+v} + \frac{1-(h/w)^2}{u+vw^2+h^2} + \frac{1-(h/w)^2}{uw^2+v+h^2}\right], \tag{3.17a}$$

$$x^1_{,uv} = \frac{2G\mu w}{h^2}\left[\frac{2}{u+v} - \frac{1}{u+vw^2+h^2} - \frac{1}{uw^2+v+h^2}\right], \tag{3.17b}$$

$$x^2_{,uv} = \frac{2G\mu}{h}\left[\frac{1}{u+vw^2+h^2} - \frac{1}{uw^2+v+h^2}\right], \tag{3.17c}$$

$$x^3_{,uv} = 0\,. \tag{3.17d}$$

In Eqs. (3.17a,3.17b), the first term diverges as we approach the midline in time of the diamond, where $u = -v$. This divergence arises because source points on the $-x$ diamond come arbitrarily close to observation points on the $+x$ diamond near the time when the string intersects itself to form a double line. We can avoid the problem either by taking into account the fact that the string has some finite thickness, which will then cut off the divergence, or by perturbing the motion to allow the two parts of the string to pass some small distance from each other in the z direction.

The remaining denominators in Eq. (3.17) do not vanish for the points to which they apply.

3.3.2 Modified null vectors

To analyze the change of shape of a loop, we will consider the null tangent vectors to the worldsheet. The function $B'(\tau_+)$, for example, which has a fixed form in flat space, accumulates changes due to the presence of $x_{,uv}$. These changes are the integral of all the effects on $B'(\tau_+)$ with τ_+ fixed and τ_- increasing through many oscillations [28]. For a fixed τ_+ in the range $0 < \tau_+ < 2$, the point in question moves alternately through $+x$ and $+y$ diamonds. In the case of A', we fix τ_- and let τ_+ vary, and for $0 < \tau_- < 2$ the point goes through $+x$ and $-y$ diamonds. The situation is shown in Fig. 3.8.

In a single diamond, u and v range from -1 to 1. But since there is no acceleration felt by points below the critical line, we only integrate u over the range $(u_c, 1)$ and v over the range $(v_c, 1)$, with the c subscript indicating the value of that null parameter on the critical line. For an arbitrary initial point, the critical line value of a null parameter is found by substituting for t, x, and y in Eq. (3.16) and solving for u or v,

$$u_c = -\frac{1+vR}{R+v}\,, \tag{3.18a}$$

$$v_c = -\frac{1+uR}{R+u}\,, \tag{3.18b}$$

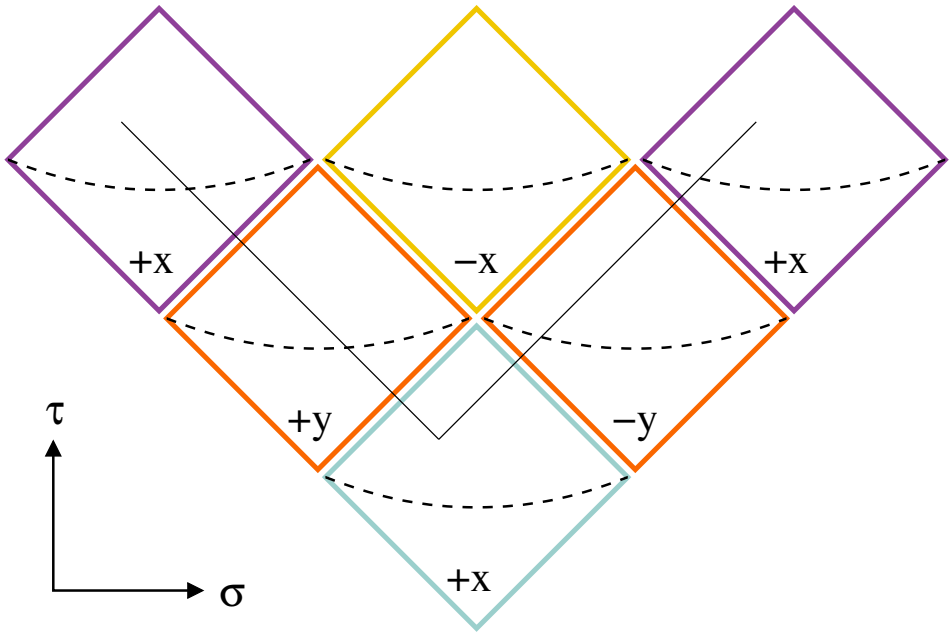

Figure 3.8: The path through the worldsheet taken by the null (solid black) lines of a point which begins in a $+x$ diamond. The lines are drawn for one full oscillation. The color choices are consistent with Fig. 3.5, as the worldsheet shown in this picture is the same worldsheet, but unfolded and scaled so that all diamonds are square. Dashed black lines indicate the critical line on each diamond, below which backreaction has no effect. Adjacent diamonds in the same row point in opposite directions. The first and third diamonds in the top row should be identified.

where $R = 1 + 2(w/h)^2$. This object has a minimum value of $R = 3$ when $\phi = \pi/4$, and increases monotonically as ϕ decreases.

Inspection of Eq. (3.17) tells us that there are only three kinds of integral whose solution we need to know, which we perform now.[1]

$$\int_{v_c}^{1} dv \frac{1}{u+v} = \ln\left[\frac{R+u}{1-u}\right], \tag{3.19a}$$

$$\int_{v_c}^{1} dv \frac{1}{uw^2+v+h^2} = \ln\left[\frac{(R'+u)(R+u)}{(1-u)^2}\right], \tag{3.19b}$$

$$\int_{v_c}^{1} dv \frac{1}{u+vw^2+h^2} = \frac{1}{w^2}\ln\left[\frac{R+u}{1+u}\right], \tag{3.19c}$$

where $R' = 1 + 2(h/w)^2$. We may recover the integrals for all other diamonds through proper exchange of $u \leftrightarrow v$ and $h \leftrightarrow w$. By applying the prefactors as given by Eq. (3.17), and adding the effects from the $+x$ and $+y$ diamonds, we find the modification to $B'(\tau_+)$

[1]The integral in Eq. (3.19a) should be understood in the principal value sense. As discussed above, there is a divergence in the acceleration when the $+x$ and $-x$ diamonds intersect. We can avoid it by letting them pass by some distance ϵ in the z direction. In that case the integrand will become $(u+v)/((u+v)^2+\epsilon^2)$, which will give the principal value on taking the limit as $\epsilon \to 0$. No other effects of ϵ remain in this limit.

for $0 < \tau_+ < 2$,

$$\Delta B'^{\lambda} = 8G\mu \left(\ln \left[\frac{(1-u)^2}{(R+u)(R'+u)} \right], \frac{1}{w} \ln \left[\frac{1-u}{R+u} \right], \frac{1}{h} \ln \left[\frac{1-u}{R'+u} \right], 0 \right) , \tag{3.20}$$

per oscillation. The modification to A' is similarly

$$\Delta A'^{\lambda} = 8G\mu \left(\ln \left[\frac{(1-v)^2}{(R+v)(R'+v)} \right], \frac{1}{w} \ln \left[\frac{1-v}{R+v} \right], -\frac{1}{h} \ln \left[\frac{1-v}{R'+v} \right], 0 \right) . \tag{3.21}$$

Equations (3.20,3.21) have a logarithmic divergence when then the null parameters are $+1$. This would imply that as we approach the kink, the modification to the direction of B becomes larger and larger, in contradiction to what we argued in Ref. [31]. This results from the intersection between the string and itself, which defeats the argument of Ref. [31] that source points close to the observation point have similar motion. If we modify the loop to avoid the self intersection and instead have the strings pass by at some distance δ, this distance will give a cutoff on the logarithmic divergence, so that we take $1 - v$ and $1 - u$ always at least δ.

For the "square" loop where $\phi = \pi/4$, we have $h = w$ and $R' = R$, so $\Delta B'^1 = \Delta B'^2$ and similarly for A'. Thus there is no change to the directions of A' and B', and the loop retains its shape. This is a consequence of the additional symmetry in this case, as discussed in Ref. [31].

We have kept the parameterization of the worldsheet in terms of $\tau_\pm$. But because of the time components of Eqs. (3.20,3.21), the relationship between these parameters and the actual time t is no longer straightforward. Nevertheless, the perturbed vectors $\tilde{A}' = A' + \Delta A'$ and $\tilde{B}' = B' + \Delta B'$ are null to first order in $G\mu$ because $A' \cdot \Delta A' = B' \cdot \Delta B' = 0$. We can integrate $\tilde{A}'$ and $\tilde{B}'$ with respect to $\tau_\pm$ to get spatially periodic functions $\tilde{A}$ and $\tilde{B}$, which have null but not unit tangent vectors. The worldsheet consists of all points which can be formed as

$$\frac{1}{2} \left[\tilde{A}(\tau_-) + \tilde{B}(\tau_+) \right] . \tag{3.22}$$

It is possible to instead reparameterize the worldsheet functions to arrive at an equivalent understanding of how backreaction changes the worldsheet; that is, where we consider $A(\tilde{\tau}_-)$ and $B(\tilde{\tau}_+)$, as we demonstrate in Appendix A.

We note that the spacetime perturbation is small and periodic, whereas changes to the string shape due to backreaction will accumulate over many oscillations. Our procedure for finding and distinguishing these secular changes from gauge effects will be to look only at how the worldsheet is modified after N oscillations, where $N \gg 1 \gg NG\mu$, so that secular

changes are much larger than oscillatory ones, but still small enough that we don't need to consider second-order effects.

3.4 The effects of backreaction

3.4.1 Energy loss

When τ_+ and τ_- have both increased by $T = 2$, the spatial position of the string loop returns to its original form. The period of the loop is the increase in the real time t. To find it we integrate the time component of $\tilde{A}'$ or equivalently $\tilde{B}'$,

$$\int_{-1}^{1} dv \left\{ 1 + 8G\mu \ln \left[\frac{(1-v)^2}{(R+v)(R'+v)} \right] \right\} = 2 + 16G\mu \left[\frac{\ln w^2}{h^2} + \frac{\ln h^2}{w^2} \right] . \tag{3.23}$$

The energy in the loop is the oscillation period times 2μ, so the change in energy due to backreaction is

$$\Delta E = 32G\mu^2 \left[\frac{\ln w^2}{h^2} + \frac{\ln h^2}{w^2} \right] \tag{3.24}$$

per oscillation. This agrees with the radiated power in Eq. (3.9) of [24].

3.4.2 Changes to A and B

To understand the modified shape of the string, we can integrate the spatial components of Eqs. (3.20,3.21). We find

$$\Delta B^1 = \frac{8G\mu}{w} F(u, R) \tag{3.25a}$$

$$\Delta B^2 = \frac{8G\mu}{h} F(u, R') \tag{3.25b}$$

$$\Delta A^1 = \frac{8G\mu}{w} F(v, R) \tag{3.25c}$$

$$\Delta A^2 = -\frac{8G\mu}{h} F(v, R') \tag{3.25d}$$

where

$$F(n, X) = \int dn \ln \left[\frac{1-n}{X+n} \right] = -(1-n)\ln(1-n) - (X+n)\ln(X+n) + \text{const.} \tag{3.26}$$

We will use the constant to keep the center of mass of the loop fixed. Equation (3.25) applies for $0 < \tau_\pm < 2$. For $2 < \tau_\pm < 4$, the signs of all components should be reversed and the constant chosen to keep A and B closed.

The total spatial change in B from $\tau_+ = 0$ to $\tau_+ = 2$ is

$$16G\mu \left[\frac{\ln w^2}{h^2} + \frac{\ln h^2}{w^2} \right] (w, h, 0) , \tag{3.27}$$

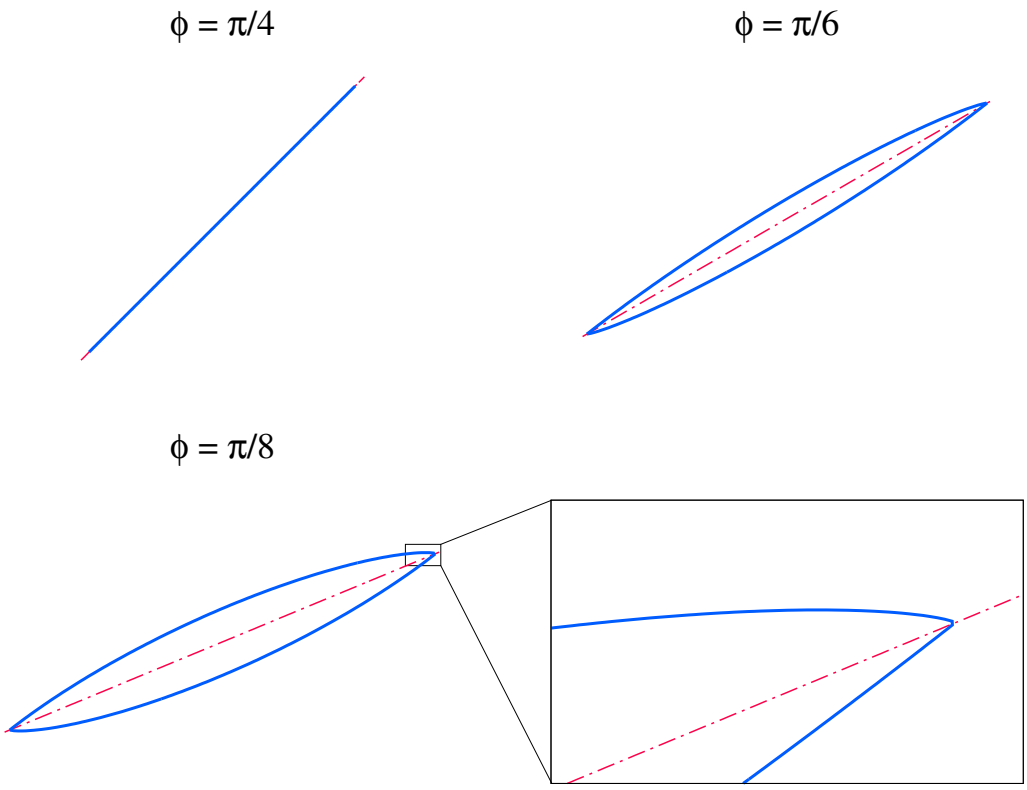

Figure 3.9: The unmodified (dashed red) and modified (solid blue) B for three different values of ϕ. Detail of the modified B as it transitions from outgoing to ingoing is given for the $\phi = \pi/8$ case. There are two general effects of backreaction: B becomes shorter, and so the loop becomes shorter as well; and the turning angle of B at its sharp ends becomes less than π, resulting in a "lens" appearance. This effect becomes weaker with increasing ϕ, to the limit that the turning angle of the $\phi = \pi/4$ case is not affected by backreaction at all. The overall direction of B (defined as the direction between the two kinks) is unchanged. We have taken $NG\mu = 7 \cdot 10^{-3}$ in all cases.

which points in the direction opposite to the unmodified B. Thus B becomes shorter by just the amount given in Eq. (3.23), but does not change its overall direction. The same argument applies to A.

We illustrate the modifications to B in Fig. 3.9. The modifications to A are given by exchange of $x \leftrightarrow -x$.

3.4.3 Changes to the loop shape

Using the new forms of A and B, we can find constant time slices of the loop's worldsheet, as shown in Fig. 3.10. We see two effects of backreaction on non-square loops: the previously

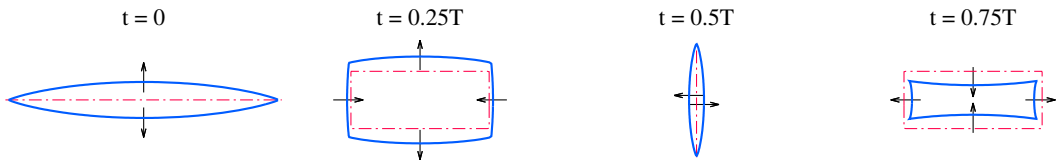

Figure 3.10: The unmodified (dashed red) and modified (solid blue) string loops at four different constant time slices. Arrows indicate the direction of motion of a segment at a given time. The effects of backreaction are to reduce the overall size of the loop, and to introduce curvature in the kink-connecting string segments for non-square loops. It should be noted that the modified and unmodified loops have different periods, and so these slices should not be taken to be at the same coordinate times, but rather at the same fraction of the loop's oscillation. What is important is that these slightly different times are constant over the entire loop. We have taken $\phi = \pi/8$ and $NG\mu = 7 \cdot 10^{-3}$.

straight segments connecting kinks acquire some bend, and the loop's oscillation is no longer symmetric. In the first half of each oscillation, the kinks have an interior angle greater than $\pi/2$, and in the second half of the oscillation, less than $\pi/2$.

The modified loop at $t = 0.25T$ in Fig. 3.10 takes up more spatial range than the unmodified loop, even though backreaction reduces its energy. While the physical length increases, the velocities of the string segments decrease by a greater amount, such that the invariant length of the modified loop decreases.

The exact nature of the crossing of the loop segments is not as straightforward for the modified loop. The string is shown in snapshots near the double line crossing in Fig. 3.11. The instantaneous double-line configuration has been replaced by a range of times of self-intersection. The time span between the start of subsequent self-intersections is $T/2$, and the range of time of self-intersection is considerably less than that.

Figure 3.11 also illustrates the important point that while A and B are opened (as in Fig. 3.9), meaning that the angle of the discontinuous jump in the tangent vector is reduced, there are time slices at which the kinks on the string loop have an angle between them of less than $\pi/2$. Examining the loop at different time slices might lead to us saying that the kinks are "opened" or "closed" at different times, and so we always refer to the changes of the worldsheet functions when we talk of kinks being opened.

3.4.4 Cusps

The changes to the tangent vectors A' and B' are also important to consider when thinking about cusp formation. For a generic loop, A' and B' trace out paths on the Kibble-Turok

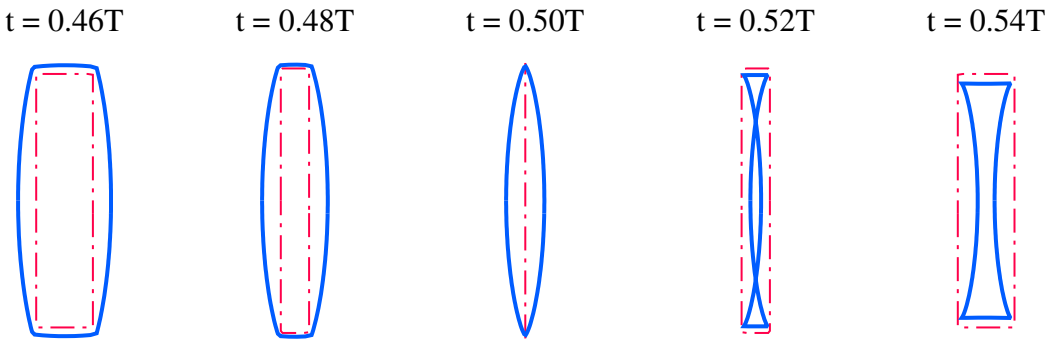

Figure 3.11: A comparison of the unmodified (dashed red) and modified (solid blue) loop configurations just before, at, and just after the "double line" configuration, halfway through one oscillation. In both loops, the inwards-moving "vertical" segments intersect along their entire lengths. While this intersection happens all at the same time for the unmodified loop, the modified loop sees the vertical segments crossing each other progressively over some period of time. We have taken $\phi = \pi/8$ and $NG\mu = 7 \cdot 10^{-3}$

[16] unit sphere. In the absence of kinks, these paths are smooth and generically intersect. These intersections produce cusps. Kinks are discontinuities in the paths of A' and B', which allow them to jump over each other instead of intersecting. Smoothing of kinks might lead to cusps that were not originally present.

The loops we discuss here are not generic but rather lie in a plane. Thus they always intersect themselves and so are not physically realistic. Nevertheless, they may shed some light on the question of kinks versus cusps. Because the loop lies in a plane, A' and B' are confined to a single great circle on the Kibble-Turok sphere. In the unmodified loop, A' and B' consist only of two points each, and angles 2ϕ and $\pi - 2\phi$ separate A' and B'. Gravitational backreaction reduces the kink angles and so increases the range of directions of A' and B'. Continued long enough, this process would cause A' and B' to overlap. The situation is shown in Fig. 3.12.

3.4.5 Kink opening

We have identified two effects of backreaction, kink opening and loop dissipation, and we would now like to compare the relative rates at which these effects take place.

The angle η between the unmodified and modified direction of B' can be found by taking the cross product of the spatial parts of B' and $\Delta B'$,

$$\eta \approx \sin\eta = w\Delta B'^2 - h\Delta B'^1 \tag{3.28}$$

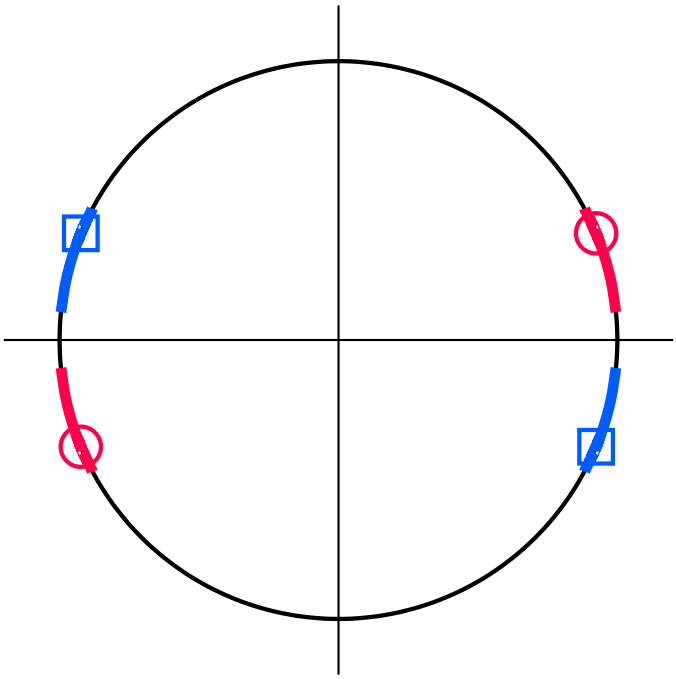

Figure 3.12: The unmodified and modified tangent vectors on the Kibble-Turok sphere. The unmodified A' and B' points are marked by blue squares and red circles, respectively, while the smearing effect of backreaction is given in blue for A' and red for B'. Backreaction has not yet acted for long enough to cause the modified tangent vectors to overlap at any point. We have chosen $\phi = \pi/8$ and $NG\mu = 7 \cdot 10^{-3}$.

At $u = -1$, this is

$$\frac{8G\mu}{hw} \ln\left[\frac{w^2}{h^2}\right] . \tag{3.29}$$

At $u = 1$, there is a logarithmic divergence, as discussed above. We will modify the string so that the string passes by itself a distance δ instead of forming a double line. Then we find that η at $u = 1$ is given by

$$\frac{8G\mu}{hw}\left[w^2 \ln w^2 - h^2 \ln h^2 + (w^2 - h^2)\ln(\delta/2)\right] . \tag{3.30}$$

Subtracting Eq. (3.30) from Eq. (3.29), we find the total angle through which B' turns between kinks,

$$\psi = \frac{8G\mu}{hw}\left[h^2 \ln w^2 - w^2 \ln h^2 - (w^2 - h^2)\ln(\delta/2)\right] . \tag{3.31}$$

The kinks in B, which originally turned by π, will now turn by $\pi - \psi$.

Now, we consider a string with $G\mu = 10^{-8}$ and take $\delta = 10^{-3}$ when comparing the rates of smoothing and dissipation. We are interested in comparing the timescales on which the

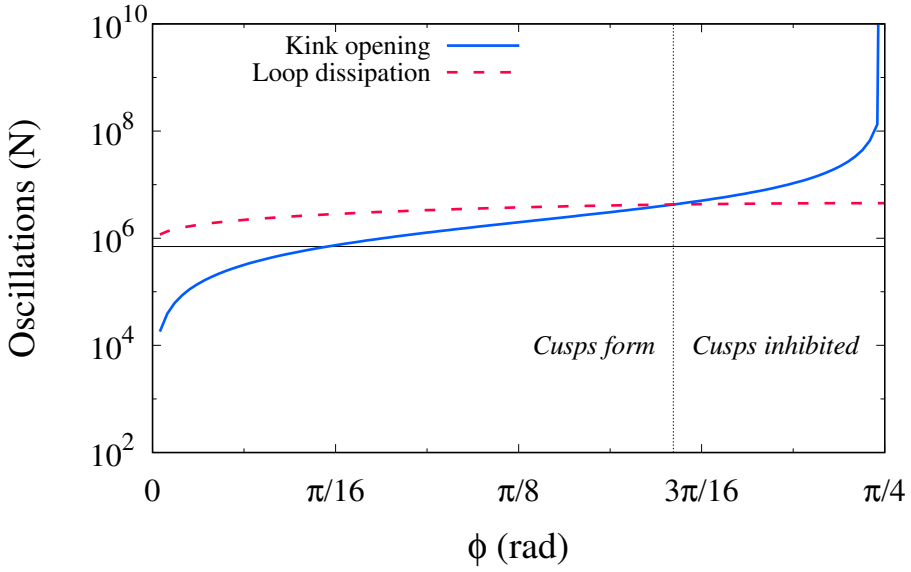

Figure 3.13: The number of oscillations (using the first-order approximation only) for a kink to be smoothed (solid blue line) and for a loop to be dissipated (dashed red line) by backreaction. For loops close to square ($\phi = \pi/4$), kink smoothing is much slower than evaporation of the loop. For small ϕ, kink smoothing is faster, and for a broad range in the middle the processes are roughly comparable. We have chosen $G\mu = 10^{-8}$, and the black horizontal line marks $N = 7 \cdot 10^5$, corresponding to $NG\mu = 7 \cdot 10^{-3}$ as used in all visualizations in Sec. 3.4.

kink angle and energy corrections become comparable to the initial angle and energy, and so we shall divide π by ψ as given by Eq. (3.31) and compare it to 4μ divided by ΔE as given by Eq. (3.24). These estimations provide us with an indication of the number of oscillations required to completely smooth the kink or to dissipate the loop. We compare the timescales of smoothing and dissipation in Fig. 3.13. When the loop is nearly square, it mostly retains its shape over the whole evaporation process, and the number of oscillations to evaporate is meaningful. Otherwise, smoothing of the kinks takes us out of the regime in which our first-order approximations apply, so the number of oscillations should not be taken literally.

3.5 Discussion

3.5.1 Maximal symmetries protect loops

As we have previously noted, the square loop does not find itself smoothed by backreaction, and maintains its initial shape as it shrinks to nothing via gravitational radiation. One should suspect that this property is connected to the extra degree of symmetry that the

square loop possesses above other rectangular loops.

We have already shown (vid. Fig. 3.12) how a non-square loop's map to the Kibble-Turok sphere is changed by backreaction. What we call attention to now is that these "smeared" sections mean there is a directionality to the modification. As u or v advances, B' or A' runs from the end of the smear closer to the y axis to the end closer to the x axis. Loosely, we could say the previously-singular worldsheet function derivatives are smeared in the direction of the x axis. This smearing does not change the symmetries that the non-square loop previously possessed.

For the square loop, attempting to smear the worldsheet function derivatives is immediately stymied. The square loop does not distinguish between the x and y axes, and there is no way for backreaction to introduce smearing without breaking this additional degree of symmetry. The square loop therefore shrinks without changing its shape.

Another case of a loop which shrinks rigidly is the ACO loop [29], studied extensively by Anderson [38, 39, 40]. This loop has one of its worldsheet functions as a circle and the other as a line perpendicular to the plane of said circle. The circle may be wound singly or multiply, and the line may go back and forth more than once; all such loops radiate and shrink without changing their shape.

We again see that it is the maximal symmetry of the worldsheet functions' arrangement which protects the ACO loop from smoothing due to backreaction. The circular function cannot be modified without breaking its rotational invariance and thus designating a preferred direction; the linear function, if it were to be smoothed by backreaction, would acquire a "bowing" in some now-preferred direction. With no direction to move in that does not result in a loss of symmetry, the loop shrinks without changing its shape.

We suspect, but offer no rigorous proof to support the claim, that the square loop and the ACO loop are the only rigidly-shrinking loops. The basic ingredients of a rigidly-shrinking loop must be linear and circular worldsheet functions only. Any piecewise function with more than two points which can satisfy the loop's closure requirement must go around the Kibble-Turok sphere in some preferred direction (the circle avoids this being a problem because it is already perfectly smooth).

Having discussed the purely linear and mixed circular-linear cases, we are left to wonder about the purely circular loop, or Burden loop [41]. It should be evident that there are only two ways to combine two circular worldsheet functions which does not have a preferred direction: when they are coplanar and cycle in the same direction, and when they are

coplanar and cycle in opposite directions. The first of these is called the *rigid rod*, and is a straight double-line rotating with some fixed angular velocity whose endpoints are persistent cusps. The second is the *breather*, and is a circular loop whose radius oscillates between zero and some maximum value.

3.5.2 The fate of kinks and cusps

We have demonstrated both broadly and for a particular class of piecewise linear loops that kinks on cosmic strings must be straightened by backreaction, and not smoothed. Such a distinction changes our expectations of what the gravitational wave spectrum from loops must look like on two counts. First, kinks produce different wave profiles than smooth segments of loop; second, because it no longer looks to be certain that loops generically (and almost immediately) develop two cusps, we must revise estimates of the frequency of cuspy signals from a population of string loops.

Because cusp-driven bursts of gravitational waves are far stronger than the stochastic background due to oscillating loops, it is the second of these effects which we are more concerned with investigating further. Because analytic solutions are impractical to come by for a completely generic loop, the clear way forward here lies in simulations, which is the subject of our future work. What follows is conjecture about important changes to our expectations for cuspy signals based on our current understanding.

The age of the loops in a network is an important determinant in the frequency of cusps. Because the functions on the Kibble-Turok sphere must be smeared such that their paths cross before cusps can develop, a loop which has been oscillating for longer is more likely to have cusps. So if one is examining a very young population, cusps are likely to be rare events, and so this effect looks to be a barrier to detection. A more optimistic view to take is that the prevalence of cusps in a population could be used to assess that population's age.

For the same reasons, it is important to determine the relative value of Γ_ζ to Γ (recall Sec. 3.1). Only when $\Gamma_\zeta \gg \Gamma$ do cusps appear soon after a network's formation. The naïve guess that $\Gamma_\zeta \sim \Gamma$ delays cusps until the loop is about halfway through its lifetime, which carries significant implications for detection, as well as similar consequences to the optimistic and pessimistic ones mentioned above.[2]

[2]In case further study does reveal $\Gamma_\zeta \sim \Gamma$, I would like to suggest here that this delay be referred to as the string loop's "midlife crisis".

We have only discussed how our findings might influence when and how many cusps appear. What we do not currently have a prediction for is how the transient signals from cusps, as well as where their peaks appear in the power spectrum, are changed by backreaction (if they are changed at all). Still, the detection of cosmic strings by gravitational wave observatories will require a bit more time, or a bit more luck, but they remain capable of spotting strings.

CHAPTER 4

GRAVITATIONAL BACKREACTION ON A PERTURBED STRAIGHT STRING

We now turn to consider how a static, straight string responds to a localized force which displaces it in space. The original intent of this investigation was to provide a naturally stepping stone from the relatively simple case of Chapter 5 to the geometrically involved case of Chapter 3 (indeed, this dissertation is presented in reverse chronological order!). We will see in Chapter 5 that the string is secondary to the problem, serving only as a wire along which superconducting current can flow; in the case we are about to discuss here, the string itself is the source of backreaction. Moreover, there are complexities which arise in this chapter which are of no consequence to the oscillating loop of Chapter 3.

The work presented in this section is unique to this dissertation.

4.1 Premise

Consider a static straight string lying on the x axis. Apply to this string some force which acts to move the point of the string which was at the origin to a point $(x, y) = (0, s)$ in unit time at a fixed velocity. The effect is to create two "sloped" segments of string connected to the "flat" segments of string at kinks, as shown in Fig. 4.1. We note that $s = \tan\theta$, with θ the acute angle between a sloped segment and the x axis.

These slopes then propagate to the left and the right, as appropriate. Picking a point in the causal future of where we first applied our force, we see a variety of different sources

Figure 4.1: A view of the string in the xy plane for a series of time slices. We have set $t = 0$ to be the instant at which the motion begins, and $t = 1$ to be when the slopes are fully formed. The slopes so produced have $s = 0.6$.

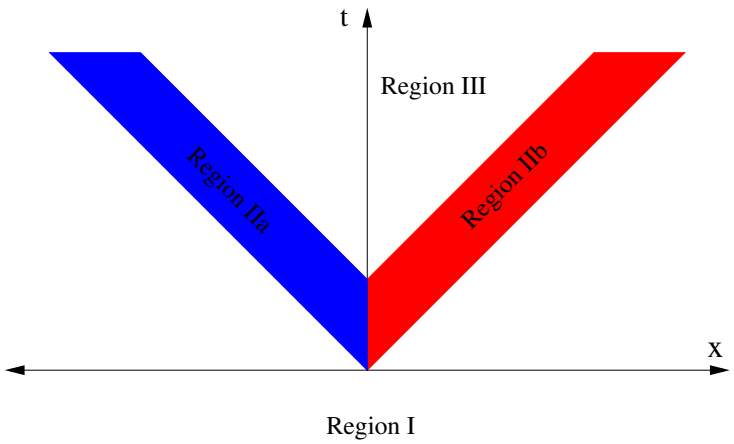

Figure 4.2: A view of the string worldsheet for the two-slope case. This view has been projected onto the tx plane. The string is static and straight in Regions I and III with a y difference of s. Regions IIa and IIb are the left- and right-going sloped regions, which propagate along the string in the $+\hat{x}$ and $-\hat{x}$ directions respectively.

(the string in different configurations) lying on our past lightcone. Similarly to how a train of charge is reduced by electromagnetic sources in its past, there should be some effect of gravitational backreaction which modifies the sloped segments of string, as well as the straight displaced segment. Our initial suspicion, again in parallel to the electromagnetic case, is that gravitational backreaction will act to decrease the angle of the sloped regions and lower the string from its displaced height back to lying entirely on the x axis.

When backreaction is not applied, we have divided the worldsheet into four distinct regions, as shown in Fig. 4.2. Regions I and III are both static straight strings, albeit with a y difference of s, while Regions IIa and IIb represent the left- and right-going sloped segments.

4.2 Worldsheet values

We begin by constructing the mathematical description of the worldsheet. In Regions I and III, the string is static and straight on the x axis, with the only difference being a fixed displacement. The tangent vectors are

$$\dot{x}^\gamma = (1, 0, 0, 0) \ , \tag{4.1a}$$

$$x'^\gamma = (0, 1, 0, 0) \ . \tag{4.1b}$$

In Regions IIa and IIb, the worldsheet and thus its tangent vectors are identical under mirror symmetry, so we will explicitly find the tangent vectors for Region IIa and reflect to

find those in Region IIb.

We take the static straight string's tangent vectors and apply two transformations: first, we rotate about the z axis by α; second, we boost the string by $|\beta| = s/\sqrt{1+s^2}$ in the direction given by $\vec{n} = \left(\frac{s}{\sqrt{1+s^2}}, -\frac{1}{1+s^2}, 0\right)$ (i.e. transverse to the rotated string's extent in the xy plane). However, we are not quite done—our conformal gauge requirement is that $\tau = t$, which requires $\dot{x}^0 = 1$. We divide both tangent vectors by the Lorentz factor γ. Thus, we obtain the tangent vectors of the sloped segment of string found in Region IIa,

$$\dot{x}^\gamma = \left(1, -\frac{s^2}{1+s^2}, \frac{s}{1+s^2}, 0\right) , \tag{4.2a}$$

$$x'^\gamma = \left(0, \frac{1}{1+s^2}, \frac{s}{1+s^2}, 0\right) . \tag{4.2b}$$

The transformations to obtain the tangent vectors of Region IIb require that we negate each vector's x component, as well as negating x'^γ in its entirety, and so we get

$$\dot{x}^\gamma = \left(1, \frac{s^2}{1+s^2}, \frac{s}{1+s^2}, 0\right) , \tag{4.3a}$$

$$x'^\gamma = \left(0, \frac{1}{1+s^2}, -\frac{s}{1+s^2}, 0\right) . \tag{4.3b}$$

Our next challenge is to introduce null coordinates u and v. It is attractive to use these coordinates because of the geometry of the problem, itself due to the property that kinks move at the speed of light. A null or lightlike line will always maintain its relative position to one of the two sloped segments. We lay down these coordinates with two requirements: that the left-going sloped section is sourced entirely by u and the right-going by v; and that the values of the null coordinates are continuous as we change regions. The first requirement is fulfilled by insisting that $x^\gamma_{,v}$ has its flat-space value in Region IIa and the same for $x^\gamma_{,u}$ in Region IIb; the second is a bit trickier, but comes down to being careful with our definitions of u and v in terms of t and σ within each region.

We discuss the details of this definition in Appendix B, but we can get at the definitions of u and v with two observations: one, that with the conformal gauge conditions, u and v are null so long as $u \propto \tau + \sigma$ and $v \propto \tau - \sigma$; two, the symmetry of the initial geometry demands that $x = (u - v)/2$ always if we are to keep u and v continuous. Thus, the null coordinates in Region IIa are defined as

$$v = \tau - \sigma \, , \tag{4.4a}$$

$$u = \left(\frac{1-s^2}{1+s^2}\right)(\tau + \sigma) \, , \tag{4.4b}$$

which leads to the null vectors being

$$A'^{\gamma} = (1, -1, 0, 0) \ , \tag{4.5a}$$

$$B'^{\gamma} = \left(\frac{1+s^2}{1-s^2}, 1, \frac{2s}{1-s^2}, 0\right) \ . \tag{4.5b}$$

(Recall that $x^{\gamma}_{,u} = B'^{\gamma}/2$ and $x^{\gamma}_{,v} = A'^{\gamma}/2$.) Similarly, the null coordinates in Region IIb are defined as

$$v = \left(\frac{1-s^2}{1+s^2}\right)(\tau - \sigma) \ , \tag{4.6a}$$

$$u = \tau + \sigma \ , \tag{4.6b}$$

which leads to the null vectors being

$$A'^{\gamma} = \left(\frac{1+s^2}{1-s^2}, -1, \frac{2s}{1-s^2}, 0\right) \ , \tag{4.7a}$$

$$B'^{\gamma} = (1, 1, 0, 0) \ . \tag{4.7b}$$

One can check that all of these vectors are properly null, i.e. that $A' \cdot A' = 0 = B' \cdot B'$. The bottom edge of Region IIa corresponds to the half-line $u = 0$, $v \geq 0$, and vice versa for Region IIb. Similarly, the top edge of Region IIa is all $u = 1 - s^2$, $v > 1 - s^2$ and vice versa for Region IIb.

Having the tangent vectors also allows us to construct the trace-reversed stress-energy tensor for the string via Eqs. (2.8,2.9).

4.3 The metric perturbation

4.3.1 General forms and simplifications

With a continuous parameterization of the string's worldsheet, we now turn to finding the metric perturbation sourced by the string at any point in spacetime. We know from Eq. (2.21) how to solve for the metric perturbation due to a region of a piecewise linear string, which we reproduce here:

$$h_{\alpha\beta} = -\frac{8G\mu\sigma_{\alpha\beta}}{A' \cdot B'} \ln\left[\frac{2A' \cdot \Omega}{A' \cdot B'} - u\right]\Bigg|_{u_+}^{u_-} \ . \tag{4.8}$$

Note that the process of obtaining this result requires that we choose to eliminate v by rewriting the Dirac delta function; the final answer is of course the same, but we may wish to obtain a result in terms of v in the case that it makes finding the limits of integration

simpler. Exchanging $A' \leftrightarrow B'$, $v \leftrightarrow u$ gives

$$h_{\alpha\beta} = -\frac{8G\mu\sigma_{\alpha\beta}}{A' \cdot B'} \ln\left[\frac{2B' \cdot \Omega}{A' \cdot B'} - v\right]\Bigg|_{v_+}^{v_-} . \tag{4.9}$$

To make a more informed choice as to which form of the metric perturbation we should choose for a given region, we examine Fig. 4.2. We find that there are three possible scenarios for how an arbitrary spacetime point's past lightcone might intersect the string worldsheet:

1. The past lightcone intersects only Region I. It crosses no borders.

2. The past lightcone intersects Regions I, IIa, and IIb. It crosses the I/IIa, IIa/IIb, and I/IIb borders. Such an intersection can only be due to a point inside the future lightcone of the origin and outside the future lightcone of $(t, x, y) = (1, 0, h)$.

3. The past lightcone intersects all regions. It crosses the I/IIa, IIa/III, IIb/III, and I/IIb borders. Such an intersection can only be due to a point inside the future lightcone of $(t, x, y) = (1, 0, h)$.

The clear choice for the perturbation due to Region IIa is Eq. (4.8), as the intersection hyperbola (if it visits Region IIa) always crosses the I/IIa border ($u = 0$). Similarly, the perturbation due to Region IIb is simplified if we use Eq. (4.9), as the intersection hyperbola always crosses the I/IIb border ($v = 0$). For Regions I or III, no form is more or less complicated than the other.

So informed, we find that in Region I or Region III,

$$h_{\alpha\beta} = -4G\mu \begin{pmatrix} 0 & 0 & 0 & 0 \\ 0 & 0 & 0 & 0 \\ 0 & 0 & 1 & 0 \\ 0 & 0 & 0 & 1 \end{pmatrix} \ln\left[\frac{t + x - u_+}{t + x - u_-}\right] . \tag{4.10}$$

In Region IIa, we have that $u_- = 0$ always, as it is the bottom border of this region.

$$h_{\alpha\beta} = -4G\mu \begin{pmatrix} s^2 & s^2 & -s & 0 \\ s^2 & s^2 & -s & 0 \\ -s & -s & 1 & 0 \\ 0 & 0 & 0 & 1 \end{pmatrix} \ln\left[1 - \frac{u_+}{(1 - s^2)(t + x)}\right] . \tag{4.11}$$

In Region IIb, we switch to expressing the metric perturbation in terms of v, for the convenience that $v_- = 0$ always. Then,

$$h_{\alpha\beta} = -4G\mu \begin{pmatrix} s^2 & -s^2 & -s & 0 \\ -s^2 & s^2 & s & 0 \\ -s & s & 1 & 0 \\ 0 & 0 & 0 & 1 \end{pmatrix} \ln\left[1 - \frac{v_+}{(1-s^2)(t-x)}\right] . \tag{4.12}$$

Now thinking about what other limits of integration we might encounter, we see there to be a limited pool to draw from: all of the I/II and II/III boundaries are constant in either u or v (at 0 and $1-s^2$, respectively), and so the only additional work we need to do to find expressions for u and v on the IIa/IIb border. Since here $u = v$, we find the value of either null parameter on the IIa/IIb border by setting $u = v(= p)$ in Eq. (2.16) and solving. Of course, we know the u and v null vectors for Region IIa and Region IIb from Eqs. (4.5,4.6), and so find

$$p = t - sy - \sqrt{(st-y)^2 + (1-s^2)x^2}\,. \tag{4.13}$$

We determine the sign on the square root term by noting that we want the solution for which $0 < p < 1 - s^2$.

We now have all of the pieces necessary to assemble the metric perturbation for any point in spacetime. There is one additional simplification we may make, having to do with the effect of the static straight string. We already know the metric perturbation of a point which sees only Region I on its past lightcone: it is the metric perturbation of a static straight string [4], with a change of sign to account for the fact that we are using different metric signatures:

$$h_{\alpha\beta} = -4G\mu\,\mathrm{diag}(0,0,1,1)\ln\left[\frac{y^2+z^2}{\delta^2}\right] , \tag{4.14}$$

with δ the string thickness.[1]

Now, consider a point whose past lightcone sees more than just Region I. It still sees Region I, albeit missing a (comparatively) small "wedge" where it sees the perturbed string instead. We know that the intersection crosses the I/IIa border at $u = 0$, and the I/IIb border at $u = (x\cdot x)/(B'\cdot x) = t + x - (y^2+z^2)/(t-x)$ (vid. Eq. (2.17)). Thus, the metric perturbation due to Region I for such a point is the perturbation of the static straight string *minus* the perturbation obtained by taking $u_- = 0$, $u_+ = t + x - (y^2+z^2)/(t-x)$ in

[1] If we did not know the static straight string's perturbation, we could find it starting from Eq. (4.10) via a process akin to finding the electric potential of an infinite line of charge.

Eq. (4.10),

$$h_{\alpha\beta} = -4G\mu\,\mathrm{diag}(0,0,1,1)\left(\ln\left[\frac{y^2+z^2}{\delta^2}\right] - \left[\frac{y^2+z^2}{t^2-x^2}\right]\right)$$
$$= -4G\mu\,\mathrm{diag}(0,0,1,1)\ln\left[\frac{t^2-x^2}{\delta^2}\right]. \tag{4.15}$$

Let us pause to consider the meaning of this result. The metric perturbation due to Region I for a point which knows about the kick, but is otherwise arbitrary, does not depend on how far from the string that point is. Instead, it only depends on how long it has been since the kick and how far from the kick it is along the string, growing with the former and shrinking with the latter.[2] While one might be concerned that, for fixed x, this perturbation grows without bound, we will later see that the perturbation due to Region III has a similar and regulatory effect.

4.3.2 Specific perturbations for all classes of point

We know that there are three different classes of point, distinguished by their position relative to the future lightcones of the start and end of the kick. We call such points, and the perturbations associated with them, in the same way that we have been classifying the worldsheet regions: a point in the past of the future lightcone of the start of the kick has a perturbation $h^{\mathrm{I}}_{\alpha\beta}$; a point between the future lightcones of the start and end of the kick has a perturbation $h^{\mathrm{II}}_{\alpha\beta}$; and a point in the future of the future lightcone of the end of the kick has a perturbation $h^{\mathrm{III}}_{\alpha\beta}$. Equations (4.10-4.12) now allow us to write the total perturbation for any such point as a sum of the perturbations of the regions visited by the point's intersection hyperbola.

From here on, for convenience's sake we shall refer to the matrix component of the trace-reversed stress-energy tensor of a flat segment of string as $\sigma^{f}_{\alpha\beta}$, of a left-going sloped segment of string as $\sigma^{a}_{\alpha\beta}$, and of a right-going sloped segment of string as $\sigma^{b}_{\alpha\beta}$. Refer to Eqs. (4.10-4.12) for the details of these components.

As we have already noted, $h^{\mathrm{I}}_{\alpha\beta}$ is the metric perturbation of a static straight string;

$$h^{\mathrm{I}}_{\alpha\beta} = -4G\mu\sigma^{f}_{\alpha\beta}\ln\left[\frac{y^2+z^2}{\delta^2}\right]. \tag{4.16}$$

[2] As the δ term was introduced as a cutoff to prevent divergences, we enforce that $t^2 - x^2 \geq \delta^2$ always, replacing anything less than δ^2 by δ^2.

For a point between the two future lightcones,

$$h^{\rm II}_{\alpha\beta} = -4G\mu \left(\sigma^f_{\alpha\beta} \ln \left[\frac{t^2 - x^2}{\delta^2} \right] + \sigma^a_{\alpha\beta} \ln \left[1 - \frac{t - sy - \sqrt{(st-y)^2 + (1-s^2)x^2}}{(1-s^2)(t+x)} \right] + \sigma^b_{\alpha\beta} \ln \left[1 - \frac{t - sy - \sqrt{(st-y)^2 + (1-s^2)x^2}}{(1-s^2)(t-x)} \right] \right) . \tag{4.17}$$

For a point in the future of both future lightcones,

$$h^{\rm III}_{\alpha\beta} = -4G\mu \left(\sigma^f_{\alpha\beta} \ln \left[\frac{t^2 - x^2}{\delta^2} \right] + \sigma^f_{\alpha\beta} \ln \left[\frac{(y-s)^2 + z^2}{(t-1+s^2)^2 - x^2} \right] + \sigma^a_{\alpha\beta} \ln \left[1 - \frac{1-s^2}{(1-s^2)(t+x)} \right] + \sigma^b_{\alpha\beta} \ln \left[1 - \frac{1-s^2}{(1-s^2)(t-x)} \right] \right) . \tag{4.18}$$

Now, we see the appearance of the "compensating" logarithm term for the flat-space part; as we move along the string far into the future in Region III, we no longer have the flat-space perturbation growing without bound. The logarithms associated with the sloped segments of string tend towards zero as we get far from the II/III boundary; that is, the perturbation will slowly forget the effects of the kink, and will eventually return to its static straight string value.

4.4 The accelerations acting on the string segments

Just as for the string loop, we find the four-acceleration felt by any point via Eq. (2.22),

$$x^\lambda_{,uv} = -\frac{1}{4} \Gamma^\lambda_{\alpha\beta} B'^\alpha A'^\beta \, . \tag{4.19}$$

Once again, we will be considering observation points which lie on the string worldsheet. It is clear that such a point is subject to some constraints—e.g. for a point in Region IIa, we set $y = s(t+x)$ and $z = 0$. In addition, a point which is on a worldsheet regions has identical null vectors to that worldsheet region. This permits the same sort of simplifications as we made before.

Most notably, a point feels no effect from the region which it is a member of, nor from distinct regions with identical null vectors. For example, a point in Region III has the same null vectors as Region I, and so it is only affected by the perturbations due to Regions IIa and IIb. A point in Region IIa has the same A' as Region I; by a similar argument to the one we presented in Sec. 3.3.1, we know that we need only consider the terms in the acceleration equation wherein A' is contracted with the direction of differentiation. Likewise, a point in

Region IIb has the same B' as Region I, and we only consider cases where B' contracts with the direction of differentiation.

We will present the accelerations in terms of u and v, as we will be integrating the accelerations over one of these parameters in order to find the correction to the null vector associated with the other. Here we must be clear about which definition of u and v we are using. All of our metric perturbations, and thus our accelerations, are currently written in terms of $txyz$. To write them in terms of uv, we use the null parameter definitions appropriate to the worldsheet region which the observation point is on.

For a point in Region IIa, the acceleration due to gravitational backreaction is

$$x^0_{,uv} = 2G\mu s^2 \left(-\frac{2}{u-v} + \frac{s^2}{s^2 u + (1-s^2)v} \right) , \tag{4.20a}$$

$$x^1_{,uv} = \frac{2G\mu s^4}{s^2 u + (1-s^2)v} , \tag{4.20b}$$

$$x^2_{,uv} = 4G\mu s \left(-\frac{1}{u-v} + \frac{s^2}{s^2 u + (1-s^2)v} \right) , \tag{4.20c}$$

$$x^3_{,uv} = 0 . \tag{4.20d}$$

For a point in Region IIb, the acceleration due to gravitational backreaction is

$$x^0_{,uv} = 2G\mu s^2 \left(\frac{2}{u-v} + \frac{s^2}{(1-s^2)u + s^2 v} \right) , \tag{4.21a}$$

$$x^1_{,uv} = -\frac{2G\mu s^4}{(1-s^2)u + s^2 v} , \tag{4.21b}$$

$$x^2_{,uv} = 4G\mu s \left(\frac{1}{u-v} + \frac{s^2}{(1-s^2)u + s^2 v} \right) , \tag{4.21c}$$

$$x^3_{,uv} = 0 . \tag{4.21d}$$

Note that these components are identical to those of Eq. (4.20) if we apply the usual mirroring transformation.

For a point in Region III, the acceleration due to gravitational backreaction vanishes,

$$x^\lambda_{,uv} = (0,\, 0,\, 0,\, 0) . \tag{4.22}$$

We can see from a fairly cursory examination of our results at current that something looks to be amiss—the acceleration at any point in Regions IIa and IIb seems to point in a direction which increases the slope angle, counter to our intuition; see Fig. 4.3. Furthermore, a point in Region III feels no acceleration. Even to first order, we would expect that backreaction would act to lower the elevated flat region of string back to its initial location

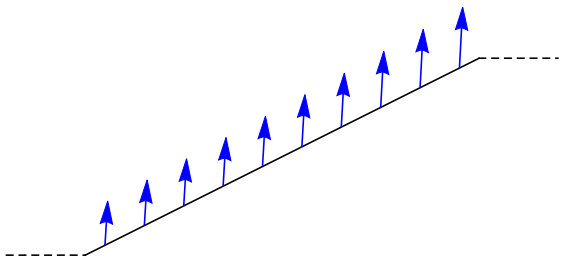

Figure 4.3: The spatial acceleration vector felt by points on the string in Region IIa at a $t = 3$ slice. Because the force increases as we move up the slope, the overall effect seems to be to increase the angle of the slope, counter to our intuition. While the y component is problematic in that it points in the positive direction, the x component opposes the direction of motion of the kink, more in keeping with our expectations.

on the x axis. It seems that we cannot infer how these accelerations change the worldsheet at a first glance, and must more carefully consider how we will interpret our results.

In the case of the oscillating loop, the metric perturbation was periodic, but changes to the loop's worldsheet accumulated over time. There, the question of interpretation was as simple as letting changes build up for many oscillations until the perturbation to spacetime was small by comparison, then examining a constant-time slice.

In the scenario now before us, there is no periodicity in the metric perturbation, and so we must devise some way to separate gauge and secular effects. Discussions of different possible techniques for doing so, and an analysis of potential pitfalls in our approach, will constitute the remainder of this chapter.

4.5 Disentangling real and unreal effects

4.5.1 Gauge transformations

A first thought is that if it is gauge effects which could confound our interpretation, why not make a gauge transformation to remove them? We know that if we perturb the coordinate system by

$$x^{\lambda'} = x^{\lambda} + \xi^{\lambda} \,, \tag{4.23}$$

then the metric will change as

$$g_{\alpha'\beta'} = g_{\alpha\beta} - \xi_{\alpha;\beta} - \xi_{\beta;\alpha} \,, \tag{4.24}$$

where the semicolon means we take the covariant derivative. Because the effect we are hoping to remove is of order $G\mu$, ξ^{λ} will also be of order $G\mu$. Any instances of our coordinates

which are either inside a logarithm or in an equation preceded by $G\mu$ we can safely leave unchanged (i.e. $x^{\lambda'} = x^{\lambda}$), as we are uninterested in second-order effects.

Of course, we still need to decide upon an appropriate change to the metric. This is best done by considering how the various elements of the perturbations grow in the far future.

Let us consider specifically a point in Region IIa. We noted previously that the contribution of Region I, given by Eq. (4.15), grows without bound when we fix x and let t increase. This remains true if we fix one of $t + x$ or $t - x$ and evolve in the direction of the other; or, as we go far into the future of Region IIa or IIb. Neither the perturbation due to Region IIa nor the one due to Region IIb seems to be up to the job of compensating for this effect, as both of them go to zero as we travel into the far future (contrast this with the second $\sigma^{f}_{\alpha\beta}$ term in Eq. (4.18)). Perhaps the contribution of Region I is the problematic term!

By inspection, we find

$$\xi^{\lambda} = -2G\mu \left(0,\, 0,\, y \ln\left[\frac{t^2 - x^2}{\delta^2}\right],\, z \ln\left[\frac{t^2 - x^2}{\delta^2}\right]\right) . \tag{4.25}$$

Note that this four-vector correctly removes h_{22} and h_{33}, but introduces nonzero $h_{(02)}$, $h_{(03)}$, $h_{(12)}$ and $h_{(13)}$. However, all of these terms fall like $1/t$ as we go into the far future of Regions IIa and IIb, so the divergent behavior is cured.

Noting that $x^{\lambda'}$ will now have some nonzero second derivatives, we ask how the acceleration is different. Disappointingly, the overall result does not greatly change; the only difference is in the y component, where we have that

$$x^{2}_{,uv} = 2G\mu s \left(\frac{2}{u - v} + \frac{1 + 2s^2}{s^2 u + (1 - s^2)v} + \frac{s^2 u}{\left(s^2 u + (1 - s^2)v\right)^2}\right) . \tag{4.26}$$

While the y component has changed, its overall sign has not.

We are now presented with two options, neither of which are particularly attractive:

1. The sloped segments of string actually become steeper. This violates our intuition and potentially causes problems in that a steeper slope has more energy (presuming the total length of the sloped segment remains the same).

2. The metric in which we have removed all unphysical effects is reached by some different ξ^{λ}. Without good motivation for how we would go about finding that particular four-vector, and with an extremely large space of possible solutions, continuing to attempt at finding the "correct" ξ^{λ} seems unlikely to bear fruit.

Not yet ready to accept the first option presented above, we turn to explore other ideas for how to extricate the physical effect from our result.

4.5.2 The motion of a bead on the string

A second idea is to consider how the propagation of a sloped segment would move an object at rest on the string. We consider a bead at rest on the string far to the left of the origin, before the left-going slope has arrived. As the slope passes by, this bead will be given some kick which changes its velocity vector. By calculating the zero component of the bead's four-velocity for a string with backreaction, we will be able to determine how the strength of the kick changes depending on when it receives the kick from the string, thereby determining how backreaction is affecting the slope.

Let us first consider what the bead feels if we are not accounting for backreaction. The bead's new velocity vector must be a linear combination of A' and B' in Region IIa, or

$$U^0 = C_a A'^0 + C_b B'^0 \,. \tag{4.27}$$

Normalized, this vector is

$$\frac{U^0}{\sqrt{g_{\alpha\beta}U^\alpha U^\beta}} = \frac{\sqrt{C_a}A'^0 + \sqrt{C_b}B'^0}{\sqrt{2C_aC_b g_{\alpha\beta}A'^\alpha B'^\beta}} \,. \tag{4.28}$$

Now, we make two observations. First is that

$$U^\lambda = \gamma\,(1, \vec{u}) \;, \tag{4.29}$$

with γ the Lorentz factor, and so the left-hand side of Eq. (4.28) is equal to γ. Second is that we wish to minimize the bead's new velocity vector; noting the see-saw dependence of the velocity on the constants C_a and C_b, we rewrite Eq. (4.28) as

$$\gamma = \sqrt{-\frac{2A'^0 B'^0}{g_{\alpha\beta}A'^\alpha B'^\beta}} \,. \tag{4.30}$$

Now, because we know the sloped segment of string to be moving with a speed $s/\sqrt{1+s^2}$, we would expect a bead given a kick by such a string—i.e. brought up to the string's velocity—to have a Lorentz factor $\gamma = \sqrt{1+s^2}$. Explicit calculation of Eq. (4.30) confirms this. So, we will interpret an increasing γ as the slope growing steeper, and a decreasing γ as the slope growing shallower.

To find the Lorentz factor for a string with backreaction, we must first calculate the correction to the null vectors due to backreaction. We find $\Delta A'$ by integrating over all

accelerations in the u-like past of a point in Region IIa, and $\Delta B'$ by integrating over all accelerations in the v-like past of a point in Region IIb. Thus,

$$\Delta A'^0 = 4G\mu s^2 \left(-2\ln\left[1-\frac{u}{v}\right] + \ln\left[1+\frac{s^2 u}{(1-s^2)v}\right]\right) , \tag{4.31a}$$

$$\Delta A'^1 = 4G\mu s^2 \ln\left[1+\frac{s^2 u}{(1-s^2)v}\right] , \tag{4.31b}$$

$$\Delta A'^2 = 8G\mu s \left(-\ln\left[1-\frac{u}{v}\right] + \ln\left[1+\frac{s^2 u}{(1-s^2)v}\right]\right) , \tag{4.31c}$$

$$\Delta A'^3 = 0 . \tag{4.31d}$$

and

$$\Delta B'^0 = 4G\mu s^2 \left(2\ln\left[\frac{v}{u}-1\right] + \frac{s^2}{1-s^2}\ln\left[s^2+\frac{(1-s^2)v}{u}\right]\right) , \tag{4.32a}$$

$$\Delta B'^1 = \frac{4G\mu s^4}{1-s^2}\ln\left[s^2+\frac{(1-s^2)v}{u}\right] , \tag{4.32b}$$

$$\Delta B'^2 = 8G\mu s \left(\ln\left[\frac{v}{u}-1\right] + \frac{s^2}{1-s^2}\ln\left[s^2+\frac{(1-s^2)v}{u}\right]\right) , \tag{4.32c}$$

$$\Delta B'^3 = 0 . \tag{4.32d}$$

With the corrected null vectors and the metric perturbation in Region IIa, we may find the Lorentz factor of a bead which, initially at rest, is given a kick by the backreacted left-going slope. This is (rewriting via binomial expansion)

$$\gamma = \sqrt{1+s^2}\left[1+\frac{4G\mu s^2}{1+s^2}\left(s^2\ln\left[\frac{s^2u+(1-s^2)v}{u}\right] + (1+s^2)\ln\left[\frac{s^2u+(1-s^2)v}{(1-s^2)v}\right] - 2s^2\ln\left[\frac{v}{u}-1\right]\right)\right]^{1/2} . \tag{4.33}$$

This clearly reduces to the flat-space $\gamma = \sqrt{1+s^2}$ we found before if there is no backreaction present. The term multiplying this one tells us how γ, and thus how the angle of the slope, is to change.

If we fix u and let v increase, then as we reach $v \gg u$ in the far future of Region IIa, we see that

$$\gamma = \sqrt{1+s^2}1 - \frac{4G\mu s^2}{1+s^2}\ln\left[\frac{v}{u}\right] . \tag{4.34}$$

At least in this limit, γ has decreased, and the slope has become shallower!

In Fig. (4.4), we consider a variety of fixed u and see how the scaling term in Eq. (4.33) changes as we evolve in v. Here, we see a curiosity: at low v, γ experiences an enhancement for larger values of u. We are not confident at this time as to the physical origin of this effect—or indeed if it is physical at all. We also note that the slope is shallower the closer

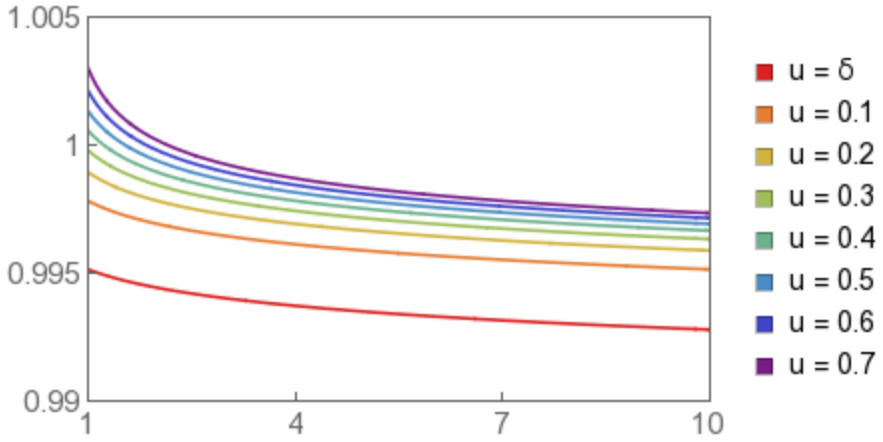

Figure 4.4: A bead at rest on a string given a kick by the left-going slope will acquire some Lorentz factor γ. We plot here how γ deviates from the flat-space case for various fixed u throughout the slope. The bead's γ is reduced more the closer we are to the leading edge of the slope. We have chosen $G\mu = 0.01$.

we are to the leading edge of Region IIa. Thus, the leading edge of the sloped region is the first to be "depleted", or brought back to the static string configuration.

This analysis gives us some confidence in our initial guess for how backreaction might change the worldsheet. However, it is not enough to explain away our earlier concerns, namely:

1. We do not know if we have found an answer which is free of gauge effects.
2. Regardless, we still should know the correct ξ^λ to remove all unphysical effects.
3. If we are to trust and use our results for the bead, Region III needs some effect which acts to modify it in order to keep the worldsheet continuous.

For now, we will step back from investigations of how backreaction changes the worldsheet and consider other aspects of the problem.

4.6 Counterpoint to the premise

We began our analysis with the presumption that the energy radiated by the moving slopes would grow without bound, thereby giving rise to a paradox. While solving the problem at hand is interesting beyond solving this paradox—for instance, when considering how small perturbations on a loop of string might be changed before the rest of the loop has had time to affect them—the paradox is still a central assumption and ought to be checked. We

already know that Region III, far from the slopes, returns to the non-radiating flat space case, but our concern is for Regions IIa and IIb.

In order to check the energy in gravitational waves, we consider the stress-energy tensor given by

$$t_{\alpha\beta} = -\frac{1}{8\pi G}\left(R^{(2)}_{\alpha\beta}[h^{(1)}] - \frac{1}{2}\eta_{\alpha\beta}\eta^{\rho\gamma}R^{(2)}_{\rho\gamma}[h^{(1)}]\right) . \tag{4.35}$$

Or, this is the stress-energy tensor constructed by taking the first-order metric perturbation, $h^{(1)}$, as input to the second-order-in-h part of the expanded Ricci tensor,

$$\begin{aligned} R^{(2)}_{\alpha\beta} = {} & \frac{1}{2}h^{\rho\gamma}h_{\alpha\beta,\rho\gamma} + \frac{1}{4}h_{\rho\gamma,\alpha}h^{\rho\gamma}{}_{,\beta} + \frac{1}{2}h^{\rho,\gamma}_{\beta}\left(h_{\rho\alpha,\gamma} - h_{\gamma\alpha,\rho}\right) \\ & - \frac{1}{2}h^{\rho\gamma}\left(h_{\beta\gamma,\alpha\rho} + h_{\alpha\gamma,\beta\rho}\right) + \frac{1}{2}\left(h^{\rho\gamma}h_{\alpha\beta,\rho}\right)_{,\gamma} - \frac{1}{4}h^{\gamma,\rho}_{\gamma}h_{\alpha\beta,\rho} \\ & + \frac{1}{2}\left(h^{\rho\gamma}{}_{,\gamma} - \frac{1}{2}h^{\gamma,\rho}_{\gamma}\right)\left(h_{\beta\rho,\alpha} + h_{\alpha\rho,\beta}\right) . \end{aligned} \tag{4.36}$$

Whether or nor general relativity is the most elegant physical theory ever devised, the arguments made for that opinion do not cite this particular expression. Still, what is tedious for the human is trivial for the machine, and so we determine the stress-energy tensor of the first-order perturbation—the stress-energy tensor of gravitational waves—to be [3]

$$t_{\alpha\beta} = 0_{\alpha\beta} . \tag{4.37}$$

So, it appears that the paradox does not need resolving. To convince ourselves of this result, we consider other investigations of radiating perturbed straight strings.

It is known that for a straight string lying on the x axis with left- and right-going waves, there is no gravitational radiation. The metric perturbation takes the form [42]

$$h^{\alpha\beta} = -4G\mu \begin{pmatrix} F'^2 + G'^2 & F'^2 + G'^2 & F' & G' \\ F'^2 + G'^2 & F'^2 + G'^2 & F' & G' \\ F' & G' & 1 & 0 \\ G' & G' & 0 & 1 \end{pmatrix} \ln\left[\frac{(y-F)^2 + (z-G)^2}{\delta^2}\right] , \tag{4.38}$$

where F and G describe how the waves perturb the string in the y and z directions, respectively. They are naturally functions of $t \pm x$.

This expression presumes the traveling waves have existed for all time, whereas our perturbation has a clear starting point. But as we go very far from that starting point into the future of either Region IIa or IIb, then the point's view of the past looks more and more

[3] To obtain this result, it is necessary to write the metric of the static straight string in its manifestly flat form, as given in Ref. [4].

like the sloped region has existed forever. In this view, we can treat the sloped region as a propagating wave of the sort whose perturbation is described by Eq. (4.38)—indeed, if we note that $F(u) = s(t+x)$ and $G = 0$ for the left-going sloped segment, then the stress-energy tensor in Eq. (4.38) matches with the one in Eq. (4.11). Perhaps it is not so surprising that we have found that the gravitational radiation from our perturbed string vanishes, rather than diverging, in the far-future limit.

4.7 Future directions

While an exact solution is not forthcoming, we have done enough work to make an educated guess about the rate at which the slopes are lowered (if indeed they are). Equations (4.31,4.32) tell us that the null vectors are modified by something proportional to $G\mu \ln(t/\delta)$, just as in Chapter 3; integrating these modifications would yield that the worldsheet modified by an effect of the same order. If we then think about the timescale on which the correction is of order unity—large enough to completely erase the slope—then even for the heaviest realistic strings, we will be waiting an extremely long time, with $t \approx \delta e^{10^8}$. Even if the modification to the slopes acts as we initially guessed, it will not significantly change a string's structure on timescales short enough to make it a dominant, or even co-dominant, effect on realistic string loops.

Here is where we abandon further investigation. While we have identified the issues with understanding and interpreting the results given in Eqs. (4.20-4.22), and have offered some approaches for curing said issues, we have not been successful in conclusively disentangling physical and unphysical effects. What we have done we have presented in the hopes that it might offer guidance, and some starting point, to someone attempting to answer this question in the future. To that end, we will now discuss some possible future directions for this work.

One issue which we have so far given little attention is the question of how, precisely, the string is initially given a perturbation. To conserve momentum at $0 < t < 1$, we add a semi-infinite "strut" to our spacetime with some pressure entirely in the y direction. The end of the strut is at the spacetime location where we need to apply the kick, and the strut itself only exists when we require its services.[4] This strut then sources its own perturbation,

[4]This does not violate causality if we imagine that all members of the strut were, long ago, given instructions on when and how hard to "push". This requires only that the string has existed for a long time before the kick.

which could change the acceleration of points on the worldsheet.

If we do not wish to pursue the strut, we can solve the issue of the injected energy by reformulating our situation to be one in which two slopes which have always existed on the string pass through each other at $t = 0$. While this situation's geometry is different, and therefore it may not be entirely analogous to the one which we have focused on, we may be able to make further headway on disentangling real versus gauge effects by this approach.

Another line of inquiry which we have not pursued is to take the acceleration effects at face value, calculate how the worldsheet changes, and then see if the final result sheds new light on any procedure thus far attempted. This is not to say we should hope that this result will somehow validate our initial guess; rather, it may be that carrying the calculation out in its entirety will permit us to diagnose with greater precision which terms are the problematic ones.

The above suggestions were not borne out by the author for the reason that the final result is far less important to the field than those presented in Chapter 3, and so investing more efforts here while more useful work awaited seemed lacking in justification. While the conclusion we hoped to reach eluded us in the end, the techniques learned and knowledge gained from this project did inform and support our future work. We do regret the lack of conclusiveness, and apologize to the reader who had hoped for more. We close on the following point:

> Science is neat, but I'm afraid it's not very forgiving.
>
> Scott Clarke, *Stranger Things*

CHAPTER 5

ELECTROMAGNETIC BACKREACTION: A TOY CASE

The problem of backreaction is not constrained to considering gravity as the motivating force. Here we consider a simpler case of electromagnetic backreaction, although there are some obvious parallels to the gravitational work we have already presented, chief of which is the reliance of both solutions on the method of Green's functions. However, our primary motivation for the work to follow is the resolution of a known paradox.

The work in this section is based upon Ref. [43].

5.1 Premise

Consider a static straight cosmic string lying on the x axis. Further assume that this string is superconducting, and so we may create massless charged particles on the string by application of some external field [8]. While such particles may carry some charge other than electromagnetic, and while they may therefore be coupled to many exotic fields, for this work we will confine ourselves to considering standard electromagnetism.

If we consider the simplest case, in which there are no external fields, then there exists an exact solution for the string's electric and magnetic fields [44]:

$$\mathbf{E}(x,\rho,\theta) = 2J^t(x)\rho^{-1}\hat{\rho}\,, \tag{5.1a}$$

$$\mathbf{B}(x,\rho,\theta) = 2J^x(x)\rho^{-1}\hat{\theta}\,, \tag{5.1b}$$

where J^t is the electric charge and J^x is the x-direction current. As the electric field is purely radial, there is no effect of backreaction, and the charges propagate unchanged along the string. However, this gives rise to an immediate paradox of divergent energy. Consider that the fields of Eq. (5.1) go as $1/\rho$, and therefore the energy density goes as $\epsilon = 1/\rho^2$. The energy per unit length is therefore

$$\mathcal{E} = \int \epsilon\rho d\rho d\theta \propto \int \frac{d\rho}{\rho}\,. \tag{5.2}$$

This is clearly logarithmically divergent as $\rho \to \infty$.

Now, we take our string, absent any charges or fields, and apply to it an electric field of arbitrary strength and pointing in the $+\hat{x}$ direction. We apply this field for a finite time

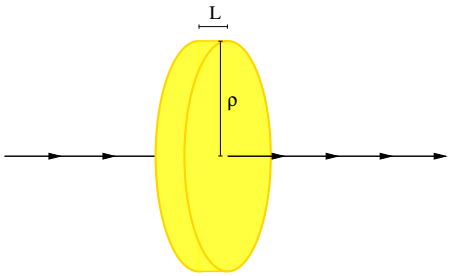

Figure 5.1: A train of charge carriers of length L, moving at the speed of light, carries with it a disk-shaped slab of electromagnetic energy.

and at the origin. What results? By charge conservation, we expect to produce two equal and opposite trains of charge—positive charge carries propagating in the $+\hat{x}$ direction, and an equal number of equal-strength negative charge carriers propagating in the $-\hat{x}$ direction.

If we apply no further external fields to these trains of charge, and do not account for backreaction, then these trains move unimpeded towards infinity, as shown in Fig. 5.1. The solution then approaches the exact form of Eq. (5.2). However, it is clearly impossible to obtain an infinite energy from a finite energy input, and so we have arrived at our paradox.

The clear resolution to this paradox lies in backreaction. More strongly, backreaction must decrease the charge density and current asymptotically to zero, for the presence of any stationary currents when backreaction ceases to act means that the paradox still exists. We will dedicate the remainder of this chapter to showing that backreaction resolves this paradox, and discuss briefly this problem's possible applications to the case of gravitational backreaction.

5.2 Induced fields and currents

We know that in the Lorenz gauge, the electromagnetic potential of a system is found from

$$\Box A^\mu = j^\mu \,, \tag{5.3}$$

where j is the charge-current density. If we consider a cosmic string with both charge and x-direction current, then $j^\mu = J^\mu(t,x)\delta(y)\delta(z)$. We may now solve for the potential via the method of Green's functions and obtain

$$A^\mu(p) = \int D_r(p,p')j^\mu(p')d^4p' = \int D_r(t,x,t',x')J^\mu(t',x')dt'dx' \,, \tag{5.4}$$

where p is the four-position of the field point and p' the four-position of the source.

Because we are interested in how backreaction changes currents on the string, we will hereafter give attention only to the electric field on the string and pointing in the x direction, as it is this field which may cause changes in the string's charge-current. This field is given in terms of the potential by

$$E_x(t,x) = F^{10} = \partial_x A^t + \partial_t A^x \,. \tag{5.5}$$

We therefore drop the subscript x on E; all instances of E from here on out refer to the x-directed field.

Inserting Eq. (5.5) into Eq. (5.4) gives us

$$E(t,x) = \int \left[J^t(t',x')\partial_x D_r(t,x,t',x') + J^x(t',x')\partial_t D_r(t,x,t',x') \right] dt'dx' \,. \tag{5.6}$$

We decompose the retarded Green's function, Eq. (2.3), into a form more useful here:

$$D_r(t,x,t',x') = -\frac{\delta\left((t-t')^2 - (x-x')^2\right)}{4\pi\,|x-x'|} \,. \tag{5.7}$$

As this depends only on $x - x'$ and $t - t'$, we can write $\partial_x G = -\partial_{x'} G$ and $\partial_t G = -\partial_{t'} G$. We then integrate by parts to find

$$E(t,x) = \int D_r(t,x,t',x') \left[\partial_{x'} J^t(t',x') + \partial_{t'} J^x(t',x') \right] dt'dx' \,. \tag{5.8}$$

The current induced by an electric field applied to a superconducting string is given by [4]

$$\partial_x J^t + \partial_t J^x = q^2 E_x \,, \tag{5.9}$$

where q is the fundamental charge. Thereby we rewrite our expression for the electric field to find

$$E(x,t) = E_{\text{ext}} - \alpha \int \frac{\delta\left((t-t')^2 - (x-x')^2\right)}{|x-x'|} E(t',x')dt'dx' \,, \tag{5.10}$$

with α the fine structure constant. This tells us that an electric field applied at a time t' leads to an electric field at some later time t. By integrating across all causally-connected electric fields, we may find the induced electric field at an arbitrary point. We have added the E_{ext} term because we wish to find the total electric field, which is external fields plus induced fields.

Our massless charge carriers move at the speed of light, and so it will be convenient to change into a null coordinate system with

$$u = \frac{t+x}{\sqrt{2}} \,, \tag{5.11a}$$

$$v = \frac{t-x}{\sqrt{2}} \,. \tag{5.11b}$$

Note that this is not what we would obtain from our usual procedure of $u = \tau + \sigma$, $v = \tau - \sigma$, $\tau = t$. This is in part because this while this choice of coordinates is excellent for analyzing the motion of a cosmic string in a flat background, the problem which we wish to solve is not really about strings at all. We could be solving for the self-interaction of massless charged particles propagating along a superconducting wire; as long as Eq. (5.9) holds, we don't care about the nature of that wire. We have instead chosen null coordinates such that the Jacobian determinants for transforming between (t, x) and (u, v) are one.

In these null coordinates, the retarded Green's function becomes

$$D_r = -\frac{1}{4\pi}\left(\frac{\delta(v-v')}{u-u'} + \frac{\delta(u-u')}{v-v'}\right), \tag{5.12}$$

and Eq. (5.10) becomes

$$E(u,v) = E_{\text{ext}} - \alpha\left(\int_0^u \frac{E(u',v)}{u-u'}du' + \int_0^v \frac{E(u,v')}{v-v'}dv'\right). \tag{5.13}$$

From this expression, we can see that the integration across causally-connected electric fields—across a given point's past light cone—has contributions from two branches. All electric fields in the past and to the left contribute through the u' integral, while all electric fields in the past and to the right contribute through the v' integral.

One sees an immediate issue of a divergence at the upper limit of integration for both integrals in Eq (5.13). This is a consequence of treating the string as a one-dimensional object, which gives it infinite self-inductance. Such a model, while good on scales much greater than the string's actual thickness, obviously breaks down on scales comparable to the string thickness. We will add a constant δ, characteristic of the string's thickness, to both integrand denominators to regulate the divergence,

$$E(u,v) = E_{\text{ext}} - \alpha\left(\int_0^u \frac{E(u',v)}{u-u'+\delta}du' + \int_0^v \frac{E(u,v')}{v-v'+\delta}dv'\right) \tag{5.14}$$

By the same transformation that gave us our null coordinates, we may split the current into left- and right-moving parts,

$$J_R = \frac{J^t + J^x}{\sqrt{2}}, \tag{5.15a}$$

$$J_L = \frac{J^t - J^x}{\sqrt{2}}. \tag{5.15b}$$

The continuity equation $\partial_t J^t + \partial_x J^x = 0$ and Eq. (5.9) tell us that

$$\partial_u J_R = -\partial_v J_L = \frac{\alpha E}{2}. \tag{5.16}$$

We interpret this as follows: if there is no electric field, then left-moving currents are independent of u and right-moving currents are independent of v. Since u and v are the left- and right-pointing null coordinates, respectively, this means that the currents propagate freely in those directions. Note that a positive J^u represents positive charge carriers moving to the right, and a positive J^v represents positive charge carriers moving to the left.

Eq. (5.16) also tells us that once we find the electric field everywhere, the current at a given point we find via

$$J_R = \frac{\alpha}{2}\int_0^u E(u',v)du' \,, \tag{5.17a}$$

$$J_L = -\frac{\alpha}{2}\int_0^v E(u,v')dv' \,. \tag{5.17b}$$

Note that Eq. (5.16) means that the currents are antisymmetric under exchange of u and v, in contrast to the electric fields, which are symmetric.

5.3 The electric field and current along the null directions

We will first consider the case where the applied field is a δ-function at the origin, $E_{\text{ext}} = \delta(u)\delta(v)$. In this case, there will be singular fields and currents along the positive u and v axes, due directly to the applied field, and non-singular fields and currents in the "interior", where $u, v > 0$, due to backreaction. We must therefore find the singular quantities first.

We write the total electric field as

$$E = E_{\text{ext}} + E_{\text{int}} + E_L + E_R \tag{5.18}$$

where E_{int} is the interior electric field, which only exists in the chronological future of the origin, and E_L, E_R are the singular fields on the positive u and v axes, respectively. Positive values of the singular fields represent a field pointing rightwards. The singular fields are equal under exchange of u and v by symmetry.

We will find E_R, then recover E_L by this symmetry. We start by considering the causal past of a generic point on the positive u axis. The null directions are those of fixed u or v, and so it is clear that only E_R and E_{ext} are in the causal past of such a point. With $E = E_{\text{ext}} + E_R$, Eq. (5.14) yields

$$E_R(u,v) = -\alpha\left(\frac{\delta(v)}{u+\delta} + \int_0^u \frac{E_R(u',v)}{u-u'+\delta}du'\right) . \tag{5.19}$$

upon integrating the $\delta(u)$ found in E_{ext}. Because E_R is constrained to lie on the line $v = 0$, we may rewrite it as

$$E_R(u, v) = -f(u)\delta(v)\,. \tag{5.20}$$

Thus, with the definition

$$h(u) = \frac{\alpha}{u + \delta} \tag{5.21}$$

and defining $*$ to mean convolution of the sort

$$(f * h)(u) = \int_0^u f(u')h(u - u')du'\,. \tag{5.22}$$

then Eq. (5.19) becomes

$$f(u) = h(u) - (f * h)(u)\,. \tag{5.23}$$

By Laplace transformations, this becomes

$$F(U) = H(U) - F(U)H(U)\,, \tag{5.24}$$

where

$$\mathfrak{L}[f](U) = F(U)\,, \tag{5.25a}$$

$$\mathfrak{L}[h](U) = H(U) = \alpha e^{\delta U} E_1(\delta U)\,. \tag{5.25b}$$

Note that E_1 is the exponential integral for complex arguments. Thus, we find the Laplace-transformed u-dependent part of E_R to be

$$F(U) = \frac{H(U)}{1 + H(U)}\,. \tag{5.26}$$

In order to take the inverse Laplace transform and find $f(u)$, we must investigate the analytic structure of $F(U)$.

We know $E_1(z)$ to have a branch cut on the negative real axis and a logarithmic singularity at the origin, but it is otherwise analytic. The singularity is easily dealt with by noting that the E_1 terms in the numerator and denominator of $F(U)$ cancel each other in the limit $z \to 1$, such that $F|_{U\to 0} = 1$.

We have shown $H(U)$ itself is not problematic, but there is the additional possibility for a divergence to arise in $F(U)$ if $1 + H(U) = 0$. We will show that this is not possible, as $e^z E_1(z)$ cannot be a negative real number. We write

$$e^z E_1(z) = \int_z^\infty \frac{e^{z-t}}{t} dt \tag{5.27}$$

from the definition of $E_1(z)$. We then take this contour go in the positive real direction until it reaches positive real infinity, then go in the imaginary direction (where it does not contribute). This is equivalent to making a transformation of variables from t to $x = t - z$, such that

$$e^z E_1(z) = \int_0^\infty \frac{e^{-x}}{z+x} dx \,. \tag{5.28}$$

Now, any z which is a real positive number gives a positive result. Complex z will always give a result with non-zero imaginary part, and so nowhere in the domain over which E_1 is defined may we obtain a $e^z E_1(z)$ which is a negative real number.

The inverse Laplace transform of $F(U)$ is then

$$f(u) = \frac{1}{2\pi i} \int_{-i\infty}^{+i\infty} F(U) e^{Uu} dU \,. \tag{5.29}$$

With the large-argument form of $E_1(z) \approx e^{-z}/z$, we see that $e^z E_1(z)$ falls like $1/z$ at infinity. We may therefore deform the contour of integration to enclose only the negative real axis, such that

$$f(u) = \frac{1}{2\pi i} \int_0^\infty \left(F(-k - i0) - F(-k + i0)\right) e^{ku} dk \,. \tag{5.30}$$

It is a property of the exponential integral that

$$E_1(-x \pm i0) = -\mathrm{Ei}(x) \mp i\pi \,, \tag{5.31}$$

and so with a change of variables to $k = \kappa\delta$ we get

$$f(u) = \frac{\alpha}{\delta} \int_0^\infty \frac{e^{-\kappa(u/\delta+1)}}{\left(1 - \alpha e^{-\kappa}\mathrm{Ei}(\kappa)\right)^2 + \left(\alpha\pi e^{-\kappa}\right)^2} d\kappa \,. \tag{5.32}$$

Equations (5.20,5.32) give an exact solution to Eq. (5.14), but the integral of Eq. (5.32) is not solvable in closed form. To find $f(u)$, we will have to make approximations.

Since we inserted δ by hand to Eq. (5.14), we do not expect our expressions to be good when $u \sim \delta$, and so we take $u \gg \delta$. This leads to exponential suppression of the integrand of Eq. (5.32) by its numerator unless $\kappa \ll 1$, so we will neglect factors of $e^{-\kappa}$ everywhere and use the small-parameter approximation $\mathrm{Ei}(\kappa) = \ln\kappa + \gamma$, with γ the Euler-Mascheroni constant. This simplifies our integral to

$$f(u) = \frac{\alpha}{\delta} \int_0^\infty \frac{e^{-\kappa u/\delta}}{(1 - \alpha(\ln\kappa + \gamma))^2 + (\alpha\pi)^2} d\kappa \,. \tag{5.33}$$

We next make the stronger approximation that $\ln(u/\delta) \gg 1$. We justify this by the observation that we are concerned with a paradox which only arises when logarithms become large. Next, we observe that the term $\ln\kappa$ has approximately the value $\ln(\delta/u)$ over the

range of integration before exponential suppression kills the integrand at $\kappa \sim \delta/u$, and so we replace $\ln\kappa$ by $\ln(\delta/u)$in the denominator. Finally, we neglect γ by comparison to the very large $\ln(\delta/u)$, and the second term in the denominator by comparison to the first, and find that

$$f(u) = \frac{\alpha}{u}\frac{1}{\left(1+\alpha\ln(u/\delta)\right)^2}\,. \tag{5.34}$$

The right-moving singular field is therefore given by

$$E_R(u,v) = -\frac{\alpha}{u}\frac{\delta(v)}{\left(1+\alpha\ln(u/\delta)\right)^2}\,. \tag{5.35}$$

and by symmetry, the left-moving singular field is

$$E_L(u,v) = -\frac{\alpha}{v}\frac{\delta(v)}{\left(1+\alpha\ln(u/\delta)\right)^2}\,. \tag{5.36}$$

Thus, after the external field is applied, the singular fields are always negative.

Having found the singular fields, the singular currents are obtained by application of Eq. (5.17). The right-moving current is found from

$$J^u_R(u,v) = \frac{\alpha}{2}\int_0^u \left(E_{\rm ext}(u',v) + E_R(u',v)\right)du' = \frac{\alpha}{2}\delta(v)\int_0^u \left(\delta(u') - f(u')\right)du'\,. \tag{5.37}$$

This has the expected Dirac delta term in v which confines it to the u axis, but we must be careful here. Our expression for $f(u)$ is not good for small u—we assumed as such in our approximations—and so we change the range of integration as follows. The definition of the Laplace transform tells us that

$$\int_0^\infty f(u)du = F(0) = 1\,, \tag{5.38}$$

and since therefore we find

$$\int_0^\infty \left(\delta(u) - f(u)\right)du = 0\,, \tag{5.39}$$

then we may rewrite Eq. (5.37) as

$$J^u_R(u,v) = -\frac{\alpha}{2}\delta(v)\int_u^\infty f(u')du'\,. \tag{5.40}$$

We see from this form that the current must fall asymptotically to zero for increasing u, i.e. a long time after the initial field is applied. This is consistent with our idea that backreaction must eventually reduce the current to zero. The integral is easily done, and we obtain expressions for the singular currents,

$$J^u_R(u,v) = \frac{\alpha}{2}\frac{\delta(v)}{1+\alpha\ln(u/\delta)}\,, \tag{5.41a}$$

$$J^u_L(u,v) = -\frac{\alpha}{2}\frac{\delta(u)}{1+\alpha\ln(v/\delta)}\,. \tag{5.41b}$$

The singular currents are always right-going and go to zero as $u, v \to \infty$. They decline exactly as quickly as is required to cancel the logarithmic divergence along the null axes. We will address the timescale of backreaction in Sec. 5.7, but for now, we note that the initial current reaches half of its initial strength when u or v, as appropriate, reaches $\delta e^{1/\alpha}$.

5.4 The electric field and current in the interior

Having found the singular fields, we may turn to finding the field and current in the interior, being the chronological future of the origin. The objects we seek we label E_{int}, J^u_{int}, and J^v_{int}. As for the singular case, we will first solve for the electric field, then use that expression to find the current.

We note two things: that E_{ext} is not causally connected to any place in the interior, and that any point in the interior sees fields to its left and to its right. This means that we will need both integrals in Eq. (5.14). By the same process that gave us Eq. (5.23), we find

$$E_{\text{int}}(u,v) = f(u)h(v) + f(v)h(u) - (E_{\text{int}}(\cdot,v) * h)(u) - (E_{\text{int}}(u,\cdot) * h)(v)\,. \tag{5.42}$$

Where we solved for the singular fields with a single Laplace transform from the domain $u \to U$, we will solve for the interior field with a double Laplace transform from the domains $u \to U$ and $v \to V$. We let $\mathcal{H} = \mathfrak{L}[E_{\text{int}}]$, so

$$\mathcal{H}(U,V) = F(U)H(V) + H(U)F(V) - \mathcal{H}(U,V)\left(H(U) + H(V)\right)\,. \tag{5.43}$$

Rearranging and solving, we find

$$\mathcal{H}(U,V) = \frac{1}{1+H(U)+H(V)} - \frac{1}{1+H(U)} - \frac{1}{1+H(V)} + 1\,. \tag{5.44}$$

Once again, we must investigate the analytic structure of $\mathcal{H}$ if we are to take the double inverse Laplace transform. The only new suspect who might give us trouble is the first term of Eq. (5.44); specifically, we wonder if we may find a pole from $1 + H(U) + H(V) = 0$. In fact, we can, provided $\alpha > 0.67$, since the minimum of $\Re\left[e^z E_1(z)\right]$ is around -0.74. Despite this seeming obstacle, we will still be able to deform the contours to enclose the negative real axes, as we argue now.

For each U, we deform the contour in V. We may discover isolated points V_i such that $H(V_i) = -1 - H(U)$, where there will be contributions like $2\pi i / H'(V_i)$. We then deform the contour in U, looking to see if we cross points at which $H'(V_i) = 0$. However, this does

not happen. We have that

$$H'(z) \propto e^z E_1(z) - \frac{1}{z} = \int_0^\infty e^{-x} \left(\frac{1}{z+x} - \frac{1}{z} \right) dx = -\frac{1}{z} \int_0^\infty \frac{x e^{-x}}{z+x} dx \,. \tag{5.45}$$

Thus, for z positive and real, the integrand is positive; for z complex, the integrand is complex. The integral can never vanish, and so we cannot have $H'(V_i) = 0$ for any V_i. We do not encounter poles when deforming our contour. As in the single-parameter case, if we take $y \to \infty$ with U fixed, we find $\mathcal{H} \sim 1/V$, and vice versa, so we may deform the contours in either order with no contribution from the contours at infinity. Thus, we have no trouble in converting the double inverse Laplace transform

$$E_{\rm int}(u,v) = -\frac{1}{4\pi^2} \int_{-i\infty}^{+i\infty} e^{Uu} dU \int_{-i\infty}^{i\infty} e^{Vv} \mathcal{H}(U,V) dV \tag{5.46}$$

to

$$\begin{aligned} E_{\rm int}(u,v) = -\frac{1}{2\pi^2} \int_0^\infty \int_0^\infty [&\mathcal{H}(-k-i0,-l-i0) - \mathcal{H}(-k+i0,-l-i0) \\ &- \mathcal{H}(-k-i0,-l+i0) + \mathcal{H}(-k+i0,-l+i0)] e^{-ku-lv} dk dl \,. \end{aligned} \tag{5.47}$$

Only the first term in $\mathcal{H}$, which depends on both U and V, survives the cancellations brought about by the form of this integrand. We change variables to $\kappa = \delta k$ and $\lambda = \delta l$ and simplify to obtain

$$E_{\rm int}(u,v) = \frac{2}{\delta^2} \int_0^\infty \int_0^\infty \frac{C q^4 e^{-\kappa(1+u/\delta) - \lambda(1+v/\delta)}}{C^4 + 2C^2 q^4 \pi^2 \left(e^{-2\kappa} + e^{-2\lambda}\right) + q^8 \pi^4 \left(e^{-2\kappa} - e^{-2\lambda}\right)^2} d\kappa d\lambda \,, \tag{5.48}$$

with $C = 1 - \alpha \left[e^{-\kappa} \mathrm{Ei}(\kappa) + e^{-\lambda} \mathrm{Ei}(\lambda) \right]$. We again approximate the null parameters to be much greater than the string thickness to find

$$E_{\rm int}(u,v) = \frac{2q^4}{\delta^2} \int_0^\infty \int_0^\infty \frac{e^{-(\kappa u + \lambda v)/\delta}}{(1 - \alpha(\ln(\kappa\lambda) + 2\gamma))^3 + 4q^4\pi^2(1 - \alpha(\ln(\kappa\lambda) + 2\gamma))} d\kappa d\lambda \,. \tag{5.49}$$

Applying the stronger approximations $\ln(u/\delta), \ln(v/\delta) \gg 1$, and ignoring the linear logarithmic term in the denominator by comparison to the cubic logarithmic term, we have quite nearly arrived at our solution. The final step is to observe the same exponential suppression we observed in Eq. (5.33) applies here for each of κ and λ, and so we again approximate the logarithm arguments as being δ/u, δ/v over the range of integration. Putting this all together gives us an expression for the interior electric field,

$$E_{\rm int}(u,v) = \frac{2q^4}{uv} \frac{1}{(1 + \alpha \ln(uv/\delta^2))^3} \,. \tag{5.50}$$

This field is always positive and goes to zero as u or v goes to infinity. It declines faster than the singular fields.

We are now interested in the interior currents. We first look for $J^u_{\rm int}$, which we know will not depend on E_R or $E_{\rm ext}$ as an integration along u which ends in the interior must be at some fixed $v > 0$. By Eq. (5.17),

$$J^u_{\rm int}(u,v) = \frac{\alpha}{2}\int_0^u \left(E_{\rm int}(u',v) + E_L(u',v)\right) du' \,. \tag{5.51}$$

The integral of E_L is trivial and yields $-f(v)$. With $E_{\rm int}$, we once again face the issue of our approximations failing for $u \sim \delta$. From the definition of the Laplace transform,

$$\int_0^\infty E_{\rm int}(u,v)du = \frac{1}{2\pi i}\int_{i\infty}^{i\infty} e^{Vv} dV \frac{F(0)H(V) + F(V)H(0)}{1 + H(0) + H(V)} \,. \tag{5.52}$$

Because $H(0) = \infty$, this simplifies to

$$\int_0^\infty E_{\rm int}(u,v)du = \frac{1}{2\pi i}\int_{i\infty}^{i\infty} F(V)e^{Vv}dV = \mathfrak{L}^{-1}[F](v) = f(v) \,. \tag{5.53}$$

Thus we have that

$$\int_0^\infty E(u',v)du' = 0 \qquad \rightarrow \qquad \int_0^u E(u',v)du' = -\int_u^\infty E(u',v)du' \,. \tag{5.54}$$

This leads us to

$$J^u_{\rm int}(u,v) = -\frac{q^4}{2v}\frac{1}{\left(1 + \alpha\ln(uv/\delta^2)\right)^2} \,, \tag{5.55}$$

and by antisymmetry,

$$J^v_{\rm int}(u,v) = \frac{q^4}{2u}\frac{1}{\left(1 + \alpha\ln(uv/\delta^2)\right)^2} \,. \tag{5.56}$$

Both of these currents are left-going, go to zero as $u, v \to \infty$, and decline faster than the singular currents. The paradox is also solved for the interior.

The behavior of the interior and singular currents is summarized in Fig. (5.2).

5.5 The current in a strip

Since the singular currents are right-going while the interior currents are left-going, we should be curious about how much these currents cancel. A simple way to get at this is to measure the u current flowing over a strip in v, say from 0 to v_0. We find

$$I^u_{\rm strip}(u,v_0) = \int_0^{v_0} \left[J^u_R(u,v') + J^u_{\rm int}(u,v')\right] dv' \,. \tag{5.57}$$

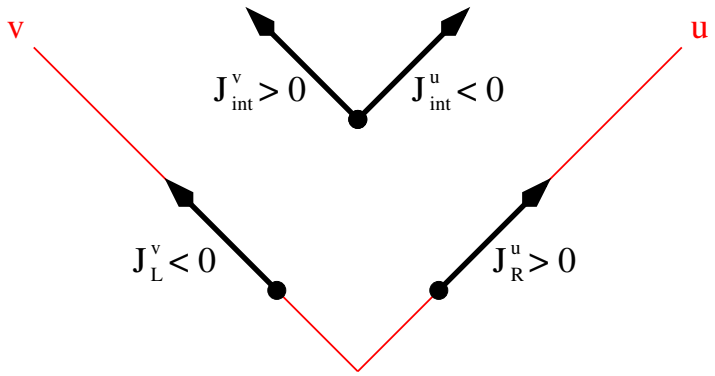

Figure 5.2: The quantities J^u and J^v represent currents flowing in the u and v directions, respectively. Since J^u_R is positive and J^v_L is negative, both represent right-going currents. Since $J^u_{\rm int}$ is negative and $J^v_{\rm int}$ is positive, both represent left-going currents.

This calls for us to integrate over a range for which our approximations are bad, but we resolve those issues as above. Unsurprisingly, we may show that $I^u_{\rm strip}(u,\infty) = 0$, and so

$$I^u_{\rm strip}(u,v_0) = -\int_{v_0}^{\infty} \left[J^u_R(u,v') + J^u_{\rm int}(u,v')\right] dv' \,. \tag{5.58}$$

Thus, the current contained in a strip of finite width in v is

$$I^u_{\rm strip}(u,v_0) = \frac{\alpha}{2}\frac{1}{1+\alpha\ln(uv_0/\delta^2)} \,. \tag{5.59}$$

This current is positive for all u, v_0 in our domain of interest, and so the singular u current is greater than the interior u current contained in any strip of finite width in v. As this width becomes very large, the interior current contained in that strip will rise to cancel out the singular current, and so the total current in the strip goes to zero.

The v current case is analogous.

5.6 The total current

Having found the current everywhere, we may define the total u and v currents as

$$J^u_{\rm tot}(u,v) = J^u_R(u,v)\theta(u) + J^u_{\rm int}(u,v)\theta(u)\theta(v) \,, \tag{5.60a}$$

$$J^v_{\rm tot}(u,v) = J^v_L(u,v)\theta(v) + J^v_{\rm int}(u,v)\theta(u)\theta(v) \,. \tag{5.60b}$$

where the Heaviside-θ functions ensure the currents only enter in the domain in which they apply.

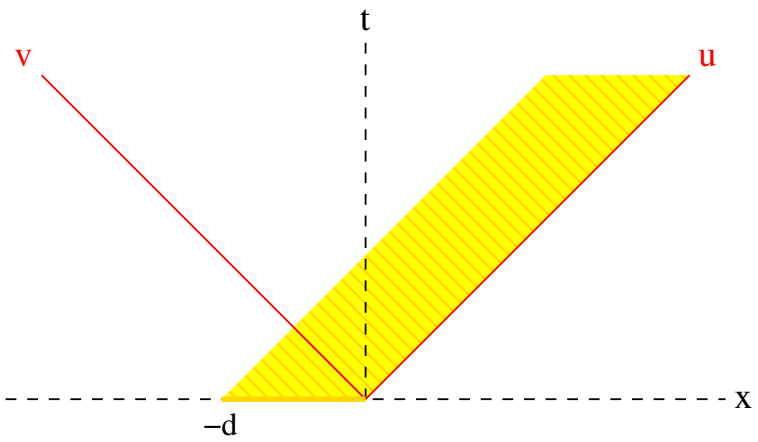

Figure 5.3: An electric field is applied along the x axis from $-d$ to 0. We are interested in the shaded region, which indicates points u-like connected to the initial distribution.

We have so far considered only the effect of applying a singular external field. For a general external field which occupies some finite space-time region, the u current is

$$J^u\left(u,v;E_{\rm ext}\right)=\int_{-\infty}^{\infty}\int_{-\infty}^{\infty}E_{\rm ext}(u',v')J^u_{\rm tot}(u-u',v-v')du'dv'\,, \tag{5.61}$$

and the v current is found in the same fashion.

To demonstrate such a solution, we consider an external field which is a top-hat distribution in x with width d and singular in time,

$$E_{\rm ext}=\delta(t)(\theta(x+d)-\theta(x))=\sqrt{2}\delta(u+v)(\theta(u-v+\sqrt{2}d)-\theta(u-v))\,. \tag{5.62}$$

Integration of Eq. (5.61) for this source over du' gives us

$$J^u(u,v;E_{\rm ext})=\sqrt{2}\int_0^{d/\sqrt{2}}J^u_{\rm tot}(u+v',v-v')dv'\,. \tag{5.63}$$

We consider the current in a region u-like connected to the initial train of charge with $0<v<d/\sqrt{2}$, as shown in Fig. 5.3. If we consider $u\gg d$, then we neglect v' in comparison to u, and so

$$J^u(u,v;E_{\rm ext})=\sqrt{2}\int_0^{d/\sqrt{2}}\left[J^u_R(u,v-v')+J^u_{\rm int}(u,v-v')\theta(v-v')\right]dv'\,. \tag{5.64}$$

Now, we consider where in this range the singular and interior currents are supported. Equivalently, where in the range $0<v',v<d/\sqrt{2}$ can $\delta(v-v')$ and $\theta(v-v')$ evaluate to true? The Dirac delta is obviously true when $v=v'$, and the Heaviside theta is true for $v>v'$. Thus, there is no contribution to the current for $v'>v$, and so we rewrite the upper limit of integration of Eq. (5.64)

$$J^u(u,v;E_{\rm ext})=\sqrt{2}\int_0^{v}\left[J^u_R(u,v-v')+J^u_{\rm int}(u,v-v')\right]dv'\,. \tag{5.65}$$

This is related to Eq. (5.57) by a simple change of variables, and so we find

$$J^u(u, v; E_{\text{ext}} = \frac{\alpha}{\sqrt{2}} \frac{1}{1 + \alpha \ln(uv/\delta^2)} \,. \tag{5.66}$$

As the train of charges moves and evolves under backreaction, how does its initial distribution change? The ratio of the current at the trailing edge (some arbitrary u and v) to the current at the leading edge (which is only the singular current) is

$$\frac{J(trailing)}{J(leading)} = \frac{1 + \alpha \ln(u/\delta)}{1 + \alpha \ln(u/\delta) + \alpha \ln(v/\delta)} \,. \tag{5.67}$$

This ratio has a range of possible values $\{1/2, 1\}$, approaching 1 in the limit that u is exponentially larger than v. While the top-hat shape of the initial distribution is distorted, it is never large, and decreases with time.

5.7 Discussion

We have shown that currents induced on a superconducting cosmic string by some finite applied electric field are reduced by backreaction. Moreover, they decline at least as fast as the inverse of $\ln(u/\delta)$ or $\ln(v, \delta)$, which is the minimum required to cancel the logarithmically-growing divergence in the energy density of the electric field off the string. In this way, the paradox presented in Sec. 5.1 is prevented.

Because the charge carriers on the string are massless, and so must move at the speed of light, we say that the effect of backreaction is to scatter these particles off of the induced field, instantaneously reversing their direction. It is the first instance of this scattering, converting u-directed particles of the singular right-going current into v-directed particles, which gives rise to the interior current; such particles are then scattered many times more, but are permanently in the interior. This depletion, and the subsequent scatterings, explain why all currents eventually go to zero.

Because $\ln(u/\delta)$ and $\ln(v/\delta)$ change more rapidly for small u, v than for large u, v, the currents drop quickly at the start but decrease more and more slowly as u, v grow large. In particular, half of the right-going singular current has vanished when $u = \delta e^{1/\alpha}$, but a fraction f remains when $u = \delta e^{(1-f)/\alpha f}$. If we consider cosmic strings of $G\mu \approx 10^{-8}$, the largest permitted by current observations (vid. Chapter 1.3), then we have a string thickness $\delta \approx 10^{-29}$ cm. An electromagnetic current on this string will have half of its initial current remaining when $u \approx 10^{30}$ cm, or roughly the size of the observable universe. It is safe to

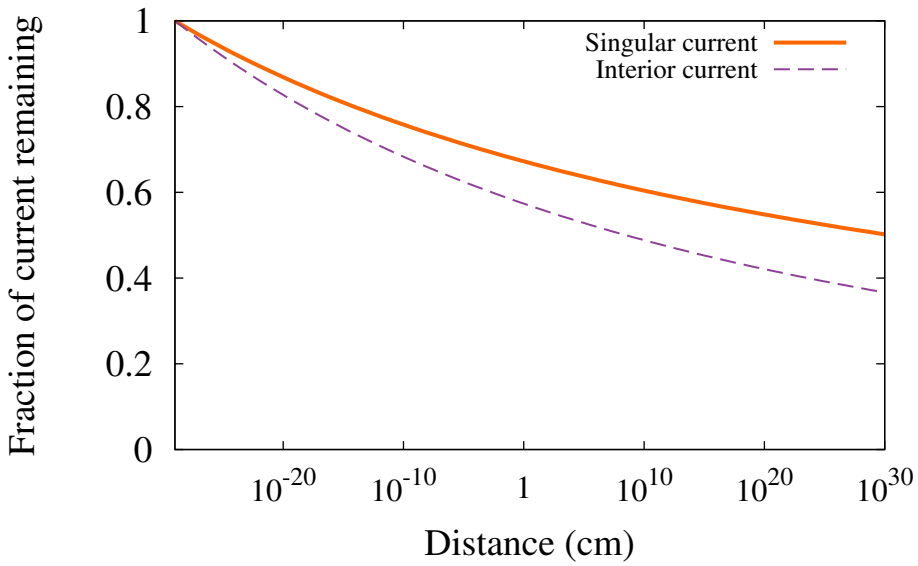

Figure 5.4: The u singular current (orange solid line) falls slower than the u interior current (purple dashed line). We have considered an interior current which is 10^2 cm behind the leading edge and evolves at a fixed v. The fraction of current remaining falls as the inverse of the logarithm at slowest, so the effect is observable right away, but never becomes huge. We assume a string thickness of $\delta = 10^{-29}$ cm.

say that we will never see backreaction reduce the current by more than half under such conditions.

On the other end of this scale, the current drops to three-quarters its initial value rapidly, when $u \approx 10^{-8}$ cm. Figure 5.4 shows this rapid initial drop-off, followed by the long tail. Such an analysis is immediately portable to particles charged by more exotic fields, as mentioned in Sec. 5.1. As long as such a field behaves like electromagnetism, or at least enough like electromagnetism that we may arrive at Eq. 5.10, we will arrive at the same result, the only change being the strength of coupling α. Weaker couplings are obviously of less interest, but stronger couplings will result in currents losing a significant fraction of their initial value before other processes can take effect.

This treatment of electromagnetic backreaction may be useful to us in the study of the gravitational backreaction of a sloped string, as we attempted in Chapter 4. If the effect of gravitational backreaction is similar to the backreaction discussed here, then we would expect the timescale of effect to scale with the replacement of α by $G\mu$. Again taking the largest possible $G\mu = 10^{-8}$, we find that $f = 10^{-6}$ at the length scale of the observable universe. This matches with our back-of-the-envelope calculation done previously. Any gravitational backreaction effect of this kind, while of theoretical interest, will not be ob-

servable in realistic strings.

CHAPTER 6

CLOSING REMARKS

We shall now summarize the results of this dissertation for each topic studied, and offer some suggestions and comments on how these results might be used or expanded upon in future work.

6.1 Electromagnetic self-interactions of charges on a string

The results of Chapter 5 show that the paradox of moving charges on an infinite, straight, and static superconducting cosmic string is resolved in an intuitive way. Due to backreactive effects, a train of charges is scattered and the current thereby reduced at least as fast as is necessary to prevent a divergence in the total energy contained in the radial electromagnetic field.

While this work focused specifically on electromagnetic charge, its results are portable to other, similarly-coupling fields. Moreover, it may be of some interest (and certainly some value) to consider how backreaction of charged particles affects currents on chiral strings. Such an investigation, when coupled with an improved understanding of how gravitational backreaction affects loops, may allow us to make some headway in addressing the problem of stabilized current-carrying loops of strings, or vortons [45].

6.2 Gravitational self-interactions of perturbed straight strings

Our investigations in Chapter 4, which ultimately bore no fruit, we still presented for completeness and in the hope that they will be useful in some future investigation. The heart of the issue lies in the question of how we would go about disentangling real and unreal effects, which we attempted to answer by considering well-motivated gauge transformations and the response of a test particle to the motion of the perturbed segment of the string.

If we assume our initial guess is correct, and the slopes are decreased by backreaction, we know enough about the worldsheet corrections to guess at the timescale on which this effect applies. Because A' and B' are corrected as logarithms, the change to the worldsheet should also be logarithmic. Thus, we guess that the decrease of the slope would happen

something like $1 - G\mu \ln t$. For realistic strings with $G\mu \approx 10^{-8}$, this means that we must wait a very long time indeed to see an appreciable change in the slopes, and so the effect is likely not important to loops.

6.3 Gravitational self-interactions of string loops

In Chapter 3, we performed both a general and specific analysis of the fates of kinks and cusps on cosmic string loops. Very significantly, we show that kinks are not rounded off by backreaction, but rather "open up" in such a way that the time at which cusps form on a piecewise linear string loop is generally delayed—and in very specific scenarios, cusp formation is prevented entirely.

This result requires that we modify our expectations for gravitational wave signals from string loops. A sub-population of the loop network for loops of the same age will have fewer cusps than we previously predicted, particularly if it is a very young sub-population. As a consequence, there will be fewer gravitational wave bursts, which has the unfortunate effect of making the detection of cosmic strings in this fashion more difficult. Moreover, we should be wary as well of whether or not we should expect the strength and shape of bursts from cusps to also change.

The specific solution of backreaction on the Garfinkle-Vachaspati loop to first order demonstrates the first of two predictions made from our general result: that kinks would be opened up, preventing the near-immediate appearance of cusps. Because our solution only holds to first order (excepting the square case, which we will address momentarily), this result does not demonstrate our second prediction: that small kinks can persist very late in the loop's life. To show this, as well as to address a host of other interesting and valuable questions, requires simulations of backreactive effects on loops.

A final note on string loops, and perhaps an object more of curiosity than great significance, is the finding that the square Garfinkle-Vachaspati loop does not change its shape at all due to backreaction, instead shrinking rigidly to nothing. The only other known example of such a rigid shrinker is the ACO loop. These unique solutions show how symmetries may protect loop shapes, but it is not clear at this time if similar effects could be present in realistic string loops.

The most obvious next step is the one we are already taking: the simulation of how gravitational backreaction changes arbitrary loops. In such a simulation, we are most interested

in understanding the distribution of when cusps first form. But what of one step beyond? There are a number of interesting problems both large and small, many of which we have mentioned above or elsewhere in the text. Certainly the results of the simulation project will inspire additional questions related to how we model, and to how we might measure, the gravitational waves emitted by string loops.

So concludes this work.

APPENDIX A

AN ALTERNATE APPROACH TO UNDERSTANDING BACKREACTION ON THE LOOP

In Chapter 3, we noted that we could distinguish secular from gauge effects by taking advantage of the fact that the metric perturbation of the loop is periodic in time, but the changes due to backreaction build up. Thus, once we had Eqs. (3.20,3.21), we needed take no further action other than waiting. However, the new null vectors are modified in their time components, and so understanding what a constant-time slice looks like by inspection is not as straightforward. Here, we present an alternate way of understanding how backreaction changes the structure of the Garfinkle-Vachaspati loop.

We wish to find a reparameterization of u and v such that $\Delta B'^0 = 0 = \Delta A'^0$. We shall work specifically on B', finding the new A' by symmetry.

First, divide $B'^\lambda + \Delta B'^\lambda$ by $B'^0 + \Delta B'^0$. Then, rewrite all fractions via $(1+x)^{-1} \approx 1-x$ for $x \ll 1$, discarding terms quadratic in $G\mu$. This results in the correction to the null vector being

$$\Delta B'^\lambda(\tilde{u}) = 8G\mu \left(0,\ \frac{1}{w}\left[h^2 \ln\left(\frac{1-\tilde{u}}{R+\tilde{u}}\right) - w^2 \ln\left(\frac{1-\tilde{u}}{R'+\tilde{u}}\right)\right],\right.$$
$$\left. -\frac{1}{h}\left[h^2 \ln\left(\frac{1-\tilde{u}}{R+\tilde{u}}\right) - w^2 \ln\left(\frac{1-\tilde{u}}{R'+\tilde{u}}\right)\right],\ 0\right). \tag{A.1}$$

Here, $\tilde{u}$ is a new null parameter which has a different range than u. That range is determined by the reduced temporal extent of the modified loop, which we know from Eq. (3.23); thus, we know that

$$\tilde{u} \in \left(-1 - 8G\mu\left[\frac{\ln w^2}{h^2} + \frac{\ln h^2}{w^2}\right],\ 1 + 8G\mu\left[\frac{\ln w^2}{h^2} + \frac{\ln h^2}{w^2}\right]\right). \tag{A.2}$$

That is, the range of $\tilde{u}$ is that of u, but scaled by the same factor that scaled the period. Note that within the logarithms, we are fine to use the range $\tilde{u} \in \{-1, 1\}$, as the difference is negligible if we are only concerned with effects to first order in $G\mu$.

For completeness, we note that

$$\Delta A'^\lambda(\tilde{v}) = 8G\mu \left(0,\ \frac{1}{w}\left[h^2 \ln\left(\frac{1-\tilde{v}}{R+\tilde{v}}\right) - w^2 \ln\left(\frac{1-\tilde{v}}{R'+\tilde{v}}\right)\right],\right.$$
$$\left. \frac{1}{h}\left[h^2 \ln\left(\frac{1-\tilde{v}}{R+\tilde{v}}\right) - w^2 \ln\left(\frac{1-\tilde{v}}{R'+\tilde{v}}\right)\right],\ 0\right). \tag{A.3}$$

$\tilde{v}$ is defined over the same range as $\tilde{u}$.

Equation (A.1) offers immediately the observation about the square loop: it is clear that for $h = w$, the entirety of $\Delta B'^{\lambda}(\tilde{u})$ vanishes, and so the new B (and A) will be that of the unmodified loop, but smaller to account for the lessened ranges of $\tilde{u}$ and $\tilde{v}$.

We can also glean the nature of the correction more easily. We examine the common term to all components of all corrections,

$$h^2 \ln\left[\frac{1-\tilde{n}}{R+\tilde{n}}\right] - w^2 \ln\left[\frac{1-\tilde{n}}{R'+\tilde{n}}\right] , \tag{A.4}$$

when the null parameter $\tilde{n}$ is at its extremes. At the lower extreme, the common term is

$$h^2 \ln\left[\frac{h^2}{w^2}\right] - w^2 \ln\left[\frac{w^2}{h^2}\right] . \tag{A.5}$$

Because we know that $w \leq h$, this expression is never positive, and is only zero when $w = h$. Conversely, at the upper extreme, the common term is

$$h^2 \ln h^2 - w^2 \ln w^2 - \left(w^2 - h^2\right) \ln\left[\frac{\delta}{2}\right] , \tag{A.6}$$

which is never negative, and is only zero when $w = h$. So, the direction in which A' and B' point changes, producing the "bowing" of A and B which we observed. Finally, we can tell that the bowing must be asymmetric; when we set $\tilde{n} = 0$, the common term becomes $w^2 \ln R' - h^2 \ln R$, which is never positive (and, in a startling break with tradition, is only zero when $w = h$ or $w = 1$). So, the turnaround point for A' and B' is in the second half of their motion. If the line connecting the kinks of A and B is to retain its angle in the xy plane, then this also means that the bowing must be more pronounced in the second half of $\tilde{n}$'s range, which is also consistent with our observations.

APPENDIX B

NULL PARAMETERIZATION OF THE SLOPED STRING

We shall now derive the null vectors of Eqs. (4.5) and (4.6) in more detail than previously given and from a geometric perspective. We begin with what we know: that the worldsheet in Region I is described by

$$x^\gamma = \left(\frac{u+v}{2}, \frac{u-v}{2}, 0, 0 \right) , \tag{B.1}$$

and in Region III by

$$x^\gamma = \left(\frac{u+v}{2} + s^2, \frac{u-v}{2}, s, 0 \right) , \tag{B.2}$$

Now, we want to insist upon the continuity of u and v as we move between regions. This straightaway gives us that we must have $x = (u-v)/2$ always. This requirement comes about because of the symmetry of the initial setup. Because the parameterizations in Regions IIa and IIb are identical under reflection through $x = 0$ and interchange of u and v, the proportionality between u and v when $x = 0$ must be unity in both regions if their (u, v) coordinates on are to agree for points on their mutual border.

Next, we consider that the y position of the left-going sloped segment is given by $y = s(t+x)$ when $1 > t + x > 0$ and $x < 0$. Because the left-going sloped segment is due to changing u, the y position should also depend entirely on u; thus, $t + x \propto u$.

Now consider a point on the line $t + x = 0$ (for some $x < 0$). This is the border between Region I and Region IIa, and so their parameterizations must agree. Because $t + x = 0 \implies u = 0$ on this time, we now know that $t = v/2 + au/2$, with a some constant.

Rewriting $y = s(t+x)$ as $y = (1+a)u/2$, we have found (up to an unknown constant a) the u null vector for Region IIa:

$$x^\gamma_{,u} = \left(\frac{a}{2}, \frac{1}{2}, \frac{(1+a)s}{2}, 0 \right) . \tag{B.3}$$

Enforcing the null requirement lets us solve $a = (1+s^2)/(1-s^2)$, and so we find the null vectors in Region IIa to be

$$x^\gamma_{,u} = \left(\frac{1}{2}\frac{1+s^2}{1-s^2}, \frac{1}{2}, \frac{s}{1-s^2}, 0 \right) , x^\gamma_{,v} = \left(\frac{1}{2}, -\frac{1}{2}, 0, 0 \right) , \tag{B.4}$$

in agreement with Eq. (4.5).

We had mentioned in Sec. 4.2 that one could check that the null vectors for Regions IIa and IIb were indeed null. This is of course no accident; while the traditional choice of null coordinates is $u = \tau + \sigma$, $v = \tau - \sigma$, there is in fact an infinite family of null parameters of this form, differing only by a constant of proportionality. Consider

$$u = C_u \left(\tau + \sigma\right) , \tag{B.5}$$

$$v = C_v \left(\tau - \sigma\right) , \tag{B.6}$$

with C_u and C_v real, nonzero constants. It is clear that this rescaling does not affect the length of the null vectors, but this means that it does not change the conformal gauge conditions either. The zero-length conditions $x_{,u} \cdot x_{,u} = 0$ and $x_{,v} \cdot x_{,v} = 0$ are just the conditions $\dot{x} \cdot x' = 0$, $\dot{x}^2 + x'^2 = 0$ rewritten for the u and v vectors. This is straightforward to work out if we consider that Eq. (B.5) implies

$$\frac{\partial}{\partial \tau} = \frac{1}{C_u}\frac{\partial}{\partial u} + \frac{1}{C_v}\frac{\partial}{\partial v} , \tag{B.7}$$

$$\frac{\partial}{\partial \sigma} = \frac{1}{C_u}\frac{\partial}{\partial u} - \frac{1}{C_v}\frac{\partial}{\partial v} . \tag{B.8}$$

Is there some danger in changing definitions of u and v at different places on the worldsheet? Certainly within each region is safe; the only question is if we might introduce some error by attempting to make invalid comparisons of or modification to the null vectors. The solution here is perform calculations with null vectors and parameters, but then to always return to $\dot{x}$ and x' when we want to interpret how backreaction has changed the worldsheet.

BIBLIOGRAPHY

[1] T. W. B. Kibble. Topology of Cosmic Domains and Strings. *J. Phys.*, A9:1387–1398, 1976.

[2] Saswat Sarangi and S.H. Henry Tye. Cosmic string production towards the end of brane inflation. *Phys.Lett.*, B536:185–192, 2002.

[3] Gia Dvali and Alexander Vilenkin. Formation and evolution of cosmic D strings. *JCAP*, 0403:010, 2004.

[4] A. Vilenkin and E. P. S. Shellard. *Cosmic Strings and Other Topological Defects*. Cambridge University Press, 2000.

[5] J. Silk and A. Vilenkin. Cosmic Strings and Galaxy Formation. *Phys. Rev. Lett.*, 53:1700–1703, 1984.

[6] R. J. Scherrer, A. L. Melott, and E. Bertschinger. The Formation of Large Scale Structure From Cosmic Strings and Massive Neutrinos. *Phys. Rev. Lett.*, 62:379, 1989.

[7] Sebastian F. Bramberger, Robert H. Brandenberger, Paul Jreidini, and Jerome Quintin. Cosmic String Loops as the Seeds of Super-Massive Black Holes. *JCAP*, 1506(06):007, 2015.

[8] Edward Witten. Superconducting Strings. *Nucl. Phys.*, B249:557–592, 1985.

[9] Veniamin Berezinsky, Eray Sabancilar, and Alexander Vilenkin. Extremely High Energy Neutrinos from Cosmic Strings. *Phys. Rev.*, D84:085006, 2011.

[10] Yun-Wei Yu, Kwong-Sang Cheng, Gary Shiu, and Henry Tye. Implications of fast radio bursts for superconducting cosmic strings. *JCAP*, 1411(11):040, 2014.

[11] Kouichirou Horiguchi, Kiyotomo Ichiki, and Naoshi Sugiyama. Primordial magnetic fields from the string network. *PTEP*, 2016(8):083E02, 2016.

[12] Jose J. Blanco-Pillado, Ken D. Olum, and Benjamin Shlaer. The number of cosmic string loops. *Phys. Rev.*, D89(2):023512, 2014.

[13] Heather Audley et al. Laser Interferometer Space Antenna. 2017.

[14] Mukunda Aryal and Allen E. Everett. Properties of $Z(2)$ Strings. *Phys. Rev.*, D35:3105, 1987.

[15] Albert S. Schwarz. *Topology for Physicists*. Grundlehren der matematischen Wissenschaften. Springer-Verlag Berlin Heidelberg, 1994.

[16] T. W. B. Kibble and Neil Turok. Selfintersection of Cosmic Strings. *Phys. Lett.*, B116:141–143, 1982.

[17] Tom Charnock, Anastasios Avgoustidis, Edmund J. Copeland, and Adam Moss. CMB constraints on cosmic strings and superstrings. *Phys. Rev.*, D93(12):123503, 2016.

[18] J. L. Christiansen, E. Albin, T. Fletcher, J. Goldman, I. P. W. Teng, M. Foley, and G. F. Smoot. Search for Cosmic Strings in the COSMOS Survey. *Phys. Rev.*, D83:122004, 2011.

[19] J. Aasi et al. Constraints on cosmic strings from the LIGO-Virgo gravitational-wave detectors. *Phys. Rev. Lett.*, 112:131101, 2014.

[20] Z. Arzoumanian et al. The NANOGrav Nine-year Data Set: Limits on the Isotropic Stochastic Gravitational Wave Background. *Astrophys. J.*, 821(1):13, 2016.

[21] Mark Hindmarsh, Kari Rummukainen, and David J. Weir. New solutions for non-Abelian cosmic strings. 2016.

[22] Jose J. Blanco-Pillado, Ken D. Olum, and Benjamin Shlaer. Cosmic string loop shapes. *Phys. Rev.*, D92(6):063528, 2015.

[23] Mark Hindmarsh, Kari Rummukainen, Tuomas V. I. Tenkanen, and David J. Weir. Improving cosmic string network simulations. *Phys. Rev. D*, 90:043539, Aug 2014.

[24] David Garfinkle and Tanmay Vachaspati. Radiation from kinky, cuspless cosmic loops. *Phys. Rev. D*, 36:2229–2241, Oct 1987.

[25] Yi-Fu Cai, Eray Sabancilar, Daniele A. Steer, and Tanmay Vachaspati. Radio Broadcasts from Superconducting Strings. *Phys. Rev.*, D86:043521, 2012.

[26] Thibault Damour and Alexander Vilenkin. Gravitational wave bursts from cusps and kinks on cosmic strings. *Phys. Rev.*, D64:064008, 2001.

[27] Charles W. Misner, K. S. Thorne, and J. A. Wheeler. *Gravitation*. W. H. Freeman, San Francisco, 1973.

[28] Jean M. Quashnock and David N. Spergel. Gravitational Selfinteractions of Cosmic Strings. *Phys.Rev.*, D42:2505–2520, 1990.

[29] Bruce Allen, Paul Casper, and Adrian Ottewill. Analytic results for the gravitational radiation from a class of cosmic string loops. *Phys. Rev.*, D50:3703–3712, 1994.

[30] Jeremy M. Wachter and Ken D. Olum. Gravitational back reaction on piecewise linear cosmic string loops. 2016.

[31] Jeremy M. Wachter and Ken D. Olum. Gravitational smoothing of kinks on cosmic string loops. 2016.

[32] Neil Turok. Grand Unified Strings and Galaxy Formation. *Nucl. Phys.*, B242:520–541, 1984.

[33] Thibault Damour and Alexander Vilenkin. Gravitational wave bursts from cosmic strings. *Phys. Rev. Lett.*, 85:3761–3764, 2000.

[34] Thibault Damour and Alexander Vilenkin. Gravitational radiation from cosmic (super)strings: Bursts, stochastic background, and observational windows. *Phys. Rev.*, D71:063510, 2005.

[35] Xavier Siemens, Jolien Creighton, Irit Maor, Saikat Ray Majumder, Kipp Cannon, and Jocelyn Read. Gravitational wave bursts from cosmic (super)strings: Quantitative analysis and constraints. *Phys. Rev.*, D73:105001, 2006.

[36] Mark Hindmarsh. Gravitational radiation from kinky infinite strings. *Phys. Lett.*, B251:28–33, 1990.

[37] Xavier Siemens and Ken D. Olum. Gravitational radiation and the small-scale structure of cosmic strings. *Nucl. Phys.*, B611:125–145, 2001. [Erratum: Nucl. Phys.B645,367(2002)].

[38] Malcolm R. Anderson. Self-similar evaporation of a rigidly-rotating cosmic string loop. *Class. Quant. Grav.*, 22:2539–2568, 2005.

[39] Malcolm Anderson. Continuous self-similar evaporation of a rotating cosmic string loop. *Class. Quant. Grav.*, 26:025006, 2009.

[40] Malcolm Anderson. Gravitational waveforms from the evaporating ACO cosmic string loop. *Class. Quant. Grav.*, 26:075018, 2009.

[41] C. J. Burden. Gravitational Radiation From a Particular Class of Cosmic Strings. *Phys. Lett.*, B164:277–281, 1985.

[42] T. Vachaspati. Gravitational Effects of Cosmic Strings. *Nucl. Phys.*, B277:593–604, 1986.

[43] Jeremy M. Wachter and Ken D. Olum. Electromagnetic backreaction from currents on a straight string. *Phys. Rev.*, D90(2):023510, 2014.

[44] Mukunda Aryal, Alexander Vilenkin, and Tanmay Vachaspati. Notes on Superconducting Cosmic Strings. *Phys.Lett.*, B194:25, 1987.

[45] R. L. Davis and E. P. S. Shellard. Cosmic Vortons. *Nucl. Phys.*, B323:209–224, 1989.